Genesis and Taphonomy of a Crinoid Lagerstätte in the Upper Pennsylvanian Barnsdall Formation of Northeastern Oklahoma

by

James Robert Thomka

A thesis submitted to the Graduate Faculty of
Auburn University
in partial fulfillment of the
requirements for the Degree of
Master of Science

Auburn, Alabama
December 13, 2010

Approved by

Ronald D. Lewis, Chair, Associate Professor of Geology
Charles E. Savrda, Professor of Geology
James A. Saunders, Professor of Geology

Abstract

A 50-cm mudstone interval within the Upper Pennsylvanian Barnsdall Formation, exposed near Copan, Washington County, northeastern Oklahoma, records prodeltaic distal shelf sedimentation in an oxygenated, low energy setting. Three thin (3-8 cm thick) horizons within this section contain abundant articulated crinoid remains, with the lowest of these horizons containing the highest genus-level crinoid diversity identified within the Pennsylvanian System. These thin units alternate with thicker (8-15 cm thick) units lacking in articulated crinoids but containing abundant endobenthic bivalve fossils. Centimeter-scale microstratigraphy, fabric analysis of mudstone slabs, taphonomic analysis of crinoid specimens, assessment of fossil content and character derived from disaggregation of mudstone slabs, and evaluation of the morphology, distribution, and physical properties of associated siderite concretions have shed light on the biological, sedimentological, and geochemical processes necessary for the occurrence and preservation of this exceptional crinoid fauna.

The crinoid-bearing units were deposited under conditions of sediment starvation associated with minor transgressive episodes. Long periods of slow sedimentation were interrupted by episodic distal storm events, which were characterized by rapid deposition of fine-grained sediment without erosion, winnowing, or strong unidirectional currents. As a result, the crinoid-bearing units are composed largely of stacked obrution layers. Individual burial layers were very thin and may have been spatially or temporally

variable in thickness, as evidenced by taphonomic variability among crinoid specimens recovered from the same horizon. Sediment starvation, by allowing obrution horizons to become bundled, appears to explain the extremely high diversity and abundance of articulated crinoids within the thin units. This mechanism is better supported than burial of a single extraordinarily diverse crinoid community.

The thicker units not bearing articulated crinoid fossils represent minor episodes of relative sea-level fall and consequent deltaic progradation. The increased proximity to sediment-source area resulted in higher sedimentation rates and more energetic storm events, as evidenced by a primarily endobenthic biofacies, thicker individual burial layers, winnowed lags, and evidence for minor erosion. These interpretations indicate that the stratigraphic expression of parasequences in distal shelf settings may be represented by such thin and subtle alternations of distinct taphofacies, biofacies, and concretion morphologies.

Taphonomic variability among crinoids within the same subclass is shown to be significant at the genus level, but is also detected among individuals of the same species. This preservational heterogeneity results from the complex interactions between morphological, ecological, and depositional factors, including rate of burial, scavenger preferences, morphology and ethology of crinoids, size of crinoid individuals, and heterogeneity in burial layer thickness.

Acknowledgments

This research was funded by research grants from the Alabama Geological Society, the Gulf Coast Association of Geological Societies, and the Southeastern Section of the Geological Society of America. Funding to present research from this project was provided by the Alabama Geological Society, the Geological Society of America, the Southeastern Section of the Geological Society of America, the Alabama Academy of Science, and the Auburn University College of Sciences and Mathematics. Access to the Copan crinoid collection and assistance during research at the University of Nebraska State Museum was provided by Roger Pabian, George Corner, and Greg Brown. Peter Holterhoff graciously provided unpublished stratigraphic data as well as helpful information on the stratigraphy and paleoecology of the deposit. Ronald Lewis provided instruction on the mudstone disaggregation technique, field and specimen photographs, unpublished field data, and generously helped with photography. Thanks are also owed to Isabel León y León for spending many hours working with disaggregated mudstone slabs; to Thomas Key, Ray Tichenor, and Jamie Kinsley for assistance and input on figure preparation; and to my committee for careful review of the manuscript and much valuable feedback.

Table of Contents

List of Tables

List of Figures

INTRODUCTION

Lagerstätten and Crinoid Taphonomy

Seilacher (1970) coined the term fossil-Lagerstätte to define a class of deposits characterized by exceptional fossil abundance (concentration Lagerstätten) or preservational quality (conservation Lagerstätten). These deposits, which result from unusual sedimentological or geochemical processes, provide unique insights into ancient ecologies, physiologies, and environments, making them capable of providing a wealth of paleobiological and paleoecological information typically removed from the fossil record by taphonomic processes (Seilacher et al., 1985). Conservation Lagerstätten are often recognized by the presence of preserved soft tissue, as in the famous Middle Cambrian Burgess Shale of British Columbia (e.g., Gould, 1989) or the Pennsylvanian Mazon Creek deposits of northern Illinois (e.g., Nitecki, 1979). However, an equally important criterion for the recognition of conservation Lagerstätten is the presence of articulated multi-element skeletons that would be found primarily as isolated elements under normal taphonomic conditions (e.g., Brett and Seilacher, 1991). These taphonomically volatile organisms are perhaps best exemplified by crinoids.

An exhaustive overview of crinoid taphonomy is beyond the scope of this study, and the reader is directed to the comprehensive reviews on echinoderm taphonomy by Lewis (1980), Donovan (1991), Brett et al. (1997b), and Ausich (2001). However, a brief introduction is necessary. Crinoids secrete a delicate endoskeleton composed of

numerous small plates (ossicles) of high-magnesium calcite that are bound together in a precise arrangement by ligaments and, in certain post-Devonian crinoids, muscle fibers (Ausich and Baumiller, 1993, 1998). These soft tissues are prone to scavenging at the sediment-water interface (e.g., Meyer, 1971) and after shallow burial (Maples and Archer, 1989) in addition to rapid bacterial decay. The disarticulation process is accelerated in agitated and oxygenated waters; this has been confirmed by actualistic observations in shallow water (Meyer, 1971; Liddell, 1975; Meyer and Meyer, 1986) and deep water (Llewellyn and Messing, 1993; see also Baumiller et al., 1995). Laboratory experiments with regular echinoids (Kidwell and Baumiller, 1990), which are taphonomically comparable to all but the most resistant crinoid morphotypes (Brett et al., 1997b), also demonstrated rapid disarticulation in oxygenated waters, although temperature was also shown to be an important factor. The net result is that the multi-element skeleton of most crinoids undergoes very rapid post-mortem disarticulation into isolated ossicles, usually in a time span between two days and two weeks (Blyth Cain, 1968; Meyer, 1971; Liddell, 1975). Prevention of this rapid degradation has historically been attributed to either rapid, deep burial or an environmental fluctuation prohibitive to scavenging and decay, such as anoxia (Lewis, 1980; Donovan, 1991; Brett et al., 1997b).

However, Allison (1988a) and Plotnick (1986) demonstrated experimentally that decay is commonly an anoxic process, meaning that burial of crinoid remains or onset of anoxia does not necessarily provide an end to decay-related taphonomic processes. In addition, Plotnick (1986), Allison (1986), and Kidwell and Baumiller (1990) utilized experiments to show that decay, even slight, drastically enhances the propensity for disarticulation of skeletonized animals, with the implication that buried crinoids, if

subsequently exhumed or disturbed by prolonged bioturbation, will likely undergo very rapid and complete disarticulation even if initially buried deeply or under anoxic conditions.

In summary, the crinoid skeleton is prone to very rapid post-mortem disarticulation as a result of a number of physical and biological factors serving to destroy or degrade the soft tissue binding together the mineralized ossicles. Preservation of intact and articulated crinoid remains is, therefore, a very rare event, and deposits featuring such fossils qualify as conservation Lagerstätten.

The Copan Crinoid Lagerstätte

A thin mudstone interval within the Upper Pennsylvanian (Missourian) Barnsdall Formation as exposed near the town of Copan, Washington County, northeastern Oklahoma (Fig. 1), contains crinoid fossils characterized by exceptional preservation, including complete crowns with intact arms, tegmens, and tegminal spines (Fig. 2), as well as tremendous diversity and uncommon abundance. Although infrequently cited and enigmatic in certain aspects (see discussion of geologic setting and previous works below), this conservation Lagerstätte lends itself to taphonomic investigations, as multi-element skeletons are high resolution recorders of environmental processes operating within the environment during deposition and after burial. Crinoid skeletons, although easily disarticulated, yield valuable information through analysis of skeletal disarticulation patterns, alignment and orientation patterns, skeletal element size distribution, early diagenetic mineralization, surface features of isolated ossicles and articulated modules, and biotic interactions recorded in fossil material (e.g., Brett and

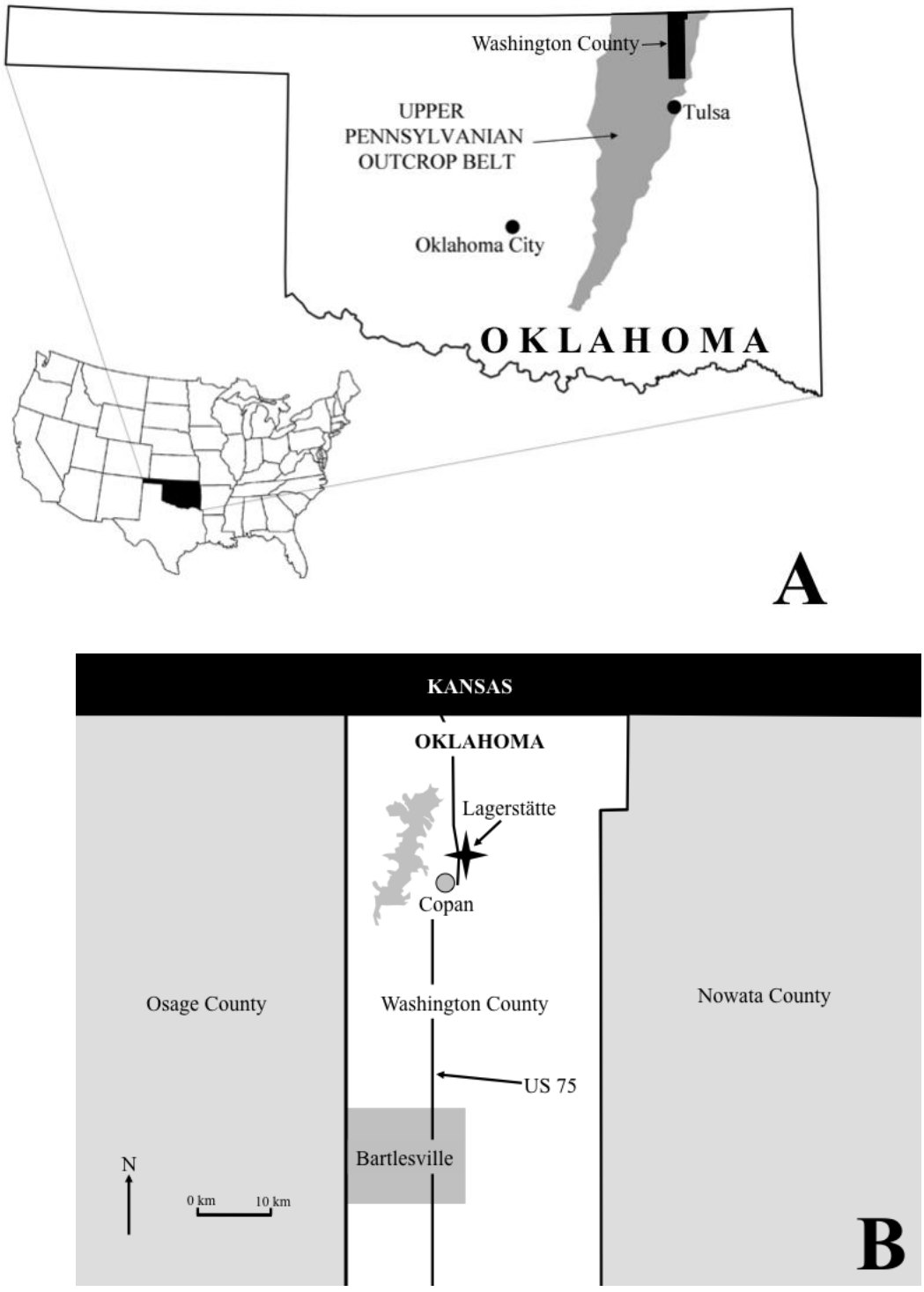

FIGURE 1—Location of study area. A) Location of Washington County, within the belt of Upper Pennsylvanian strata (gray) of Oklahoma. B) Location of Lagerstätte within northern Washington County, roughly 4 km northeast of Copan. The large water body west of the town of Copan is Copan Lake.

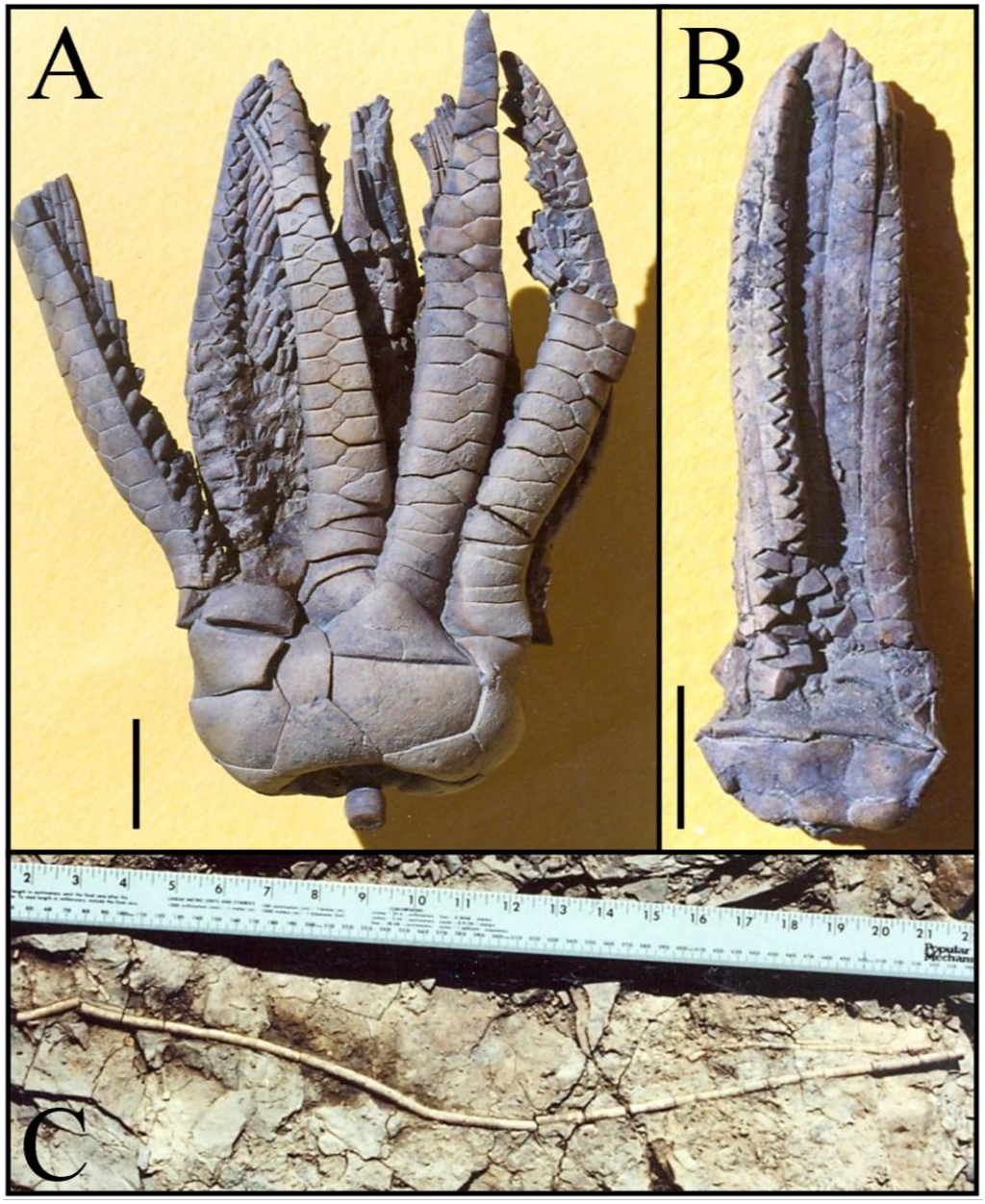

FIGURE 2—Examples of excellent preservation in crinoids recovered from the Copan Lagerstätte. A) *Delocrinus subhemisphericus* crown complete with articulated multi-pinnular pinnules; scale bar = 1 cm. B) *Erisocrinus typus* crown with minor disruption in proximal arms; scale bar = 1 cm. C) Articulated column totaling nearly two feet in length, lacking both a holdfast and an attached crown. Photographs provided by R. D. Lewis.

Baird, 1986a; Speyer and Brett, 1986; Allison, 1988b; Lewis et al., 1990; Parsons and Brett, 1991). The abundance of crinoidal material within this thin interval makes the Copan Lagerstätte rich in paleontologic and paleoenvironmental data capable of shedding light on subtle, but potentially significant patterns involving sedimentation, geochemistry, and paleoecology in what may otherwise appear to be a deposit suitable only for fossil collecting and crinoid taxonomy.

GEOLOGIC SETTING

The Late Pennsylvanian Midcontinent Sea was a vast but relatively shallow water body that persisted from the Middle Pennsylvanian to Early Permian and covered a sizeable portion of the North American craton (Algeo and Heckel, 2008; Fig. 3). An Upper Pennsylvanian outcrop belt consisting of a series of essentially east-west trending, laterally extensive, depth-related facies spanning the area from Iowa in the north to central Oklahoma in the south records deposition within this epicontinental seaway. Shallow carbonate-platform facies susceptible to occasional subaerial exposure dominate in the north (i.e., through most of Iowa) as evidenced by the presence of correlatable paleosol horizons (Boardman and Heckel, 1989) and a recognizable meteoric influence on diagenesis (Xiong and Heckel, 1996). Further south, open marine conditions prevailed, with a phylloid algal mound complex developing through much of southern Kansas. In contrast, the Early Pennsylvanian uplift of the Ouachitas and subsequent shedding of abundant clastic material, coupled with increased subsidence near the Arkoma Basin, resulted in the loss of extensive carbonate units near the Kansas-Oklahoma border and the development of the terrigenous detrital facies belt of Heckel (1977, 1978) to the south. Northern Oklahoma, therefore, is dominated by fine-grained clastic units deposited at the southern margin of this epicontinental sea and in the adjacent basinal environment (Heckel, 1977, 1978; Algeo and Heckel, 2008, and references therein).

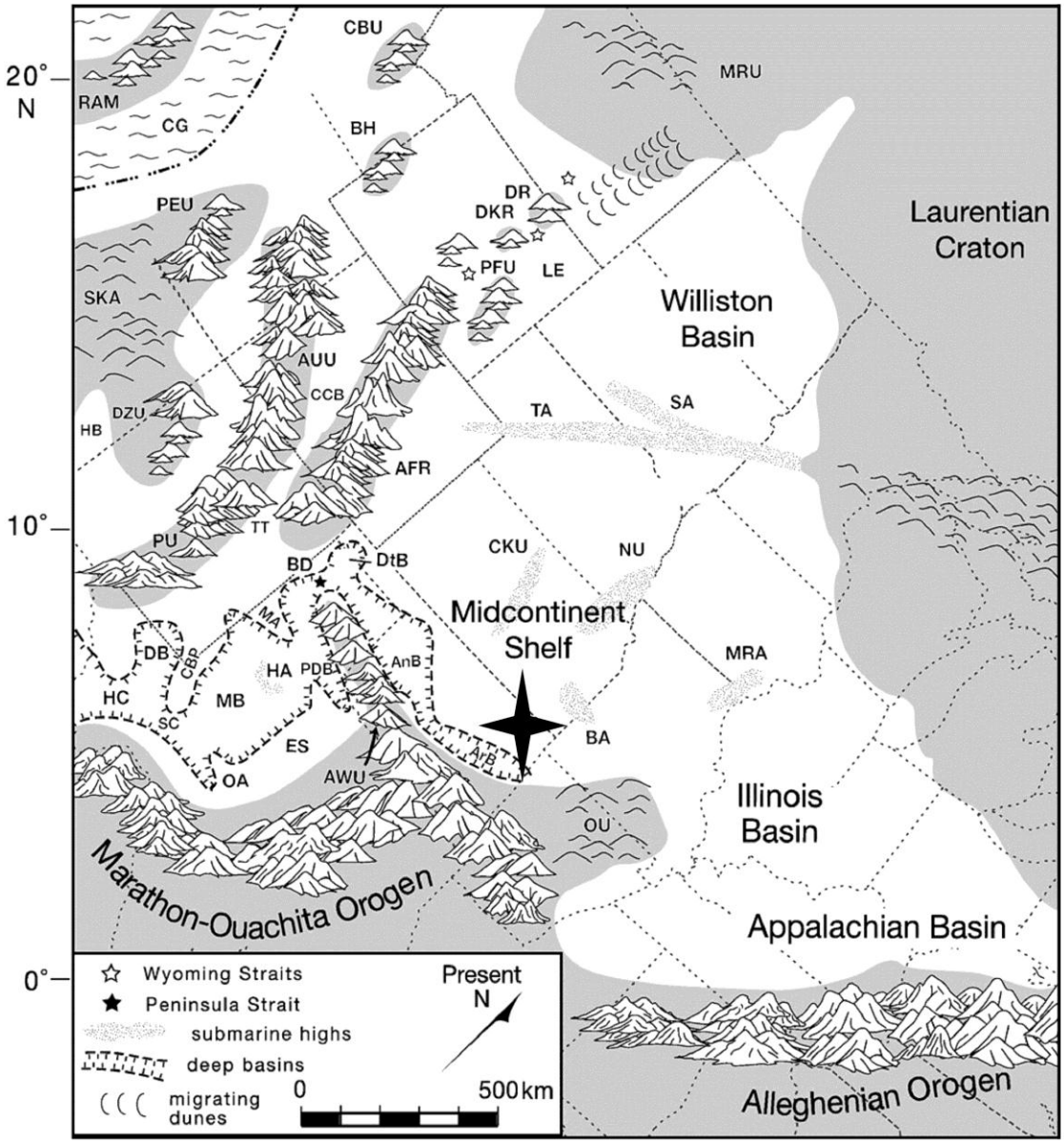

FIGURE 3—Late Pennsylvanian paleogeography of midcontinent North America, showing the extent of the Late Pennsylvanian Midcontinent Sea. The star marks the approximate location of the Copan Lagerstätte in northeastern Oklahoma, then a distal shelf environment close to the source of clastic sediment derived from the Ouachitas. Modified from Algeo and Heckel (2008).

Much of the Pennsylvanian System of North America is characterized by cyclic deposition, representing fluctuations in relative sea-level driven by combined tectonic and eustatic controls (Klein and Willard, 1989; Read and Forsyth, 1989; Klein, 1990) operating on the Late Pennsylvanian Midcontinent Sea. Whereas Pennsylvanian cyclothems of the Appalachian and Illinois basins appear to have been influenced primarily by tectonic subsidence (Klein and Kupperman, 1992), midcontinent cyclothems appear to have resulted primarily from eustatic sea-level fluctuations (Heckel, 1977, 1978, 1980, 1984, 1986, 1994). Cyclothem periodicity suggests that Milankovitch cyclicity, specifically orbital eccentricity, was the driving force behind these eustatic sea-level changes (Heckel, 1986); these orbital perturbations resulted in the waxing and waning of Gondwanan continental glaciers, which were present throughout the Late Pennsylvanian (Crowell, 1978).

Midcontinent cyclothems, or Kansas-type cyclothems of Heckel (1977), ideally consist of five units and represent a single rise and fall of relative sea-level (Fig. 4). An outside shale, potentially containing terrestrial facies, and overlying middle limestone constitute a transgressive phase; a core shale, typically black or dark grey and bearing pelagic fauna and phosphate nodules, represents maximum highstand and the development of thermohaline water-column stratification (see detailed discussion of sedimentology in Bisnett and Heckel, 1996; paleontology in Malinky and Heckel, 1998; and paleoceanography in Algeo and Heckel, 2008); finally, an upper limestone and outside shale constitute the regressive phase, which is disconformably overlain by the next cyclothem. The core shale unit is often used as a marker for lithostratigraphic correlation across broad portions of the midcontinent (e.g., Boardman and Heckel, 1989),

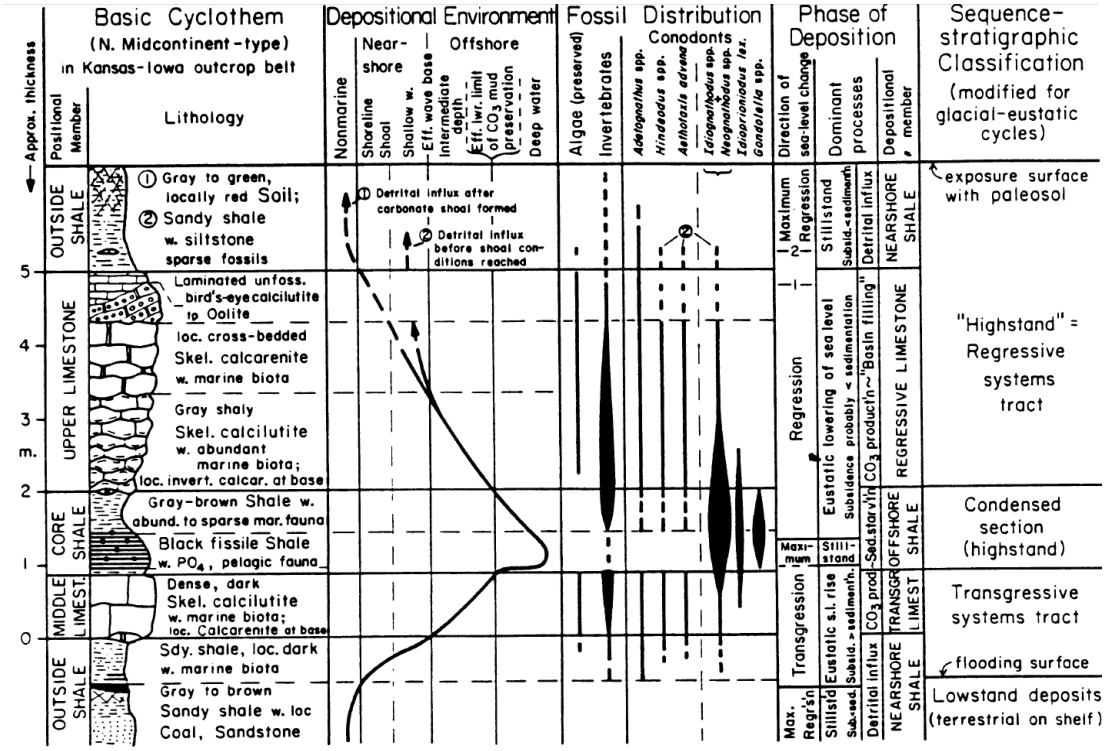

FIGURE 4—Ideal Kansas-type cyclothem, as commonly encountered in the North American midcontinent. The Copan Lagerstätte occurs in the upper core shale facies, above maximum highstand. From Heckel (1994).

as it is easily recognizable lithologically, contains a unique and distinctive fauna relative to surrounding units, and occurs in a consistent position within the cyclothem.

In many cases, however, the core shale portion can be divided into two lithofacies: the lower core shale, as described above, and the overlying upper core shale, which is green to grey in color and contains a diverse benthic marine invertebrate fauna. This upper core shale is deposited during relatively high sea level, but during an initial period of regression; as a result, water-column stratification is broken down, and increased benthic oxygenation permits the replacement of dysaerobic faunas (sensu Boardman et al., 1984; Kammer et al., 1986) by normal marine faunas, while sedimentation rate and environmental energy remain low. It is this oxygenated, low energy, low turbidity environment that allows benthic invertebrates to flourish. The low sedimentation rate and relatively slow rate of sea-level fall results in highly fossiliferous upper core shale facies throughout the midcontinent (Holterhoff, 1996).

The crinoid Lagerstätte near Copan falls within the upper core shale facies of the Stanton cyclothem. The Stanton cyclothem constitutes the youngest midcontinent cyclothemic sequence of Missourian age in the midcontinent and is represented by the Stanton Formation of the Lansing Group in Kansas, where the cyclothem was first described and is most complete (Heckel, 1986; Boardman and Heckel, 1989). However, neither lithostratigraphic unit (Lansing Group or Stanton Formation) is formally recognized in Oklahoma, where the marine portion of the Stanton Formation correlates to the Barnsdall Formation of the Ochelata Group (Holterhoff, 1997a). This difference in stratigraphic classification and nomenclature reflects the major disparity between carbonate-dominated, shelf lithofacies of Kansas and the clastic-dominated, basinal

lithofacies of Oklahoma.

The Barnsdall Formation represents the last major transgressive event of the Missourian Stage, and in northern Oklahoma and southeastern Kansas, a complex mosaic of facies is present, including elements of an anoxic basin (i.e., lower core shale), an oxygenated basin to distalmost shelf (i.e., upper core shale), and various shallow marine environments, including delta-front deposits (see detailed stratigraphic analysis in Watney et al., 1989, and brief discussion in Holterhoff, 1997a). Local and regional scale lithologic variation, coupled with structural deformation (e.g., Rascoe, 1975) makes precise stratigraphic interpretations and correlations within the Barnsdall Formation quite difficult. For instance, lowstand incised channels and prograding deltas serve as antecedent topographic lows and highs, respectively, and profoundly influence later deposition (i.e., younger deltaic wedges accumulating between older deltaic wedges; lowstand incised valleys serving first as catchments for deep-water turbidites and later as funnels for deltaic progradation [P. F. Holterhoff, pers. comm., 2010]).

At the study area, part of the middle portion of the Barnsdall Formation is exposed at a hillside outcrop located roughly 4 km northeast of Copan (Fig. 1B). Here, the transition from lower core shale to upper core shale facies, and eventually to regressive, shallow marine facies, is recorded (Fig. 5). The lower core shale is represented by a thin unit of dark gray, platy, phosphatic, sparsely fossiliferous shale containing a distinctly dysaerobic molluscan fauna (Boardman et al., 1984); this unit correlates to the Eudora Shale Member of the Stanton Formation (Heckel, 1978; Holterhoff, 1997a). This is transitionally overlain by the upper core shale facies, represented by a green to gray, thoroughly bioturbated, densely fossiliferous mudstone

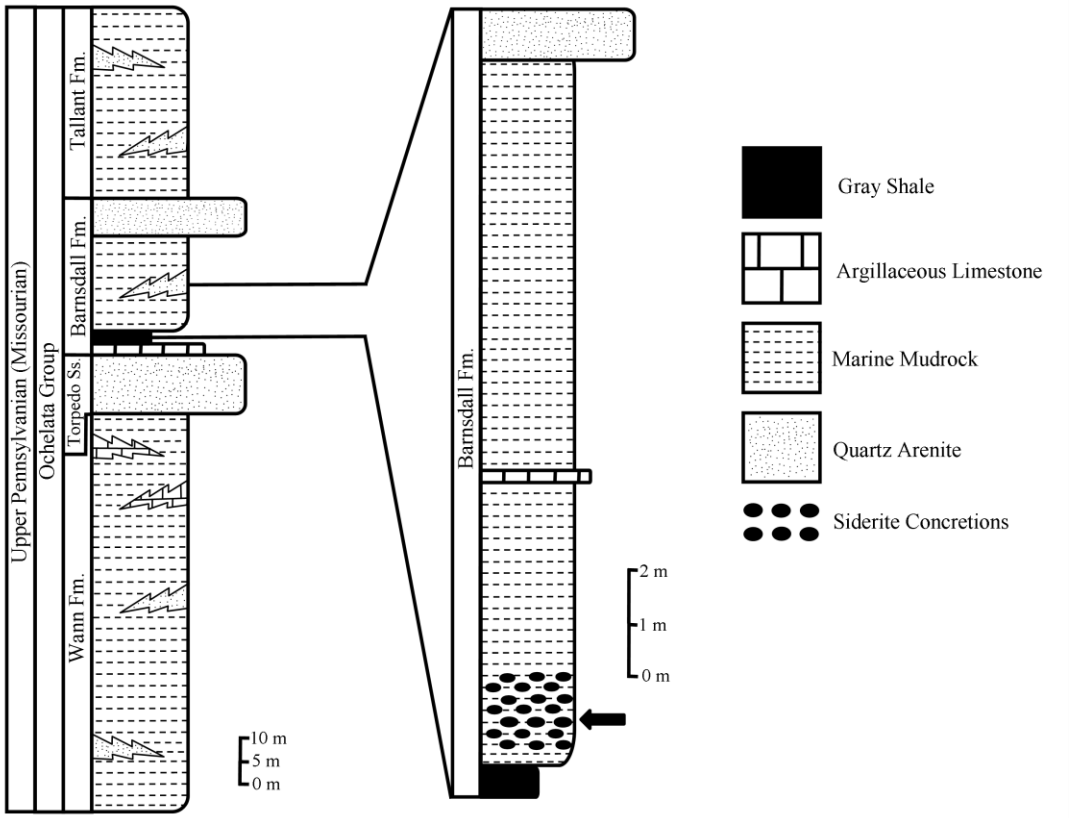

FIGURE 5—General regional stratigraphy of northern Washington County, Oklahoma (left) and stratigraphy of hillside exposure near Copan (right). The arrow marks the location of the Lagerstätte. Although mudrocks are undifferentiated in this figure, sediments near the arrow are densely fossiliferous, with overlying mudrocks generally barren (see text for further explanation). Data derived from Oakes (1940), Tanner (1956), Rascoe (1975), and P. F. Holterhoff (pers. comm., 2010).

containing abundant siderite concretions and a diverse benthic fauna, including the thin horizons containing articulated crinoid fossils. This facies is overlain by a thick sequence of nonfossiliferous silty sandstones and sandy shales representing relatively shallow shelf environments, with well-sorted quartz sandstone representing proximal delta deposits capping the sequence (P. F. Holterhoff, pers. comm., 2010).

PREVIOUS WORKS

The history of research at the Copan site begins in the 1940's, when Harrell Strimple collected a number of crinoid specimens he found weathering out of the hillslope. He termed this site the Tank Dike Locality, named after the petroleum storage tank that had once been there, and whose emplacement had resulted in excavation of the hillslope and consequent exposure of the articulated crinoids. Several new crinoid taxa were described (Strimple, 1949a, b, 1950, 1951, 1952, 1977; Moore and Strimple, 1969), although some were later synonymized. Strimple collected from the site for decades and suspected that the well-preserved crinoid specimens were originating from a single source layer, but was never able to locate it, and instead continued to describe specimens not found in place.

The site was re-discovered in 1984 by Daniel Mosher, a professor at nearby Bartlesville Wesleyan College. As an amateur fossil collector, Mosher was familiar with Strimple's research, and began to visit the Tank Dike Locality as his time permitted. After finding several intact crinoid crowns weathering out of the slope, he searched for the source bed by marking the location of each well-preserved crinoid specimen he found with a penny. Eventually, the location of the highest pennies allowed the recognition of a thin interval of very poorly indurated mudstone that appeared to be producing the crinoids. Mosher collected this 5-8 cm layer with a trowel and buckets over a period of five and a half years, sieving the mudstone over a 3-mm screen and saving all fossil

material recovered. Approximately 1021 kg (~2250 lbs) of material was sieved, producing over 1057 crinoid cups and crowns over an area of roughly 11.9 square meters (~128 square feet; D. Mosher, unpublished data). This sieving technique, although effective at recovering all but the most minute fossil material, was destructive, resulting in the loss of information on spatial relationships between fossil material, fossil associations, orientation patterns, and microstratigraphic features within the crinoid-bearing unit. In addition, it contributed to disarticulation of delicate crinoid modules such as intact columns and particularly fragile crowns; the columns would be reduced to a collection of pluricolumnals, while crowns would be separated from their associated stems and/or distal arms.

After the recognition of the Copan crinoid fauna's paleontologic significance, examination of the site without mudstone disaggregation was deemed necessary, and an excavation phase was initiated in 1992. A backhoe was used to remove the overburden and expose the crinoid-bearing layer along with beds immediately overlying it. This allowed researchers to examine fossils in position and obtain information on the lithology and stratigraphy of matrix sediment. An archaeological-style grid was established in order to map the positions of newly discovered fossils, and any crinoid fossils were carefully examined for associated elements (e.g., stems were traced to see if cups or crowns were attached).

Pabian (1987) and Pabian et al. (1995) presented a preliminary report of the systematics of crinoid taxa recovered from the Copan locality, with a further revised list of crinoid taxa included within Lewis et al. (1998). An updated list of crinoid taxa is given in Table 1. Forty-four genera and 50 species are currently recognized from this

TABLE 1—Crinoid taxa recovered from the Copan deposit. Derived primarily from unpublished data by R. K. Pabian, but modified following Moore and Teichert (1978) and Lewis and Strimple (1990).

- Subclass Camerata
  - Family Dichocrinidae
    - *Dichocrinus* sp. cf. *D. nola*
  - Family Acrocrinidae
    - *Dinacrocrinus elegans*
- Subclass Disparida
  - Family Allagecrinidae
    - *Kallimorphocrinus copani*
    - Gen. and sp. undet.
- Subclass Cladida
  - Family Codiacrinidae
    - *Lecythiocrinus* sp. cf. *L. ollicuaeformis*
  - Family Scytalocrinidae
    - *Melbacrinus* sp.
    - *Hypselocrinus littlecaneyensis*
  - Family Blothrocrinidae
    - *Elibatocrinus leptocalyx*
  - Family Pelecocrinidae
    - *Exoriocrinus* sp. cf. *E. rugosus*
  - Family Laudonocrinidae
    - *Laudonocrinus subsinatus*
  - Family Stellarocrinidae
    - *Stellarocrinus virgilensis*
    - *Celonocrinus* sp. cf. *C. angulatus*
    - *Copanicrinus platulus*
  - Family Pachylocrinidae
    - *Plummericrinus* sp.
  - Family Anobascicrinidae
    - *Sciadiocrinus* sp. A
    - *Sciadiocrinus* sp. B
    - *Sciadiocrinus* sp. C
  - Family Decadocrinidae
    - *Clathrocrinus clathratus*
    - *Glaukosocrinus* sp.
    - *Trautscholdicrinus carinatus*
  - Family Cromyocrinidae
    - *Aglaocrinus* sp. cf. *A. compactus*
    - *Terpnocrinus* sp.
    - *Ulocrinus* sp. cf. *U. buttsi*

TABLE 1, **continued—**Crinoid taxa recovered from the Copan deposit. Derived primarily from unpublished data by R. K. Pabian, but modified following Moore and Teichert (1978) and Lewis and Strimple (1990).

Family Erisocrinidae
Erisocrinus typus
Family Diphuicrinidae
Graffhamicrinus sp.
Family Catacrinidae
Delocrinus subhemisphericus
Family Apographiocrinidae
Apographiocrinus typicalis
Contocrinus sp. cf. *C. stantonensis*
Family Pirasocrinidae
Perimestocrinus granuliferus
Plaxocrinus crassidiscus
Plaxocrinus sp.
Polygonocrinus baumani
Stenopecrinus planus
Triceracrinus spinosus
Triceracrinus sp. cf. *T. altamontensis*
Vertigocrinus parilis
Gen. sp. undet.
Family Galateacrinidae
Galateacrinus ornatus
Galateacrinus sp. cf. *G. allisoni*
Amphitriticrinus acis
Amphitriticrinus poolerensis
Family Cymbiocrinidae
Aesiocrinus detrusus
Allosocrinus bronaughi
Halogetocrinus sp. cf. *H. paucus*
Family Exocrinidae
Exocrinus multirami
Subclass Flexibilia
Family Synerocrinidae
Euonychocrinus magnus
Gen. and sp. undet.
Family Mespilocrinidae
Cibolocrinus detectus
Family Dactylocrinidae
Aexitrophocrinus washingtonensis
Family Euryocrinidae
Paramphricrinus oklahomaensis

locality, making this Lagerstätte the most diverse crinoid deposit recognized throughout the global Pennsylvanian System. Despite the tremendous diversity, the vast majority of specimens are represented by a few dominant genera; Lewis et al. (1998) report that approximately 81% of individuals belong to four genera, in descending order: *Exocrinus multirami*, *Apographiocrinus typicalis*, *Kallimorphocrinus copani*, and *Erisocrinus typus*. Most of the crinoids recovered from this deposit belong to the subclass Cladida, which is not unexpected, as cladid and disparid crinoids comprise the dominant portion of global crinoid diversity during the late Pennsylvanian (e.g., Holterhoff, 1997b; Simms, 1999). The high alpha diversity, although remarkable, is also not entirely unexpected. Holterhoff (1997b) documented the evolutionary paleoecology of crinoids through the Paleozoic, noting that the Pennsylvanian was a period characterized by maximum diversity in offshore shelf settings, reflecting the transition of stalked crinoids from shallow carbonate hardground encrusters inhabiting reef and shoal settings to soft substrate dwellers following the loss of the extensive Mississippian epeiric seas, coupled with the range expansion of deep basinal taxa to slightly shallower environments. Furthermore, the majority of crinoid taxa are relatively small and unornamented, fitting with observations made by Pabian and Strimple (1970, 1979, 1985, 1993) and Heckel and Pabian (1981), who noted that diverse assemblages of diminutive crinoids are common in offshore facies in the North American midcontinent, and were interpreted to represent colder water faunas. These differ markedly from lower diversity assemblages of large, robust, ornamented crinoids found in coeval nearshore environments.

Holterhoff (1988, 1997a) studied the comparative crinoid paleoecology of the various facies within the Barnsdall-correlative Stanton Formation, including the Copan

site as one of his data sources. He recognized a great deal of diversity in crinoid feeding strategies (as reflected by arm morphology), indicating a trophically diverse and strongly tiered fauna. This interpretation, in addition to lithologic evidence, suggested stable, moderate, unidirectional currents typical of that operating in basinal to distal shelf environments. Based on the transitional contact with underlying dysaerobic sediments, Holteroff (1997a) postulated that the Copan fauna may have experienced some degree of oxygen stress. Most importantly, Holterhoff (1988, 1997a) noted that most of the crinoid taxa present at the Copan Lagerstätte were present in other facies within the Barnsdall Formation or coeval units, but the relative abundance of key taxa defined different biofacies. The Copan site was unique from the standpoint of biofacies because of the dominance of *Exocrinus* and *Apographiocrinus*, despite the presence of these taxa in shallower and deeper facies; *Exocrinus* was reported only from shallower facies in this study (Holterhoff, 1997a) but was reported in lower core shale facies by Boardman et al. (1984). This observation means that transportation of exotic crinoids into the deeper facies represented by the Copan deposit would be relatively difficult to recognize by analysis of crinoid occurrence alone.

Pabian et al. (1997) studied biotic interactions preserved on macrofaunal remains from the Copan site, focusing heavily on interactions involving crinoids. A number of forms of interaction were documented on crinoid fossils, including interactions that occurred prior to death, such as parasitism, predation, and commensalism (including the presence of coprophagous platyceratid gastropods), as well as after death (e.g., encrustation). These indicate a diverse and ecologically healthy environment, most likely enriched by the presence of the crinoids themselves (Meyer and Ausich, 1983), and the

presence of post-mortem encrusters indicates oxygenated conditions and low sedimentation rates. In addition, genus-level variations in biotic interaction were noted, as certain taxa appeared more prone or more resistant to specific forms of interaction (i.e., certain species were generally devoid of all signs of parasitism or encrustation). These patterns, although relatively poorly understood, are consistent with trends observed in crinoids from the Stanton Formation in Kansas (Pabian, 2003) and may reflect the presence of host-specific parasites, crinoids that are repulsive in some way to other organisms, or preferential consumption of certain taxa over others, either by predators or scavengers. These variations have important taphonomic implications, as differences in organismal interactions between crinoid taxa may shed light on patterns of preservation, particularly at the genus or species level.

Lewis et al. (1998) summarized the results of the excavation phase with regard to taphonomy, making the significant observation that articulated crinoid fossils are present at two thin horizons overlying the interval sampled by Mosher. Although considerably less productive than what was termed the Main Crinoid Bed, these overlying beds (Bed 1 and Bed 3) yielded articulated crowns, cups, and considerable lengths of column in noticeably greater abundance than the interbedded, more barren mudstone units (Fig. 6). Associated with the articulated crinoid fossils, and concentrated in the Main Crinoid Bed, Bed 1, and Bed 3, are siderite concretions, which mark the horizons in outcrop. The presence of such abundant siderite was crucial to locating these beds in the field (Lewis et al., 1998), as all units are otherwise lithologically homogeneous. After several years of fieldwork within this framework, little more than 100 new crinoid cups and crowns were discovered, suggesting that the majority of the crinoid specimens in the area had been

recovered by Mosher; in addition, the margins of the excavated area were examined for articulated crinoid fossils with little success, indicating that the geographic extent of crinoid-rich sediments near Copan is limited to the area sampled by Mosher and exposed by removal of overburden (Lewis et al., 1998).

Orientations of fossils within the Main Crinoid Bed were mapped by Lewis et al. (1998), but no clear patterns were observed (Fig. 7), indicating that the event responsible for the preservation of articulated crinoids was not accompanied by exceptionally strong unidirectional or bidirectional currents. The discovery of distal portions of crinoid columns with pronounced tapering and intact radicular cirri typical of crinoid adaptations for life in soft, muddy substrates (Seilacher and MacClintock, 2005; Fig. 8), in addition to productid brachiopods in living position with delicate spines still attached and burrowing bivalves preserved in living position, led to the recognition that at least some, if not most, of the fauna is autochthonous to parautochtonous. Siderite concretions were interpreted as early diagenetic, based on relationships with fossils and surrounding sediment (see Maples, 1986, for some indicators of diagenesis in mudrocks). Stable isotopic analysis of concretions from the Main Crinoid Bed indicated that methanogenesis was not responsible for concretion genesis (but see Whiticar et al., 1986), and that early suboxic diagenesis in the shallow subsurface led to siderite precipitation.

Based on the presence of abundant endobenthic macrofauna, evidence for thorough bioturbation, and light-colored lithology, anoxia was ruled out as a killing mechanism for the articulated crinoids. Instead, rapid burial (obrution) was put forth as both a killing and preservation mechanism, as echinoderms are particularly prone to death by burial in fine-grained sediment, which serves to clog the ambulachral grooves

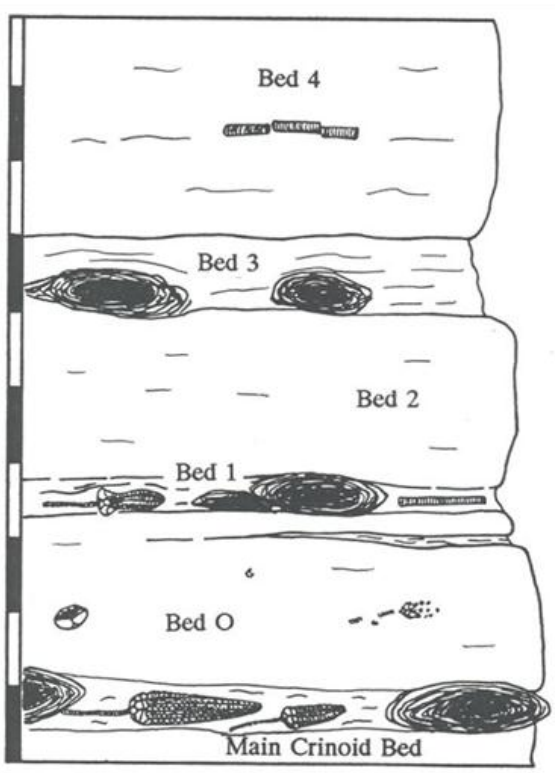

FIGURE 6—Preliminary microstratigraphy of the Copan deposit from Lewis et al. (1998) showing alternations between beds containing articulated crinoids and siderite concretions and beds containing sparse, disarticulated crinoid remains. Scale bars represent 5 cm.

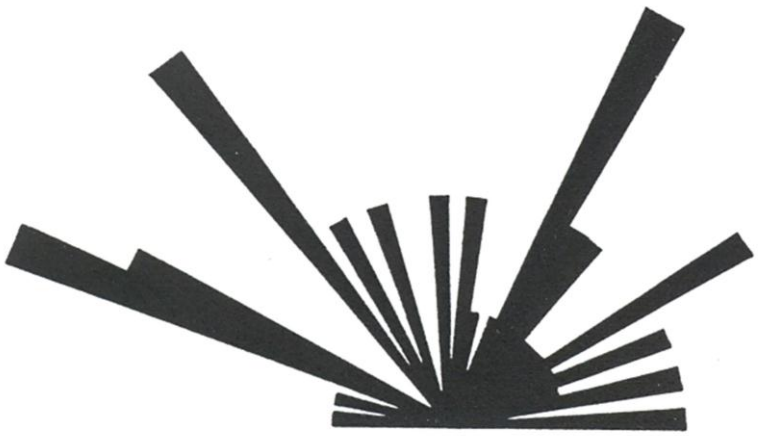

FIGURE 7—Rose diagram of fossil orientations (N = 46) measured within the Main Crinoid Bed by Lewis et al. (1998). Note the lack of a strong unimodal or bimodal pattern.

FIGURE 8—Distal portion of crinoid column recovered from the Main Crinoid Bed. Note the pronounced taper toward the distalmost end and the attached cirri marked by arrows. This specimen provides good evidence that at least some of the well-preserved crinoid specimens represent autochthonous or parautochthonous individuals. Scale bar = 2 cm.

and essentially asphyxiate the organism (Rosencranz, 1971; Shäfer, 1972; Brett and Seilacher, 1991). However, no evidence for discrete rapid burial events associated with storms or turbidity currents, such as graded beds, tool marks, groove casts, scour-produced firmgrounds, hummocky cross-stratification (e.g., Kreisa, 1981; Kreisa and Bambach, 1982; Aigner, 1985), or even coarser deposits preserved as burrow-fill sediment (the "tubular tempestites" of Tedesco and Wanless, 1991), were recognized, indicating that rapid burial of crinoids was likely accomplished by locally derived sediment that would be indistinguishable from background sedimentation. This, coupled with pervasive biogenic mixing, left the articulated crinoid skeletons themselves as the only evidence of rapid burial events (Lewis et al., 1998).

OBJECTIVES

Despite the success of previous investigations of the Copan Lagerstätte in recognizing significant stratigraphic relationships, identifying the taxonomic affinities of the diverse crinoid assemblage, and interpreting the paleoecologic and taphonomic characteristics of the macrofaunal assemblage, no research to date has focused on the physical, biological, and geochemical mechanisms responsible for the genesis of this deposit. This information, in turn, may shed light on some of the relationships between crinoid diversity, crinoid preservation, and paleoenvironment, as well as reveal the causes and implications of the alternation between thin crinoid/siderite beds and thicker "barren" beds.

Therefore, the objectives of this research project are to (1) re-investigate previous paleoecological interpretations, allowing the state of the environment prior to, as well as immediately following, the event or events responsible for crinoid mortality to be determined; (2) obtain an understanding of the nature of the killing mechanism and its immediate taphonomic effects on the crinoid assemblage; (3) unravel the complicated post-event taphonomic history of the deposit; and (4) identify the cause of the apparent cyclicity present within this densely fossiliferous interval. These data will then be integrated into a model for the genesis of the Lagerstätte that incorporates all available sedimentologic, stratigraphic, taphonomic, paleoecologic, and geochemical information.

These goals were accomplished through analysis of material recovered from the

site by previous researchers during the time period between 1984 and 1998. In particular, research has focused on four sources: field notes and videotapes recorded during excavation of the site, which allow a detailed microstratigraphic section to be constructed and patterns of fossil distribution and orientation to be recognized; mudstone samples collected from various horizons during the excavation phase and the fossil material within these samples; crinoid specimens, including both Mosher's initial collection from the Main Crinoid Bed and specimens from all horizons discovered during the subsequent excavation; and siderite concretions from all horizons, with particular emphasis on the large concretions within the beds yielding articulated crinoids.

MICROSTRATIGRAPHIC ANALYSIS

Methods

Previous investigations have been successful at placing stratigraphic constraints on the location of the Copan crinoid Lagerstätte, as discussed previously. However, the occurrence of articulated crinoid fossils at three separate horizons (Main Crinoid Bed, Bed 1, and Bed 3) within a single 50-cm interval and without a documented cause (Lewis et al., 1998) highlights the need for detailed microstratigraphic analysis of the fossiliferous section. Subtle shifts in the properties of fossils and their enclosing sediment may hold the key to understanding the nature of the events responsible for crinoid preservation as well as determining the underlying cause of the repetition of crinoid/siderite beds. Unfortunately, the exposure containing the crinoid Lagerstätte is not partially filled and overgrown and is on private property; as a result, the crinoid-bearing horizons are no longer available. Although taking direct measurements in the field is now impossible, some of the necessary information can be revealed through careful scrutiny of video recordings, field notes, and still photographs taken during fieldwork conducted from 1994 to 1998.

These sources, particularly the videotapes, which total over five hours in duration, were studied in detail, with information retrieved from direct observation of images, comments made by recorded individuals, and references to still photographs of significant features, which were then examined. In addition, observations made by R. D.

Lewis and P. F. Holterhoff were available through consultation. For all of these media, I cross-checked and recorded the stratigraphic location and taphonomic state of each crinoid fossil. The morphology, size, and stratigraphic location of siderite concretions were noted, as well as any other potentially significant macrofossils and lithologic features. Measurements of individual units were obtained by paying close attention to scale objects visible in images, as well as the observations and notations of field workers; thickness values were evaluated by comparison with available mudstone blocks.

Analysis of mudstone slabs provided a great deal of information to supplement and verify patterns observed in these field records. However, because the slabs used for microstratigraphic studies are the same as those used for fabric analysis, they are discussed in the following chapter. Collectively, these data were used to construct a centimeter-scale microstratigraphic section for the half-meter of strata containing the three crinoid-bearing horizons. For the purposes of consistency, terminology of this stratigraphic section follows that of Lewis et al. (1998) shown in Figure 6.

Results and Discussion

Centimeter-scale microstratigraphy for the approximately 50-cm interval containing the articulated crinoids, based on data derived from both field notations and mudstone blocks, is shown in Figure 9. This stratigraphic column is an idealized representation; in reality, there is a great deal of heterogeneity in individual unit thickness and, in some cases, unit character (see below). Horizons measured in the field frequently had a pinch-and-swell geometry, likely resulting from anisotropy within the very strongly compacted sediment. As a result, thicknesses given in Figure 9 are typical and representative, but

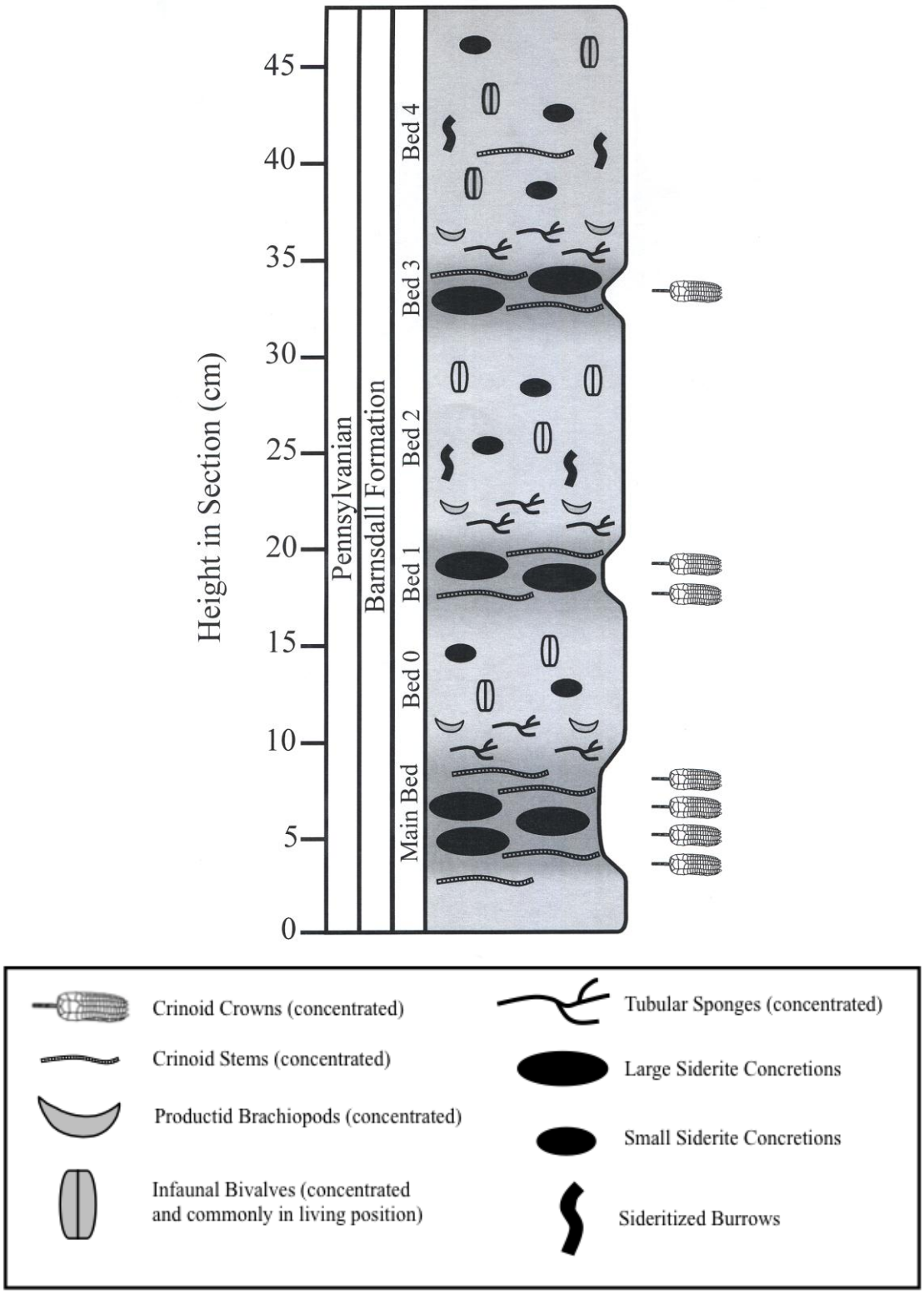

FIGURE 9—Microstratigraphic column of studied interval. Note that fossil symbols represent concentrations of depicted organisms, not simply occurrences. See text for detailed explanation.

not necessarily identical to any particular site within the excavated area.

A number of consistent macroscopic patterns are also apparent, the most striking of which, first noted by Lewis et al. (1998), is the alternation between (1) thinner units easily recognized by the presence of abundant articulated crinoid skeletons and large siderite concretions (Main Crinoid Bed, Bed 1, and Bed 3), and (2) thicker units characterized by small siderite concretions, numerous endobenthic mollusks, and an absence of abundant articulated crinoid material (Bed 0, Bed 2, and Bed 4). The various lines of evidence supporting the distinction between these two repeating units are discussed individually below, accompanied by a brief discussion of paleoenvironmental or paleontologic implications. Note also that the microstratigraphic patterns of siderite concretion morphology will be discussed in a separate section, but are also used in differentiating between the thinner and thicker units.

Biofacies

All units shown in Figure 9 are rich in fossil material, and several particularly common fossil types, including fenestrate bryozoan fronds, productid brachiopod shells, tubular sponges, bivalve shell debris, and disarticulated crinoid debris, are ubiquitous throughout the section. There are, however, notable differences in the relative abundances of these skeletal components. The thinner units are dominated by a diverse assemblage of crinoids, a diverse assemblage of articulate brachiopods, particularly productids, and fenestrate bryozoans. Secondary faunal elements include tubular sponges, scaphopods, and regular echinoid spines, with inarticulate brachiopods and bivalve mollusks as present, but relatively rare. In contrast, the thicker units are

dominated by bivalve mollusks, with tubular sponges, scaphopods, inarticulate brachiopods, and fenestrate bryozoans as secondary faunal components.

The distinction between these two biofacies has significant paleoecologic implications. With thinner units characterized by an epibenthic, sessile biofacies, an environment with stable, low turbidity, low sedimentation conditions must persist in order to permit suspension feeding by the abundant crinoids, articulate brachiopods, and bryozoans. The subsequent development of a biofacies dominated by an endobenthic, vagile molluskan fauna indicates a transition to an environment conducive to deposit feeding. This transition commonly occurs as a result of increased sedimentation rate, which serves to exclude suspension feeders by interfering with their particle capture apparatuses (e.g., clogging filtration fans), while simultaneously increasing the amount of particulate organic matter brought into the environment.

Taphofacies

Taphonomic analysis of many fossiliferous units, including Lagerstätten, has revealed that fossil assemblages are often composed of two distinct assemblages: the event assemblage, representing individuals preserved through episodic rapid burial events, and the background assemblage, comprising multiple generations of skeletal remains contributed to the seafloor sediment over long periods of normal sedimentation (Speyer and Brett, 1991). Consequently, these two assemblages have contrasting taphonomic signatures. The event assemblage is characterized by such features as articulated multi-element skeletons, organisms in living position, and preserved microstructural details of skeletal material; whereas the background assemblage shows

evidence of considerable time in the taphonomically active zone, with typical features including completely or primarily disarticulated multi-element skeletons, organisms in orientations and positions not adopted during life, skeletal elements in a generally degraded condition (e.g., corroded, abraded, fractured, corraded), and delicate fossils or features completely destroyed (Speyer and Brett, 1991; see also Brett and Baird, 1986a and Speyer and Brett, 1986).

Both assemblages are present within both the thinner and thicker units of the section under study here. The event assemblage of the thinner units is dominated by articulated crinoid remains, represented by both complete and partial crowns and long columns (see Fig. 2). In addition to crinoidal material, the thinner units also contain numerous productid brachiopods retaining surface ornamentation and, in some cases, featuring attached spines and preserved in living position; and particularly abundant and large fronds of fenestrate bryozoans found intact as flat-lying to slightly undulose sheets. These well-preserved fossils provide evidence of rapid burial by fine-grained sediment. The background assemblage of thinner units consists of isolated crinoid ossicles representing completely disarticulated individuals, regular echinoid spines, fragments of fenestrate bryozoan zoaria, degraded and commonly broken scaphopod, brachiopod, and bivalve material, and portions of tubular sponges.

Although there is considerable similarity between the event and background assemblages in these units, a significant discrepancy is represented by the conspicuous absence of any mobile fauna within the event assemblage. Although the delicate spines and plates of regular echinoids (*Archaeocidaris* sp.) are moderately common constituents of sediment within the thinner units, not a single intact or even partial specimen has been

discovered, despite their slow locomotion. Likewise, despite the presence of scaphopods and bivalves in the Main Crinoid Bed, Bed 1, and Bed 3, these organisms invariably display evidence of considerable exposure at the seafloor and are never preserved in living position. This is strong evidence that the burial events responsible for preservation of the articulated crinoids (and associated fauna), although rapid, resulted in beds sufficiently thin to allow the escape of mobile fauna and only entomb stationary organisms such as crinoids, articulate brachiopods, and bryozoans. The presence of an associated background assemblage indicates that these burial events were separated by long periods of normal sedimentation, resulting in little net sediment accumulation.

The event assemblage in thicker units is very different from that described above. Very few articulated crinoid crowns were recovered from Bed 0, Bed 2, and Bed 4, and although some relatively long columns were observed in these horizons, they were overwhelmingly within the lower 3-5 cm of each unit. Instead, the event assemblage is dominated by large, thin-shelled endobenthic bivalves preserved articulated and in living position, as well as scaphopods and productid brachiopods preserved in living position (Fig. 10). Some large fenestrate bryozoan fronds are present as well, although they are not as numerous as those in the Main Crinoid Bed, Bed 1, and Bed 3. The background assemblage in thicker units is fairly similar to that of the thinner units, with crinoid ossicles, tubular sponge fragments, fenestrate bryozoan fragments, and degraded and/or broken material from bivalves, scaphopods, and acrotretid (inarticulate) brachiopods.

The presence of numerous endobenthic mollusks preserved as part of the event assemblage is very significant, as these organisms are not only mobile, but are adapted for proficiency at moving vertically through sediment. Furthermore, bivalve functional

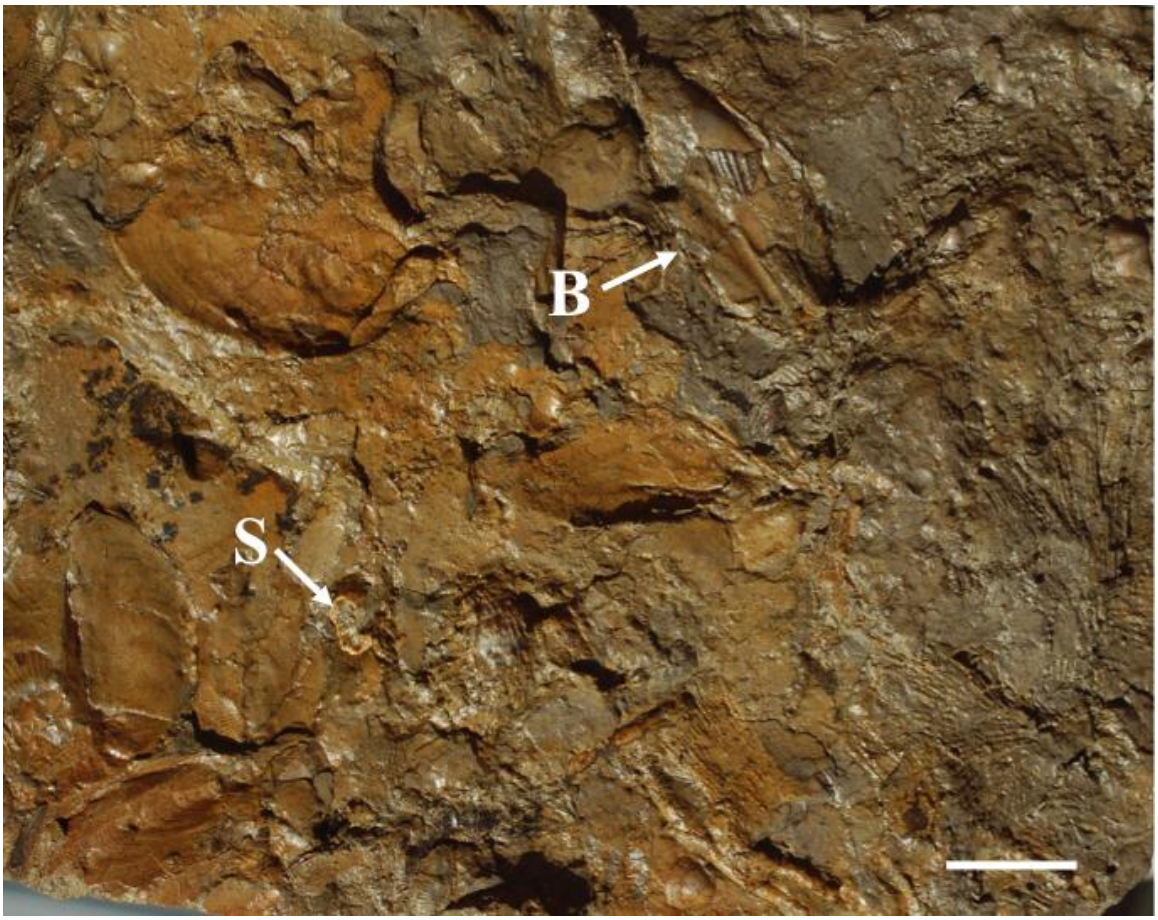

FIGURE 10—Representative event assemblage from thicker units. This slab, recovered from Bed 2, is dominated by mollusks, in sharp contrast to the primarily non-molluskan assemblage from the thinner units. The S marks a scaphopod in living position and the B marks a large bivalve preserved in living position. The presence of these efficient burrowers in living position indicates a thick, rapidly deposited sediment blanket. Note also the numerous molluskan (mytiloid?) organisms on the left side of the picture. Scale bar = 2 cm.

morphology (i.e., anterior-posterior elongation, thin valves) indicates that these are moderately deep burrowers (Stanley, 1970), capable of escaping rapidly deposited sediment, especially the thin sediment blankets typical of the thinner units (Kranz, 1974; Peterson, 1985). The inability of the bivalves to escape this sediment blanket reflects a markedly increased thickness of event layers capable of entombing not only the few epibenthic organisms, but the more common endobenthic organisms as well. The orientation of these bivalves is unlikely to be the result of post-mortem reworking, as the rapid decay of the adductor muscles creates a tendency for the shell to splay open at the hinge rather than remain articulated (Allmon, 1985). Thus the thinner and thicker units are distinct not only in terms of the dominant organisms preserved (see above), but also in the nature of rapid burial events. The evidence for increased sedimentation rates and thicker burial events appear to indicate an environment closer to a sediment source area for Bed 0, Bed 2, and Bed 4.

Ichnofabrics and Lithologic Properties

Much of the ichnofabric and lithologic data come from fabric analysis and will be discussed in greater detail in the following section. However, a few major distinctions are relevant to the microstratigraphic framework established for the Copan section. Ichnofabrics are essentially identical in both the thicker and thinner units, and are characterized by a lack of discrete large biogenic sedimentary structures of any kind. However, the sole exception to this is the presence of relatively uncommon, fairly large diameter, sideritized burrows found consistently within the lower portion of Bed 2 and the middle portion of Bed 4 (Fig. 11). Burrow morphology is difficult to ascertain, as the

FIGURE 11—Sideritized burrows from the thicker units. A) In place burrow from the bottom of Bed 2. Scale bar = 1 cm. B) Burrow recovered as float. Note the branching at the bottom of the specimen and the fracturing, resulting from weathering. Scale bar = 1 cm.

burrows tend to fracture into segments that weather out of the outcrop individually. Branching is observed on some specimens (Fig. 11B), and there is considerable variation in burrow orientation, with subvertical, subhorizontal, and even seemingly spiriform orientations observed (R. D. Lewis, pers. comm., 2009).

The preferential sideritization of these biogenic structures indicates a major porosity difference between burrow-filling sediment and the surrounding sediment into which the structure was excavated. In addition, a large burrow would have been highly unstable in muddy, fluid-rich sediment such as that indicated for the environment represented by the studied section. Both of these lines of evidence indicate that these large burrows were emplaced into firmer substrates that were briefly available. The absence of a major shift in biota or morphology (e.g., discoidal crinoid holdfasts replacing recumbent runner-type distal columns), pervasive seafloor encrustation, or reworked sedimentary material or concretions suggests that this firm substrate was unlikely to have been exposed at the sediment-water interface; instead, only the upper portion of the fluid-rich mixed layer may have been removed, permitting the deepest bioturbators to encounter partially de-watered, stiff mud that was normally too deep for excavation.

In terms of lithologic properties, a remarkable degree of similarity is observed in grain size and composition between the thinner and thicker units (Fig. 12). Seemingly, this fairly calm environment was far enough from sources of clastic sediment to be affected only by relative sedimentation rates, without any appreciable changes in grain size, even in event layers. One notable difference in macroscopic lithologic properties does exist between the thinner and thicker beds, however. The thinner beds, although

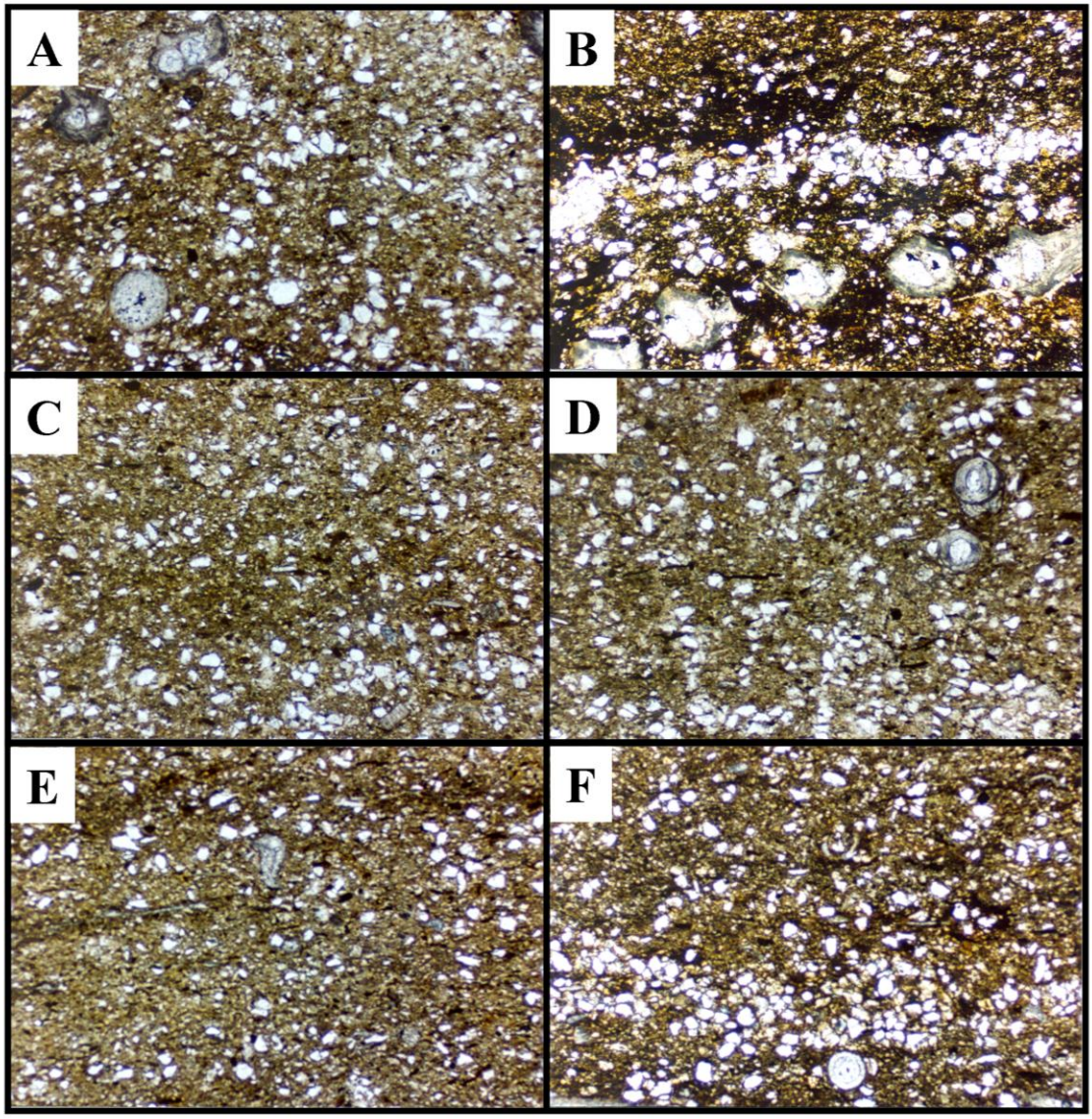

FIGURE 12—Thin sections depicting representative fabrics of intervals within the microstratigraphic section. A, B) Samples from Bed 0 immediately above the Main Crinoid Bed. C, D) Samples from the Main Crinoid Bed. E, F) Samples from below the Main Crinoid Bed. Note the similarity between all samples and the absence of primary fabric. Note also the discrete silt layer in B. Field of view in all pictures is approximately 2 mm wide. Photographs provided by R. D. Lewis.

rich in skeletal material, do not contain any distinct skeletal lags or sharply defined fossil concentrations, while the thicker units are host to numerous thin, sharply based, densely packed skeletal horizons (Fig. 13; see also thin silt layer in Fig. 12B). These appear to represent lags resulting from winnowing of fine-grained sediment during periods of increased current velocity. Some of these lags are laterally discontinuous to channelform in cross-section (see the lowermost labeled horizon in Figure 13); such features have been interpreted as subtle gutter casts in other mudstone sequences (Brett and Allison, 1998). Lag horizons are relatively common in mud-dominated shelf sequences and are frequently generated by increased energy associated with distal storm events (e.g., Aigner, 1985).

The consistent and nonrandom occurrence of two distinct structures associated with increased energy and resultant erosive effects provides strong evidence that Bed 0, Bed 2, and Bed 4 were not only characterized by higher sedimentation rates and thicker event layers, but also increased energy associated with event deposition. Evidently, the thinner units accumulated under conditions of low sedimentation punctuated by rapid burial events where a thin sediment blanket was deposited over the benthic fauna without associated scouring; the thicker units accumulated under conditions of higher sedimentation punctuated by rapid burial events where a thicker layer of sediment, accompanied by occasional winnowing and erosion, was deposited over the seafloor. Such interpretations are in agreement with the proximality trends of Aigner and Reineck (1982), Aigner (1985), and Seilacher and Brett (1991), where distal event deposits are dominated by sediment smothering with minor erosion, and distalmost events involve only deposition of thin layers.

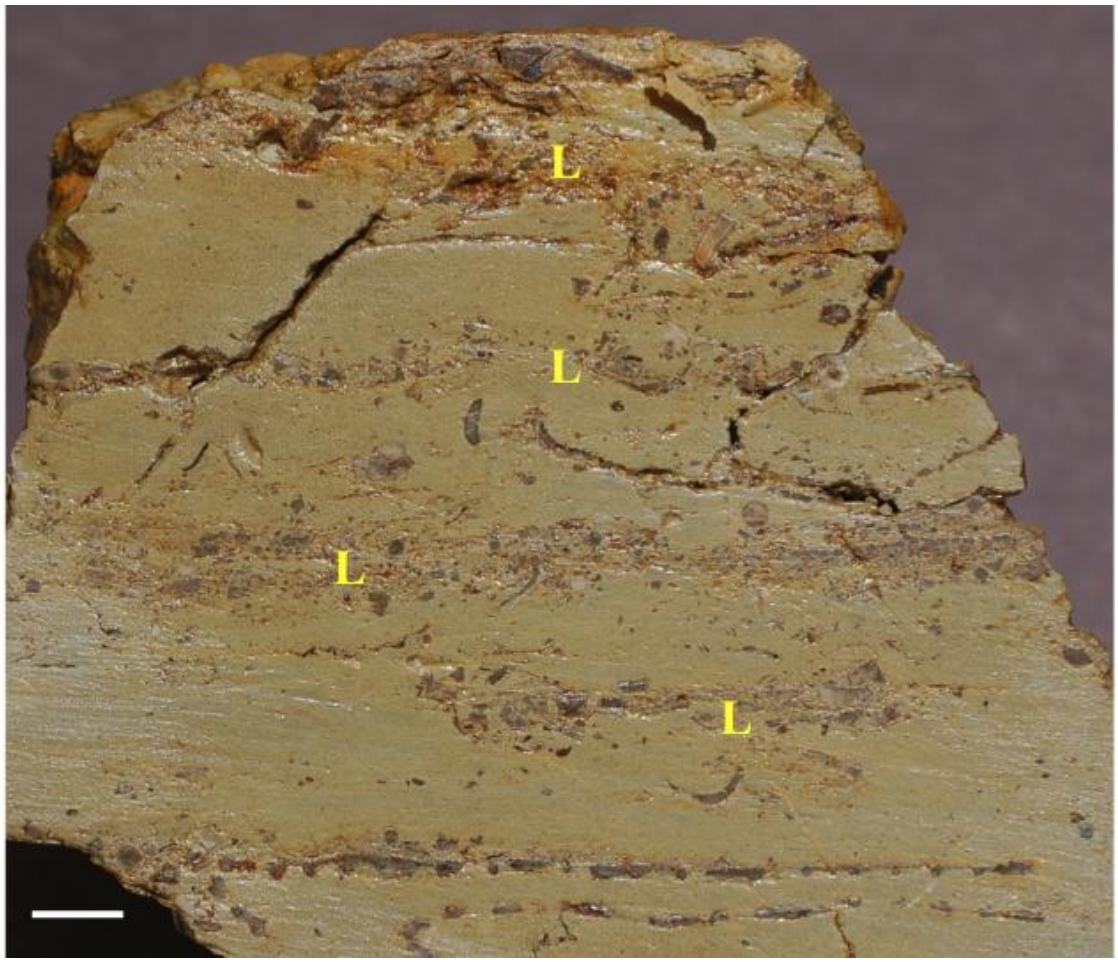

FIGURE 13—Winnowed lags (L) of concentrated skeletal material in a sample from Bed 2. Note the repetition of these horizons, representing repeated reworking. Also note the relatively sharp lower boundaries of the concentrations. Scale bar = 1 cm.

FABRIC ANALYSIS OF MUDSTONE SLABS

Methods

Lithologic samples collected during the excavation stage of the study and stored at Auburn University were used for detailed fabric analysis in order to verify measurements derived from the above sources, to supply sub-centimeter microstratigraphic data on select intervals, most notably the Main Crinoid Bed, and to provide paleoenvironmental data. Large mudstone blocks were coated with a thin layer of clear enamel and then cut perpendicular to presumed bedding with a tile saw. Such measures are necessary due to the very poorly indurated nature of the mudstone, as exposing the blocks to water or liquid lubricant would result in complete disaggregation. Samples were cut perpendicular to bedding to produce a series of slabs 5-10 cm thick, depending on the shape of the block, thereby maximizing the sediment fabric exposed per sample. Cut faces were ground against increasingly fine grades of sandpaper, typically beginning with 150 and ending with 600 grade, until all saw marks and scratches were removed. These faces were then examined, and potentially significant features were photographed and digitally magnified.

This inspection allowed comparison between samples from the same horizon and from other beds in an attempt to detect changes in biofacies, taphofacies (sensu Brett and Baird, 1986; Speyer and Brett, 1986), ichnofabrics (sensu Savrda, 1995), and lithologic properties. Attributes noted included the presence and identity of any distinct biogenic or

physical sedimentary structures; fossil identity, abundance, and taphonomic state; distribution or density of skeletal material, particularly concerning evidence of winnowing; occurrence, morphology, and size of diagenetic siderite, particularly if associated with fossils; and any recognizable changes in sediment grain size or composition.

Results and Discussion

Detailed fabric analysis of mudstone blocks has revealed a number of consistent microstratigraphic patterns not evident through evaluation of other materials, specifically concerning detailed trends within and directly above the Main Crinoid Bed. Being both the thickest of the thinner units and the most paleontologically significant horizon, the Main Crinoid Bed was the source of more bulk lithologic samples than either Bed 1 or Bed 3, allowing for detailed analysis of the bed. Thus, the Main Crinoid Bed serves as a template against which patterns observed in the other thin units can be compared. Figure 14 shows examples of fabrics from the Main Crinoid Bed; patterns evident in such samples are further described below. The same patterns are consistently observed within Bed 1 and Bed 3, although the thinness of these units makes photography of the patterns considerably more difficult.

Although the Main Crinoid Bed, Bed 1, and Bed 3 are characterized by the presence of numerous articulated crinoid crowns and large siderite concretions, these elements are actually concentrated primarily in the lower portion of the units, with the upper portions dominated by disarticulated crinoid debris and fenestrate bryozoan fronds. Scattered crowns and cups do occasionally occur in the upper parts of the horizons,

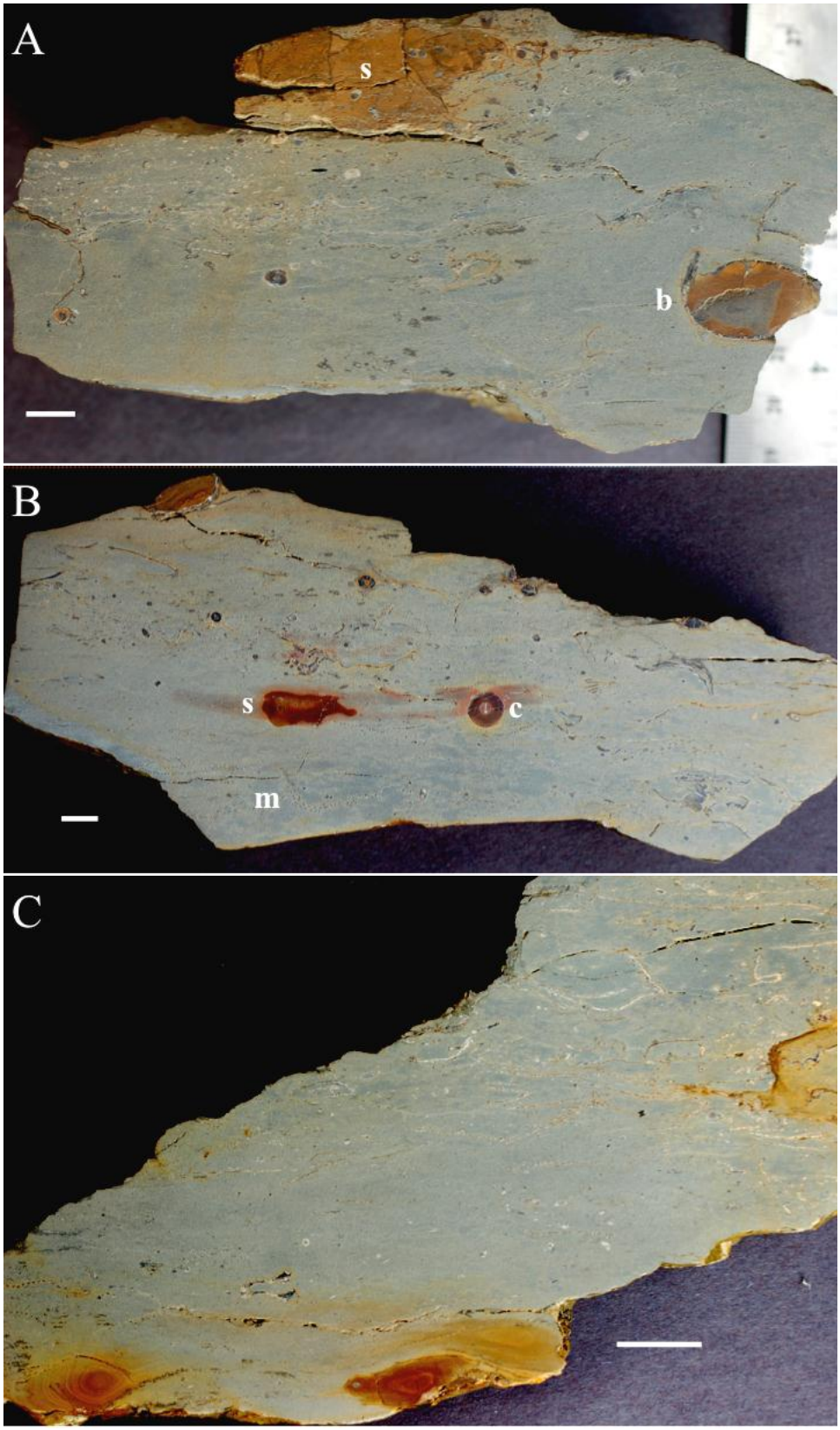
A
s
b
B
s
c
m
C

(from previous page) **FIGURE 14—**Fabric of the Main Crinoid Bed. A) Sample from lower portion containing siderite concretion (s), abundant skeletal material, and productid brachiopod in living position and infilled with siderite (b); scale bar = 1 cm. B) Sample containing irregular siderite concretion (s), large diameter crinoid columnal (c) serving as a nucleus for a siderite concretion, and pronounced mottled fabric (m); scale bar = 1 cm. C) Sample showing nearly the entire thickness of the unit. Note the siderite concretions concentrated in the lower portion and the abundant disarticulated and fragmented skeletal material higher up; scale bar = 2 cm.

however, and column segments ranging in length from short pluricolumnals to long, nearly complete columns as well as articulate brachiopods are common throughout each thin unit. Directly above this zone, at the very base of the overlying thicker beds, is a 1-4 cm horizon consisting nearly entirely of concentrated tubular sponges (Fig. 15). Overlying this zone is a 3-5 cm layer of tubular sponges and productid brachiopods, both in living and overturned orientations, and in varying degrees of completeness, ranging from intact to fragmented (Fig. 16). Above this zone is the typical mollusk-dominated assemblage described in the above sections. The upper 3-5 cm of the thicker units contain articulated columns in greater abundance than the middle, possibly reflecting sampling from the base of overlying thinner units where microstratigraphic relationships were unclear, or some sort of transition zone between thicker and thinner units.

An interesting and surprising result of fabric analysis is that the Main Crinoid Bed, Bed 1, and Bed 3, although stratigraphically thin, are not single-event beds, but rather represent the stacking of thin obrution horizons formed over an extended period of time. The strongest evidence for this interpretation is the presence of several articulated productid brachiopods in living position separated by several millimeters of sediment (Fig. 17); a similar pattern was observed with intact fenestrate bryozoan fronds. This

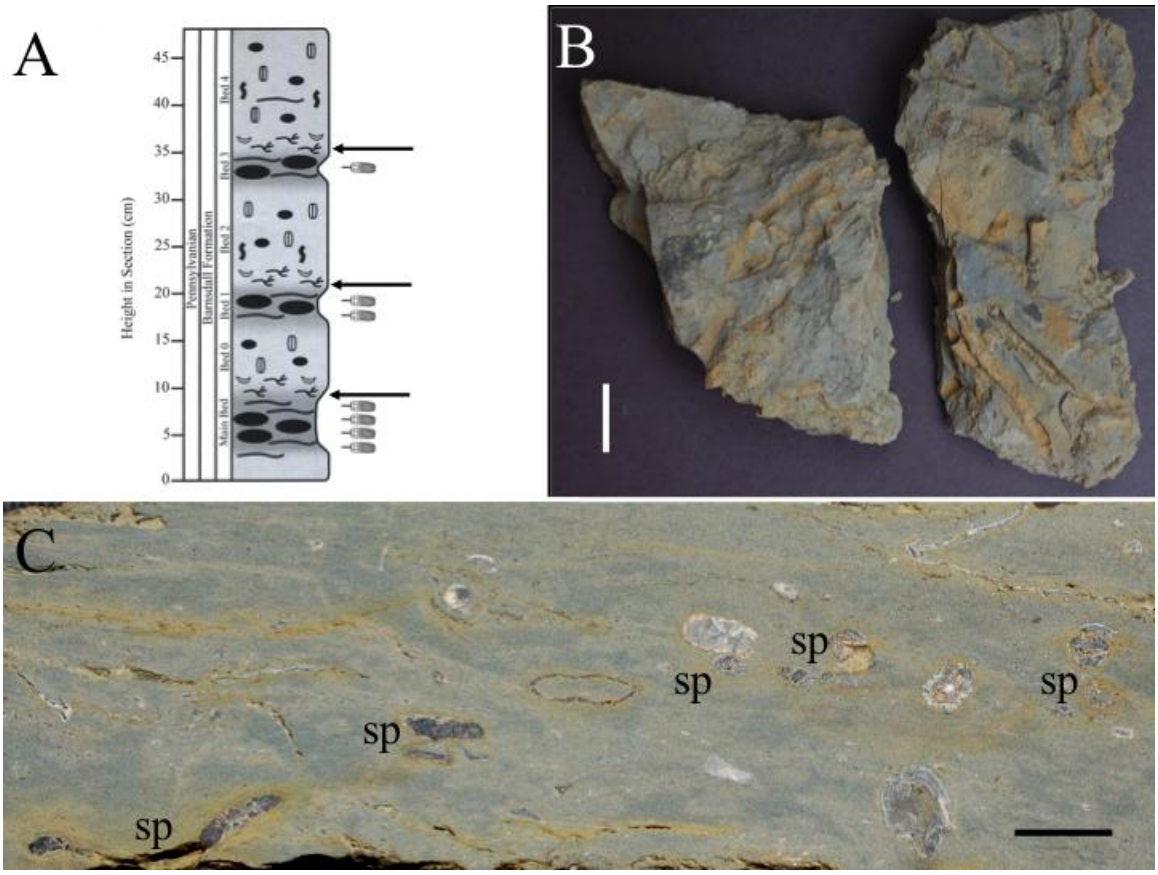

FIGURE 15—Examples of material from the sponge-rich horizons overlying the crinoid-rich units. A) Location of sponge-rich beds (arrows) in the Copan microstratigraphic section. B) Hand sample from the base of Bed 0 containing abundant tubular sponges covering bedding surface; scale bar = 2 cm. C) Fabric of sponge-rich bed from the base of Bed 2. Note the mottled texture and numerous sponge tubes in cross-section (sp); scale bar = 1 cm.

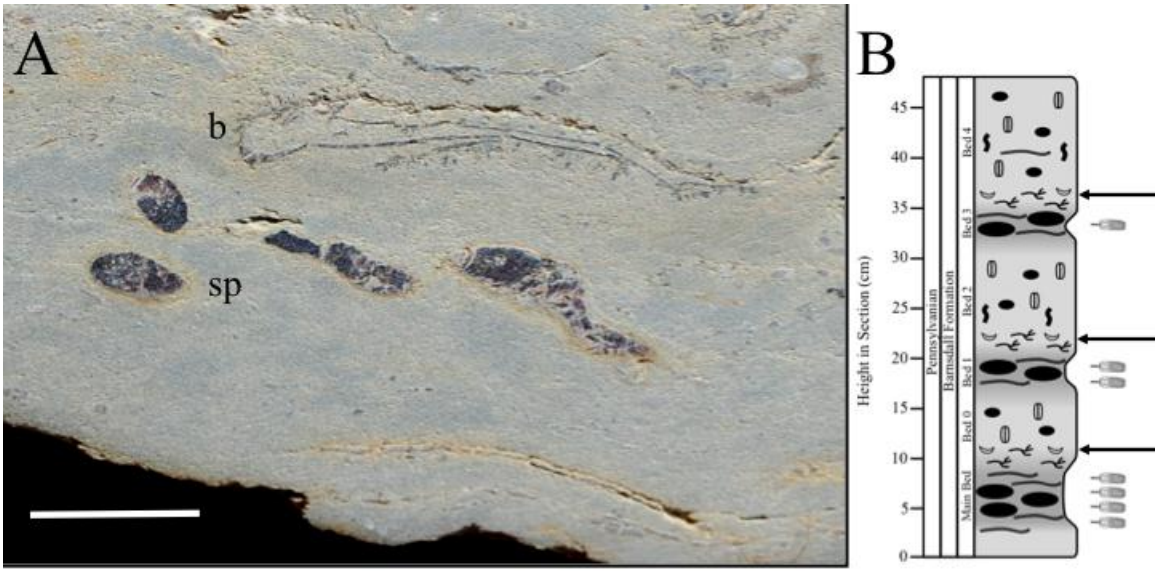

FIGURE 16—Example of material from the sponge and productid brachiopod-rich horizons overlying the thinner units. A) Fabric of sponge (sp)/brachiopod (b) bed from lower Bed 0; scale bar = 1 cm. B) Location of horizons (arrows) within the microstratigraphic section.

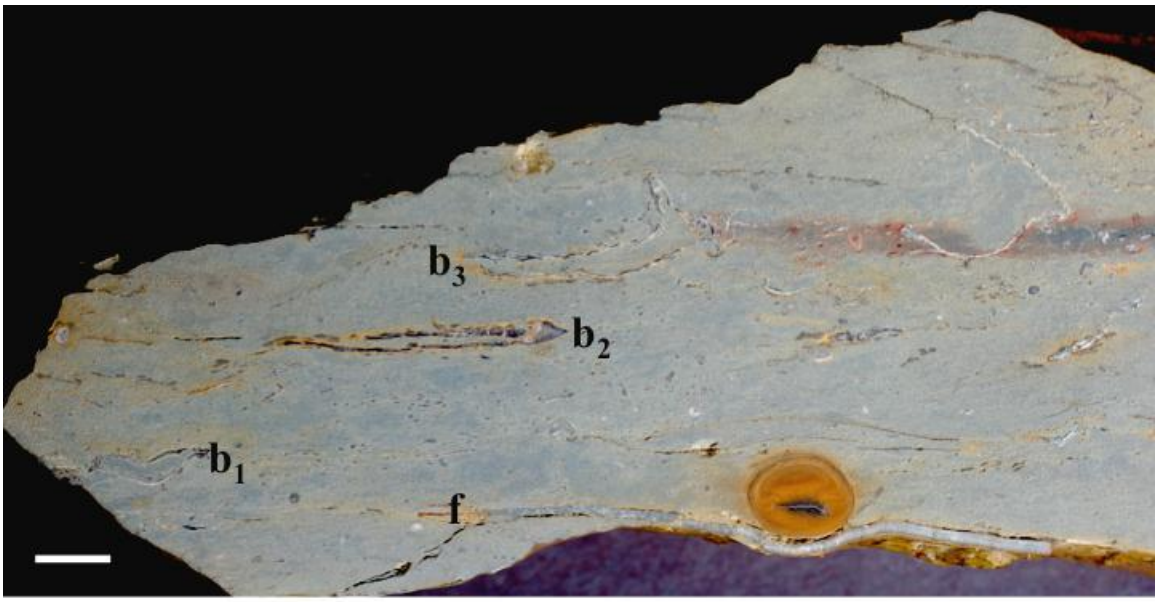

FIGURE 17—Sample from the Main Crinoid Bed containing articulated productid brachiopods in living position (convex side down) at three closely spaced horizons (b_1-b_3). Although brachiopod b_2 is more compacted than the other two, it is still evident that the convex valve is facing downwards. This indicates that several rapid burial events comprise the Main Crinoid Bed and other thinner units. Note the deformed fenestrate bryozoan frond (f) in the bottom of the slab, which may count as a fourth horizon below b_1. Scale bar = 1 cm.

could not have been produced by a single episode of rapid burial, as the brachiopods are neither in the hydrodynamically stable convex-up position (which can result from reworking by relatively gentle currents in muddy substrates [Brenchley and Newall, 1970]), nor are they found at the same level, as would be expected from a hydraulically sorted bed. Likewise, this pattern could not result from normal, ambient sedimentation, as the slow sedimentation rate and active bioturbation within the environment would not lead to preservation of organisms in living position or with articulated valves (Holland, 1988).

Aspects of ichnofabrics relevant to differentiating between thinner and thicker units, specifically the presence of discrete sideritized burrows, was discussed in an earlier section, but more detailed ichnologic analysis was performed on sectioned mudstone slabs. Evidence for pervasive bioturbation included a lack of any recognizable physical sedimentary structures in cross-section or on the tops or bottoms of mudstone slabs; a lack of any recognizable biogenic sedimentary structures; and a pronounced mottled texture in samples from all horizons. In many samples, small (generally 1/10 – 1/5 mm in diameter), circular to elongate, densely spaced structures recognized by a slightly darker sediment color were recognized, and may be compressed *Chondrites* (Fig. 18). This interpretation makes sense in light of the observation that *Chondrites* often occupies the deepest levels of tiered substrates (Bromley and Ekdale, 1984) and, therefore, may be the best candidate for preservation within a bioturbated, fluid-rich environment, where it would overprint the homogeneous background created by migration of shallower tiers (Savrda, 2007). These structures, although revealing little new paleoenvironmental information, support previous interpretations that the benthic environment was

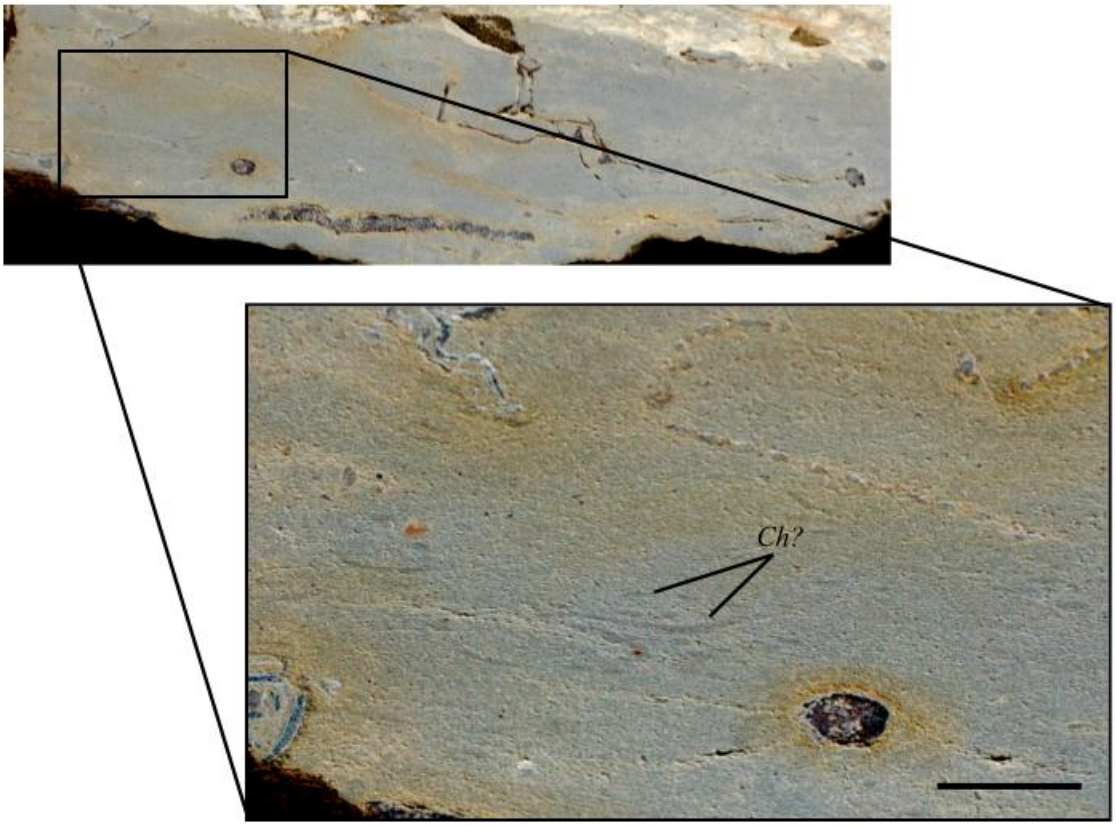

FIGURE 18—Possible compressed *Chondrites* (*Ch?*) in a sample from lower Bed 0 (note the tubular sponge fossils). Inset highlights the very small size and subtlety of this structure, which is found throughout the entire section. Scale bar = 0.5 cm.

oxygenated throughout deposition, and that bioturbation was extensive even within the primarily epibenthic thinner units.

Comparison between the fabric of thinner and thicker units revealed some consistent differences. Numerous samples from the thicker units showed distinct skeletal material-rich and skeletal material-poor layers (Fig. 19), which were absent from the thinner units. The relatively barren layers frequently exhibit some of the best examples of mottled fabric (Fig. 19B). Whether this pattern reflects concentration of fossil material by minor winnowing followed by fallout of fine-grained sediment from suspension is possible, but purely speculative, despite occurring with clear skeletal concentration layers, as described in the previous section (see Fig. 13).

Little evidence for diagenetic processes beyond siderite precipitation has been documented for the Copan section (e.g., Lewis et al., 1998) due, at least in part, to the preservation of crinoids in a seemingly unaltered mineralogic state and the lack of cement in non-sideritic mudstone. While the current study also found little evidence for diagenetic processes beyond siderite precipitation and compaction, samples were analyzed for signs of carbonate dissolution, which can be an important factor in fossil preservation in offshore marine deposits. Indeed, in a detailed study of core shale taphonomy involving both lower and upper core shale facies of midcontinent Upper Pennsylvanian cyclothems, Malinky and Heckel (1998) determined that migration of the lysocline resulted in geographic variations in the occurrence of calcitic and aragonitic fossil components. The Copan fauna is variable in terms of resistance to dissolution, with some calcitic skeletal material represented only by complete or partial external molds (commonly bryozoans and productid brachiopods), and some originally aragonitic

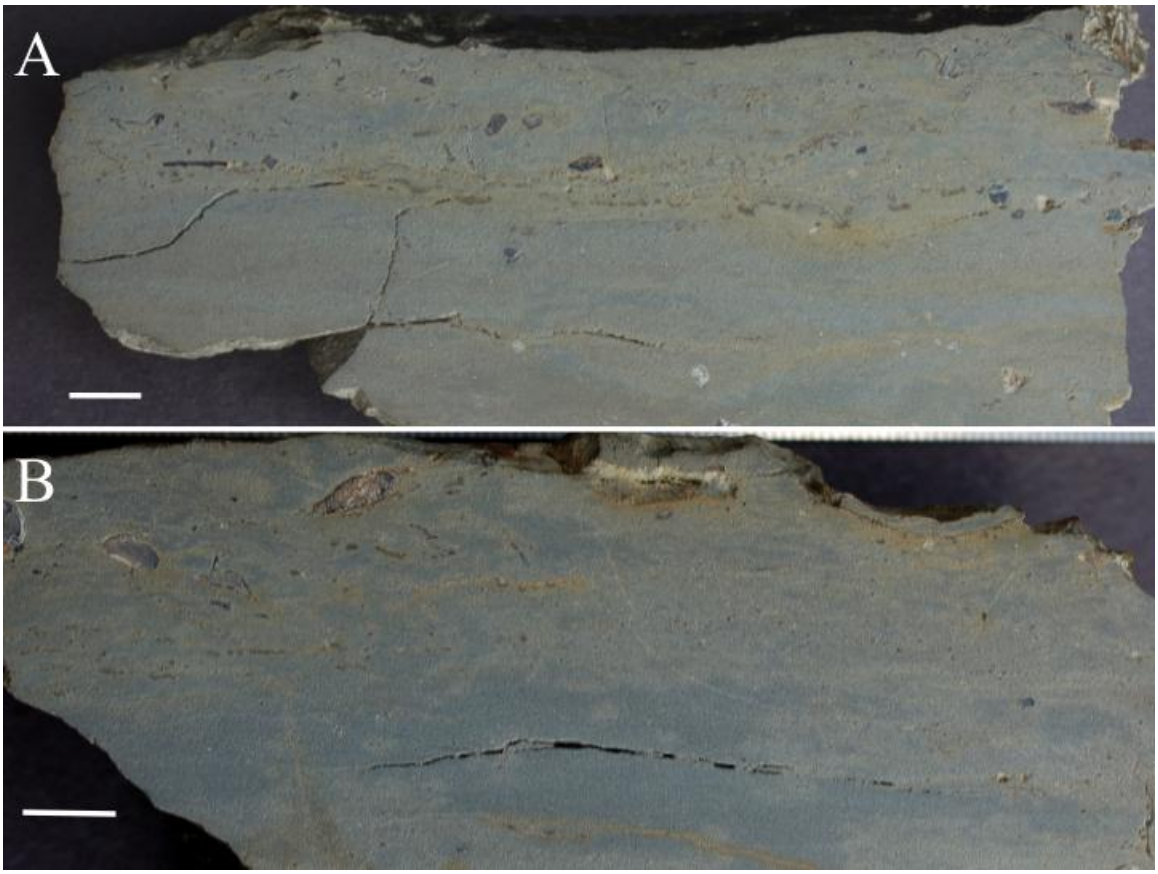

FIGURE 19—Examples of minor concentrations of skeletal material observed in the thicker units. A) Sample from the bottom of Bed 2 displaying a sharp-based (erosional?) concentration of fossil material at the upper portion of the slab; scale bar = 1 cm. B) Sample from lower Bed 4 showing a concentration with a gradational contact with the mottled zone below; scale bar = 1 cm.

molluskan material preserved without evidence of any dissolution. Regardless of the underlying cause, certain mudstone slabs display a pattern in which a lateral change in the relative visibility of preserved skeletal material can be observed within a single horizon (Fig. 20). Here, calcareous fossils are clearly visible on one part of the slab, with few visible fossils on the opposite side, and an oxidized surface separating them. This may represent some form of small-scale diagenetic front operating within the outcrop. Unfortunately, the inconsistent occurrence of this feature, both laterally and stratigraphically, makes further interpretation impossible.

FIGURE 20—Possible diagenetic front preserved in a block from Bed 2. Note the abundance of clearly visible fossil material on the left and poor visibility of material on the right, with oxidation surface in between. This may show the effects of dissolution on fabric. Scale bar = 2 cm.

SPATIAL DISTRIBUTION AND ORIENTATION OF FOSSILS

Methods

The archaeological-style grid system dividing the excavated area into 0.5 m x 0.5 m squares (Lewis et al., 1998) was used to plot the the fossils discovered during excavation. In addition, data were gathered on the bearing of fossils with a long axis that might signify paleocurrent direction. These data were recovered from the videotapes, field notes, and still photographs taken during the excavation. In addition, some mudstone blocks and fossils collected with associated matrix were marked with a north arrow. However, records concerning some fossils were found to be incomplete (e.g., some fossils have a documented orientation and location, but lack an identified source horizon).

Results and Discussion

Figure 21 shows the spatial distribution of macrofossils from the excavated area. It is apparent that many records are incomplete, due in large part to the number of crinoid specimens which were collected early in the excavation seasons, when the collecting grid was still being re-established and corrected from previous fieldwork. These specimens could be included as part of the orientation analysis, but could not be part of the spatial distribution analysis. Despite the small number of specimens definitively mapped in

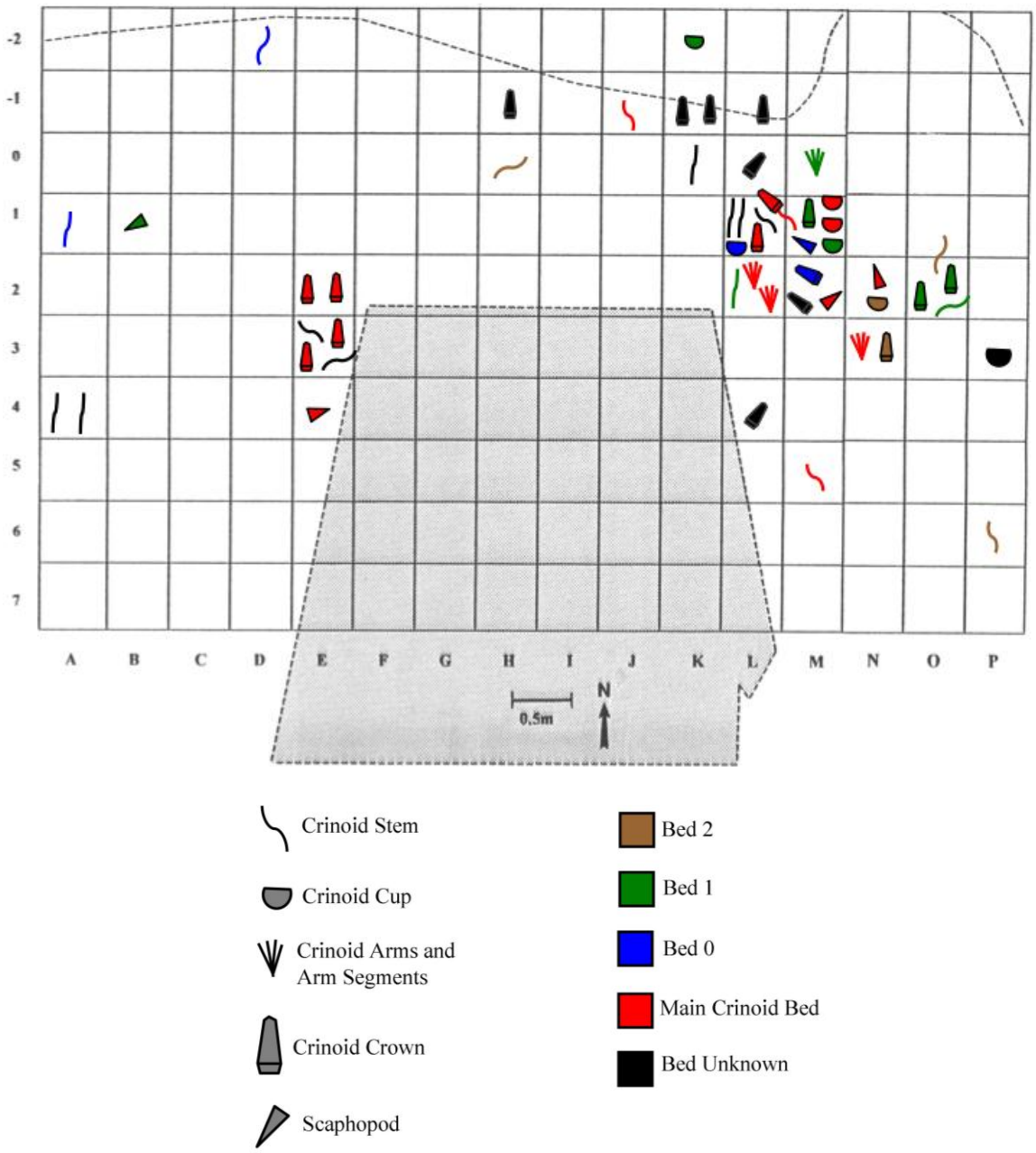

FIGURE 21—Distribution of macrofossils identifiable from analysis of field records. Fossils for which no orientation was measured are oriented due north. The stippling represents the area sampled by Mosher (see text for further explanation). Grid figure from Lewis et al. (1998).

place, a number of observations can be made. In particular, the degree of spatial patchiness of crinoidal material within the study area becomes apparent. Clusters of crinoid crowns and stems were discovered at several locations within the collecting grid, most notably in the areas near M1-M2 and E2-E3. This patchiness was even detected by Mosher in the late 1980's, who thought that the entire colony had been collected or that he had lost the source horizon several times during his bulk collecting (D. Mosher, unpublished data). Furthermore, many of the clusters containing articulated cups or crowns were composed of individuals belonging to the same species. This taxonomic association provides suggestive evidence that the crinoid assemblage is autochthonous, as monospecific clusters often result from the settling of larvae on local hard substrates (e.g., Meyer, 1997; Brett and Allison, 1998).

The summary data from orientation measurements are presented in Figure 22. Unfortunately, no orientations are available from Bed 3 or Bed 4, and 9 measured fossils have no identified source horizon; nevertheless, 51 long-axis orientation measurements were taken, primarily from the Main Crinoid Bed. The combined data from all horizons show considerable variation, with no consistent modal orientation of linear fossils (Fig. 22A). Orientation data from each horizon, however, provide a number of interesting results (Figs. 22C-G). The Main Crinoid Bed yielded a wide range of orientations, with two maxima approximately 90 degrees from one another (Fig. 22C). These orientations came from two main sources: articulated crinoid columns and scaphopods. Despite the similarity in shape between these two types of fossils, scaphopods, being essentially one-part skeletons, and crinoid columns, being multi-element skeletons, are not taphonomically comparable; long lengths of articulated crinoid column indicate rapid

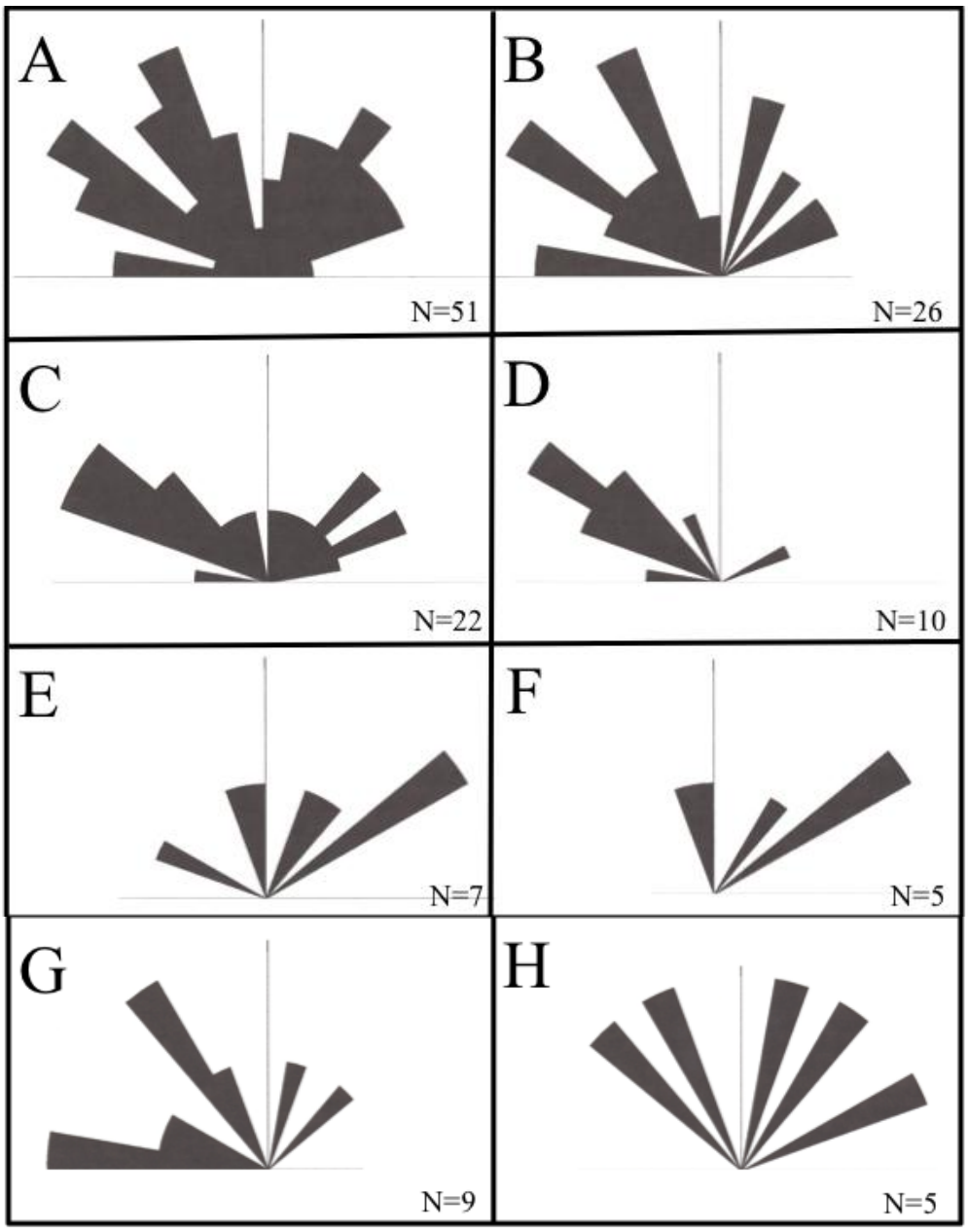

FIGURE 22—Orientation data for fossil material at various horizons. A) All measured fossil material from all horizons. B) Crinoid stems from all horizons. C) All fossils from the Main Crinoid Bed. D) Stems from the Main Crinoid Bed. E) All fossils from Bed 1. F) Stems from Bed 1. G) All fossils from Bed 0. H: All fossils from Bed 2.

burial, while intact scaphopods may not. Therefore, the orientations of long crinoid columns were plotted separately in order to provide information on the event assemblage of the Main Crinoid Bed (Fig. 22D). Interestingly, the crinoid stems do show a preferred orientation, with a prominent maximum at approximately 310 degrees, indicating that burial events responsible for the preservation of articulated crinoids in the Main Crinoid Bed may have been associated with currents directed predominantly to the northwest.

Orientation measurements from Bed 1 show a somewhat similar pattern to that of the Main Crinoid Bed (Fig. 22E-F), although there are fewer measurements, the maximum is less well-defined, and only two of the measurements are from scaphopods. For Bed 1, crinoid stems are aligned in a predominantly north-northeast direction, indicating that current directions associated with rapid burial events may have shifted in between deposition of the Main Crinoid Bed and Bed 1, although this inference is made cautiously in light of the small number of orientation measurements. In contrast to the Main Crinoid Bed and Bed 1, measurements from Bed 0 and Bed 2 show no clear pattern (Fig. 22G-H), although, as noted above, the small number of measurements makes interpretation difficult. Bed 0 may show an orientation maximum at approximately 295 degrees, but this may be an artifact of the small sample size and/or the inclusion of several measurements taken from an area where distinguishing between the upper portion of the Main Crinoid Bed and the base of Bed 0 is difficult. Furthermore, all measurements from Bed 2 are from crinoid stems, making a comparison between crinoidal and non-crinoidal fossils impossible. Consequently, little can be concluded about current direction in the thicker units of the section.

Such results are rather ambiguous, but not entirely unexpected, as interpreting

paleocurrent parameters from crinoid fossil orientation is notoriously difficult (see Brett and Baird, 1986; Brett and Allison, 1998; Ausich, 2001). The most common problem with analyses of crinoid-column orientation patterns, including the current study, is that crinoid columns frequently lack a definite unidirectional orientation, and instead exhibit a bent or contorted configuration (e.g., Fig. 8). This is often the case for crinoids that underwent live burial by sediment that was deposited rapidly, but without a strong associated current; in this setting, the ambulachra become clogged by sediment and crinoids become preserved in their death posture rather than becoming aligned or re-oriented. Orientation studies focused on crinoids include a combined flume and field study of crinoid pluricolumnals by Schwarzacher (1963), who concluded that crinoid stems are aligned with a modal orientation that does not correspond to current direction, resulting from crinoid stems rolling before rotating parallel to current, and that current direction is indicated by a secondary peak; he further concluded that current-parallel rotation occurs more readily on muddy substrates than on sandy substrates. In another study, Nagle (1967) documented unimodal alignment in pluricolumnals, but in a direction perpendicular to current. It is important to note, however, that these studies used shorter column segments (i.e., pluricolumnals) than the long, articulated columns measured here, which have been the focus of few current-alignment studies. A notable exception is work by Baumiller and Ausich (1996), who noted that only "blow-down" scenarios characterized by very strong unidirectional currents would leave a distinct and unambiguous alignment signature in crinoid stalks, and that crinoids buried under normal or moderately elevated current velocities may exhibit a curved or arched stalk posture.

Two other significant observations regarding the orientation of crinoid remains

must be noted. The first involves the occurrence of aligned stems that cross-cut other stems that are aligned in a different direction. An example of this, in a slab recovered from Bed 3, is shown in Figure 23. Here, the stems in each of the two sets are very strongly aligned with one another, but are offset by nearly 40 degrees from the other set. In addition, there is a consistent cross-cutting relationship between the sets, with the stem set oriented vertically in Figure 23 clearly underneath the set oriented oblique to it, but separated by less than a millimeter of sediment, where intervening sediment is present at all. This appears to indicate shifting current directions associated with the rapid burial of crinoids. Although confounding in terms of orientation patterns, multidirectional paleocurrent indicators have been reported from distal shelf tempestites by Gray and Benton (1982), and were even put forth, along with well-preserved fossils, as important indicators of storm activity in environments lacking in coarse sediment and physical sedimentary structures.

The second observation involves the occurrence of several long stems that are parallel, but aligned in an arcuate pattern, rather than a simple unidirectional pattern (Fig. 24). The cause of arched, but parallel, crinoid stems is somewhat enigmatic. Wetzel and Meyer (2006) interpreted the alignment of curved *Chariocrinus württembergicus* stems as evidence of dragging by currents or waves. An alternative explanation could involve turbulent eddies swirling stems into arcuate orientations, a mechanism proposed by Webber et al. (2008) to explain the radial orientation pattern of *Uintacrinus socialis* aggregations. Clear evidence for either explanation is lacking in the Copan Lagerstätte, but this pattern indicates that the events responsible for burial of crinoids may have been associated with energetic events more complex than simple unidirectional flow.

FIGURE 23—Two sets of parallel stems from Bed 3. The underlying set of three strongly aligned stems is oriented toward the top of the page (see arrows). The overlying set of three strongly aligned stems is oriented oblique to the underlying set (see arrows), and is separated by less than a millimeter of sediment, although some stems are in direct contact. Scale bar = 2 cm.

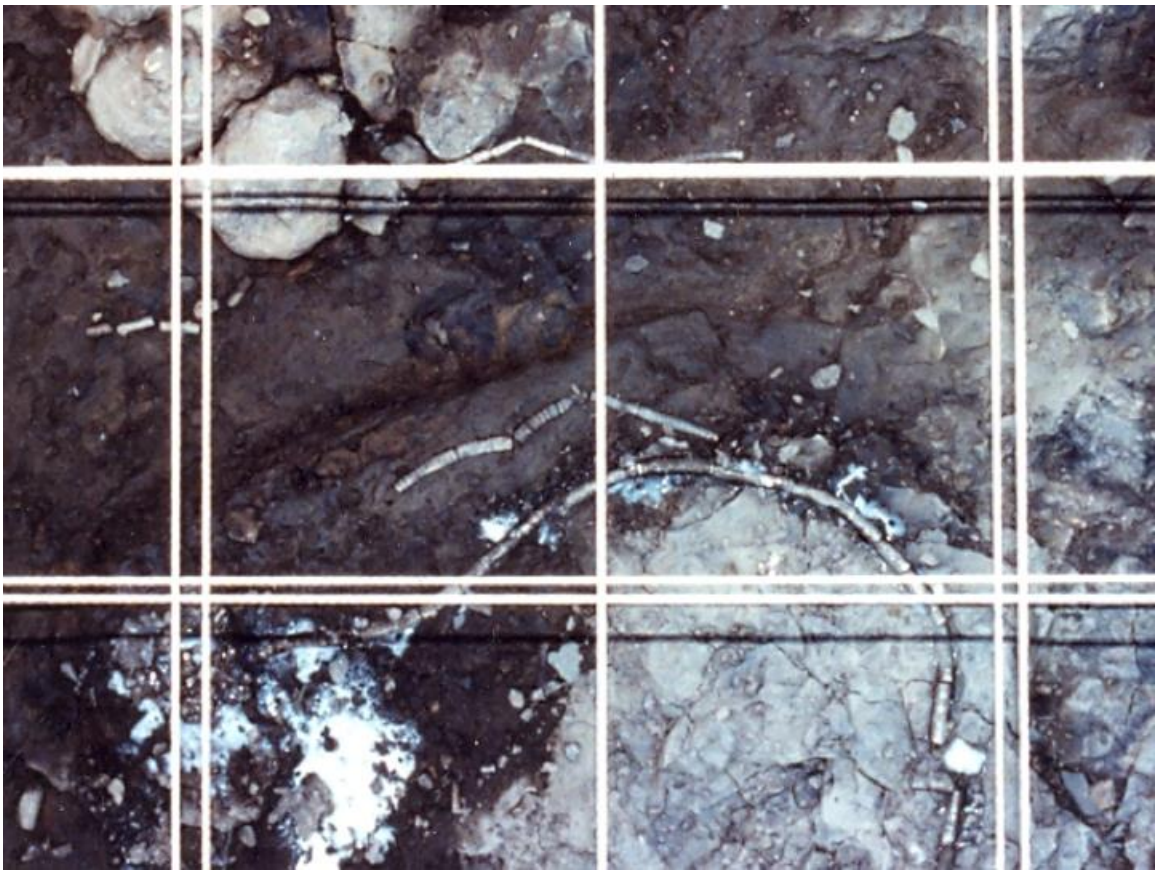

FIGURE 24—Three crinoid columns arranged into arcuate, but parallel orientations in the Main Crinoid Bed. The fact that these do not display simple, unidirectionally aligned configurations or random, individually contorted orientations may indicate some form of complex hydrodynamic activity. Each square is 10 cm x 10 cm. Photograph provided by R. D. Lewis.

CRINOID TAPHONOMY

Background and Methods

The large collection of articulated and partially articulated crinoid specimens recovered by Mosher during the period from 1984 to 1989, as well as some of the specimens discovered during the subsequent excavation, are stored at the University of Nebraska State Museum in Lincoln, Nebraska. Over 1214 specimens are represented, ranging from partial cups to complete crowns with attached columnals. The taphonomy of this impressive collection (excluding holotypes) was assessed during portions of the spring and summer of 2009, with the goals of understanding the magnitude and causes of taphonomic variability within the crinoid assemblage, and gaining insight into the processes responsible for the taphonomic state of event-buried crinoids. In order to achieve these goals, several features were documented for each crinoid specimen, including degree of completeness, axis of compaction, arm position, and presence and nature of other decay- or scavenging-related features.

Evaluation of the degree of completeness of crinoid fossils was accomplished through the development of a taphonomic grade system, wherein each specimen is placed into one of a series of classes defined by taphonomic state, thereby allowing semi-qualitative comparisons to be made. This technique has been used successfully to compare crinoid preservation among facies and to compare the relative propensity for disarticulation of high-level taxonomic groups (Meyer et al., 1989; Ausich and

Sevastopulo, 1994; Taylor and Brett, 1996; Webster, 1997; Gahn and Baumiller, 2004; Wetzel and Meyer, 2006; see also Brandt, 1989). These studies, with the exception of Gahn and Baumiller (2004) and Wetzel and Meyer (2006), adopted a holistic approach to crinoid taphonomy, with each grade describing state of an entire specimen. However, research on Paleozoic stalked crinoids (Ausich and Baumiller, 1993; Gahn and Baumiller, 2004), modern stalked crinoids (Baumiller and Ausich, 1992; Baumiller et al., 1995), and modern comatulid crinoids (Meyer, 1971; Liddell, 1975; Meyer and Meyer, 1986) has shown that different parts of the skeleton disarticulate at different rates, with the most notable disparity between the muscular articulations of the arms and the ligamentary articulations of the cup and column. This makes separate description of column, cup, and arm disarticulation a more precise technique for assessing crinoid taphonomy (Gahn and Baumiller, 2004). Cups were described as either complete or partial; arms and columns were described as absent, proximal, or considerable, with partial defined as measuring less than twice the height of the cup. This made possible an 18-grade classification system that accounts for all possible taphonomic states, which is described in Table 2 and visually depicted in Figure 25. It is important to note that this system is designed to account for all possible specimen states, and as a result, some taphonomic grades are much less likely to be encountered than others.

Compaction was examined for each specimen to understand the relationships between specimen completeness and compaction, to determine the relative proportion of specimens that have undergone noticeable compaction, and to identify the orientation of crinoids within the substrate following burial. Compaction orientations documented are (1) lateral compaction, where compaction occurred perpendicular to the long axis of the

TABLE 2—Taphonomic grades, illustrated in Figure 25, used to describe crinoid specimens stored at the University of Nebraska State Museum. See text for explanation of considerable vs. proximal.

	CUP	COLUMN	ARMS
A	Partial	Absent	Absent
B	Complete	Absent	Absent
C	Partial	Absent	Proximal
D	Partial	Proximal	Absent
E	Partial	Proximal	Proximal
F	Complete	Absent	Proximal
G	Complete	Proximal	Absent
H	Complete	Proximal	Proximal
I	Partial	Absent	Considerable
J	Partial	Proximal	Considerable
K	Partial	Considerable	Considerable
L	Complete	Absent	Considerable
M	Complete	Proximal	Considerable
N	Complete	Considerable	Considerable
O	Partial	Considerable	Absent
P	Partial	Considerable	Proximal
Q	Complete	Considerable	Absent
R	Complete	Considerable	Proximal

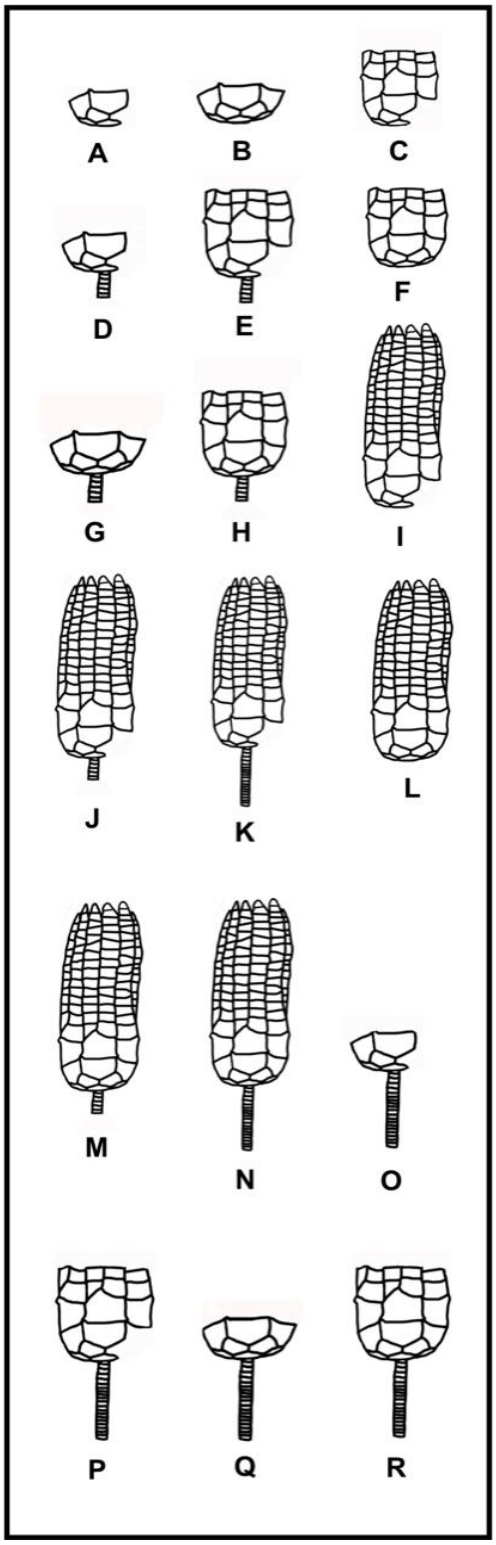

FIGURE 25—Taphonomic grades described in Table 2.

crown, resulting in a flattening of the crown; (2) oral-aboral compaction, where compaction occurred parallel to the long axis of the crown, commonly resulting in a telescoping of cup circlets; (3) oblique compaction, where compaction occurred oblique to the long axis of the crown, resulting in "smearing" of arms to one side; and (4) no recognizable compaction, in which the specimen appears to retain its original dimensions (Fig. 26).

Arm configuration was documented for each specimen in order to understand the relationships between arm position and other taphonomic attributes and processes. All specimens with at least primibrachials on two arms were documented. Arm positions recorded are (1) the shaving brush posture, where all arms are aligned parallel to the long axis of the crown and closed tightly, often with inwardly curled distal arm tips; (2) the closed position, where arms are aligned parallel to the long axis of the crown but appear somewhat relaxed rather than being tightly closed; and (3) the open position, where arms are splayed or otherwise not aligned in any dominant orientation. Arm positions can be further described as indistinct, referring to specimens with only proximal arms that do not allow identification of any recognizable posture; or absent, where no brachials are attached to the cup. Selected examples of arm positions are shown in Figure 27.

An understanding of arm positions is important because it provides evidence of timing and crinoid response to burial events. Work with Recent isocrinids has shown that these crinoids adopt the shaving-brush posture as a stress response to increased current velocities (Meyer, 1997; Baumiller et al., 2008). Hence, common occurrence of this position may indicate more energetic conditions not otherwise evident. This is not universal, however, as most allagecrinids, including *Kallimorphocrinus copani* (the

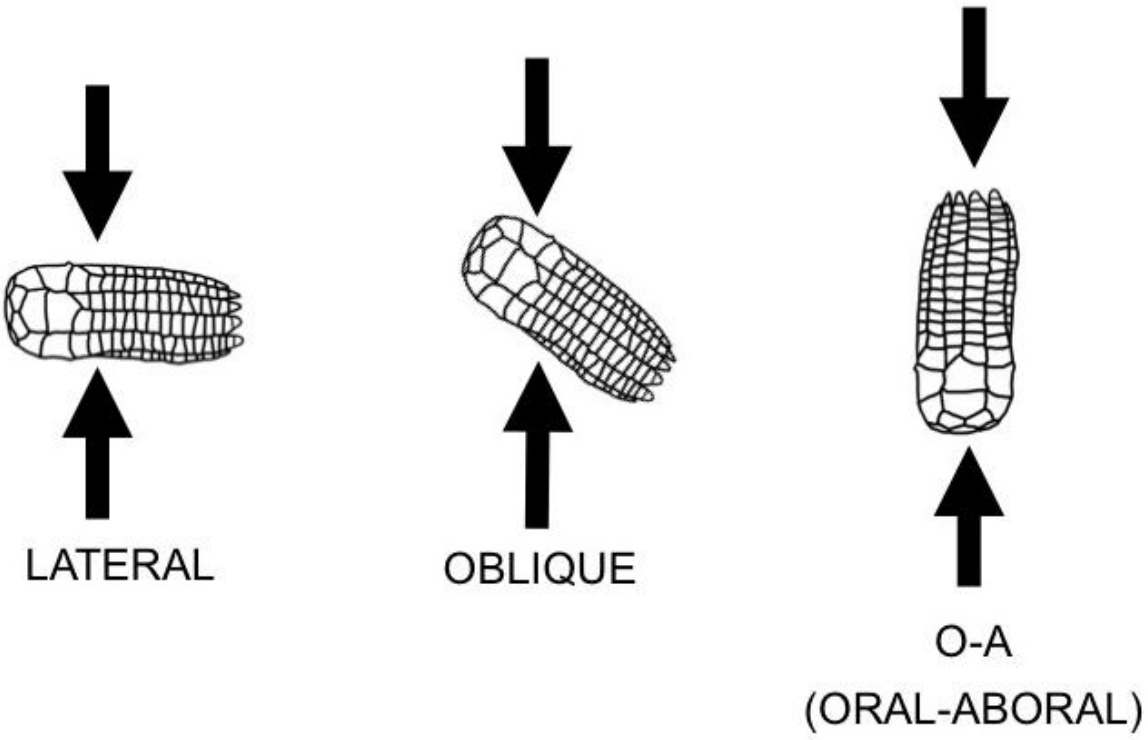

FIGURE 26—Compaction orientations and terminology used to describe crinoid specimens stored at the University of Nebraska State Museum. Note that lateral compaction would result in a flattened specimen, oblique compaction would result in a specimen with arms curved to one side of the cup, and O-A compaction would result in a specimen with splayed arms and/or lower cup circlets pushed into the interior of the cup.

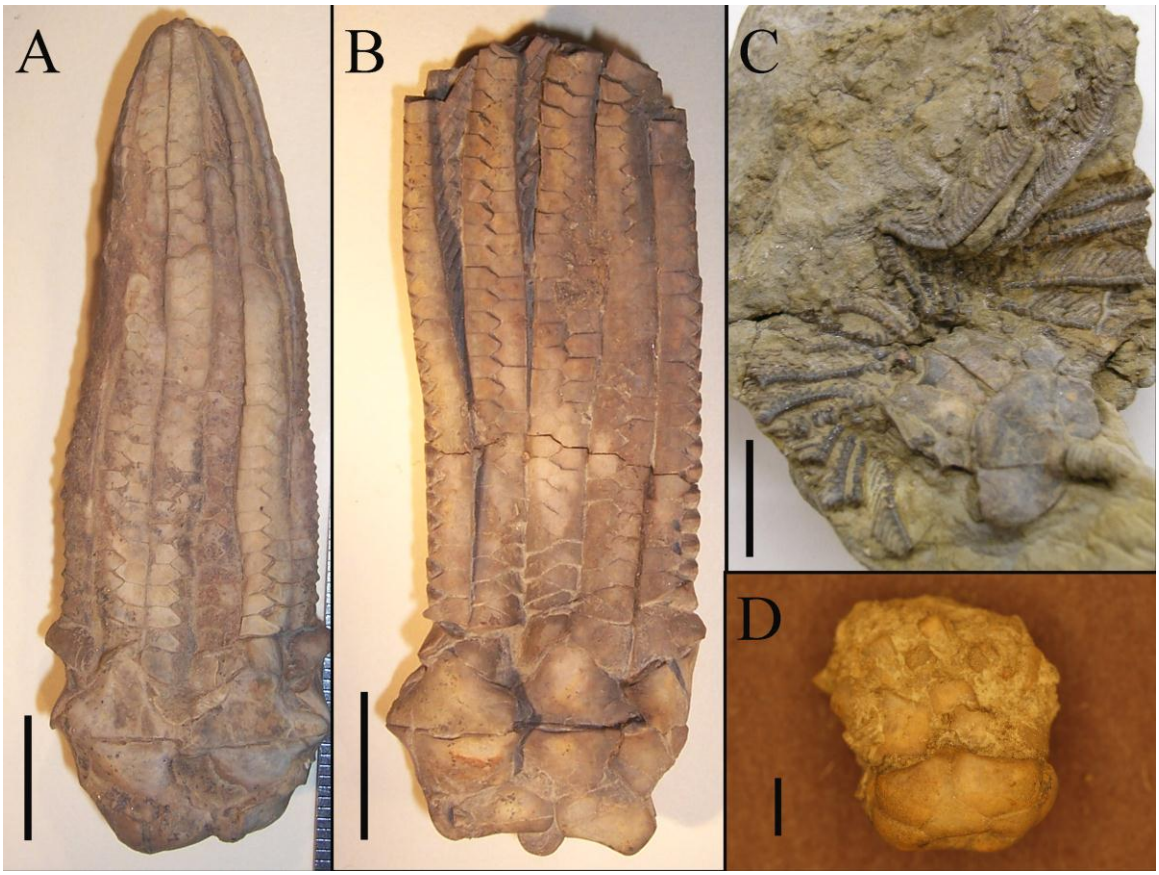

FIGURE 27—Examples of arm positions documented for crinoids in the UNSM collection. A) *Erisocrinus typus* exhibiting the shaving-brush posture, with aligned and tightly closed arms; scale bar = 1 cm. B) *Erisocrinus typus* exhibiting the closed posture, with aligned, but slightly relaxed arms; scale bar = 1 cm. C) *Dichocrinus* sp. exhibiting the open posture, with arms widely splayed; scale bar = 1 cm. D) *Apographiocrinus typicalis* exhibiting an indistinct arm configuration, where proximal brachials are present, but are not arranged into any recognizable posture; scale bar = 2 mm.

third most common component of the Copan crinoid fauna), maintain the shaving-brush position as a normal living posture not strictly indicative of trauma (Sevastopulo, 2008). The closed position likely represents a decay-induced loosening of a specimen formerly exhibiting the shaving-brush posture (Gahn and Baumiller, 2004), and indicates a brief period of exposure or a relatively thin sediment blanket. The open position likely represents burial rapid enough to prevent the crinoid from adopting a trauma position, or burial in a vertical, mouth-down orientation.

Other taphonomic features documented for each specimen assessed are (1) any jumbling of crown plates, which is commonly indicative of the activity of scavenging organisms; (2) the loss of distal arm tips, possibly resulting from decay; (3) the presence of a concavity at the base of the arms but without any associated plate jumbling or disarticulation; and (4) the presence of any siderite associated with all or part of the specimen. Noting the jumbling of crown plates is significant in that the tegmen, which contained the nutrient-rich gonads in Paleozoic crinoids (Lane, 1984), and inter-brachial muscle tissue in the arms were the targets of scavengers, making disruption in the plate sequence of the proximal arms a common signature of scavenging (Maples and Archer, 1989; Fig. 28A). In contrast, the loss of the distal arms is one of the initial stages in incipient crinoid decay due primarily to the small cross-sectional attachment area between adjacent pinnular and brachial plates (Lewis, 1980; Fig. 28B). The two other attributes noted also deal with presumed soft-tissue decay. Since the vast majority of a crinoid's visceral mass is concentrated within the cup, post-burial decay of this material may cause a collapse of overlying plates into the cup, thereby creating the concavity described above. Decay of soft-tissue also may create an ionically reactive

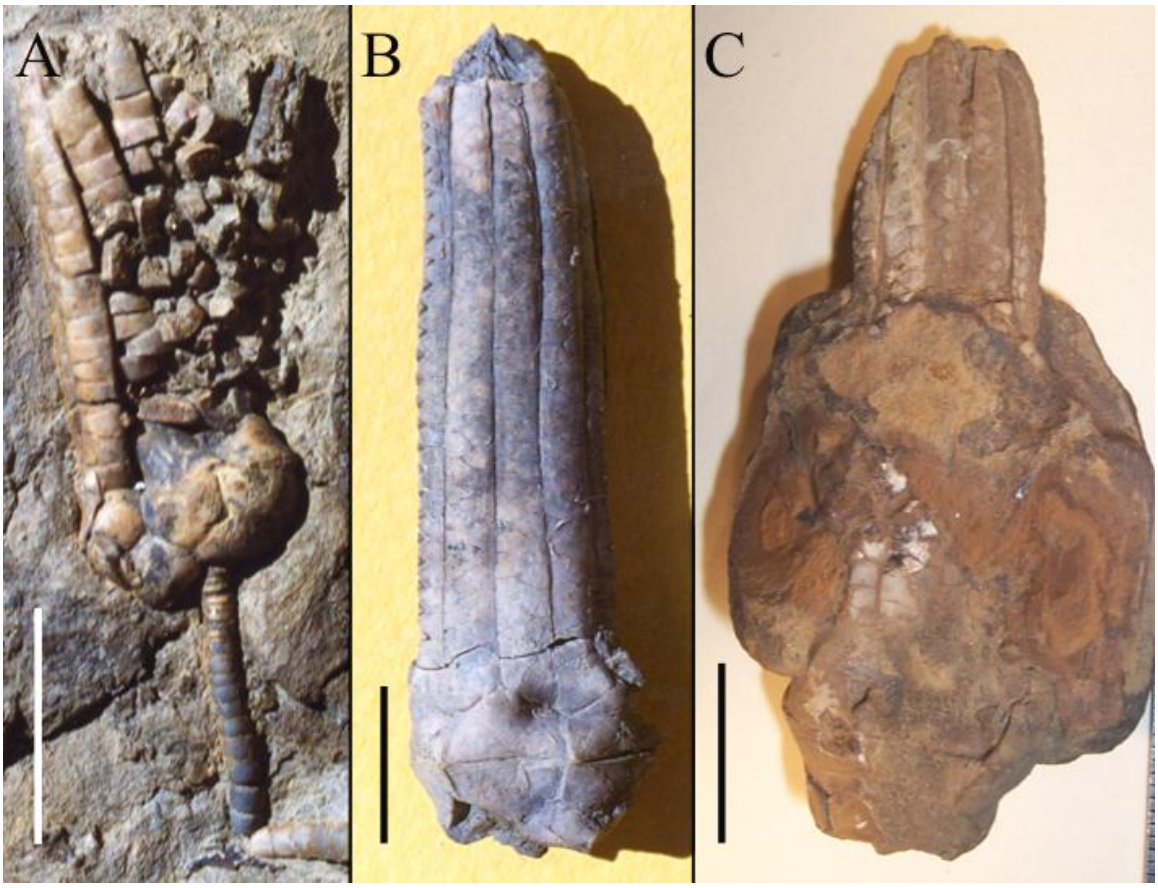

FIGURE 28—Examples of scavenging- or decay-related taphonomic features documented as part of the taphonomic assessment of the UNSM Copan crinoid collection. A) *Apographiocrinus* with jumbled proximal arm plates; the absence of any disturbance to other parts of the skeleton, as well as one completely undisturbed arm, suggests that this is the result of scavenging. Scale bar = 1 cm; photograph provided by R. D. Lewis. B) *Erisocrinus* with missing distal arm tips, possibly indicating a brief period of incipient decay prior to burial. Scale bar = 1 cm; Photograph provided by R. D. Lewis. C) *Erisocrinus* with a siderite concretion nucleated around the proximal arms, seemingly generated by decay of the tegmen; scale bar = 1 cm.

microenvironment conducive to the precipitation of early diagenetic minerals such as siderite (Allison, 1988a, b; Fig. 28C).

Results and Discussion

Taphonomic assessment of the UNSM collection of Copan crinoids yielded some interesting results. Summary data for all 1214 specimens surveyed are presented in Figures 29-32. The generally articulated nature of the crinoid assemblage is reflected by the dominance of taphonomic grades F and L (see Table 2); in total, over 65% of specimens retain at least proximal arms, and over 78% of specimens have a complete cup. Despite the abundance of specimens with attached arms, relatively few specimens contain attached columns of any length, with only 20% of specimens retaining at least proximal columnals. Furthermore, even though H is the fifth most common taphonomic grade, many of these specimens are from *Kallimorphocrinus*, which is commonly preserved with a distinctive proxistele that remains attached to the cup longer than other parts of the column (Lane and Sevastopulo, 1981, 1982). The relative absence of columns attached to complete or partial crowns in taxa besides *Kallimorphocrinus* does not typically result from brief periods of decay at the sediment-water interface, as experimental studies with modern stalked crinoids have shown that separation of proximal columnals from the cup is one of the final stages in disarticulation under normal conditions (Baumiller, 1994, 2003). Instead, this may reflect one or more of several factors: (1) compaction preferentially separating crowns from columns at what is likely a weak spot on the crinoid skeleton (Llewellyn and Baumiller, 1993); (2) the processing

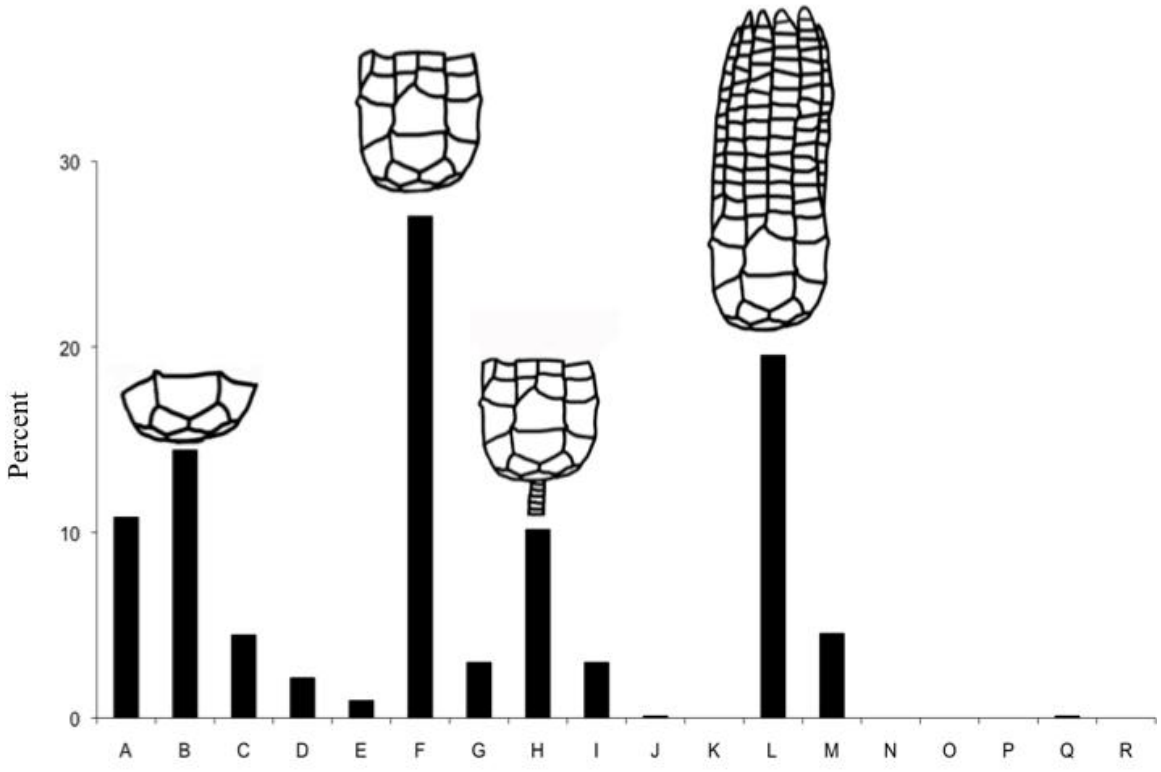

FIGURE 29—Summary taphonomic grade data for UNSM crinoid collection.

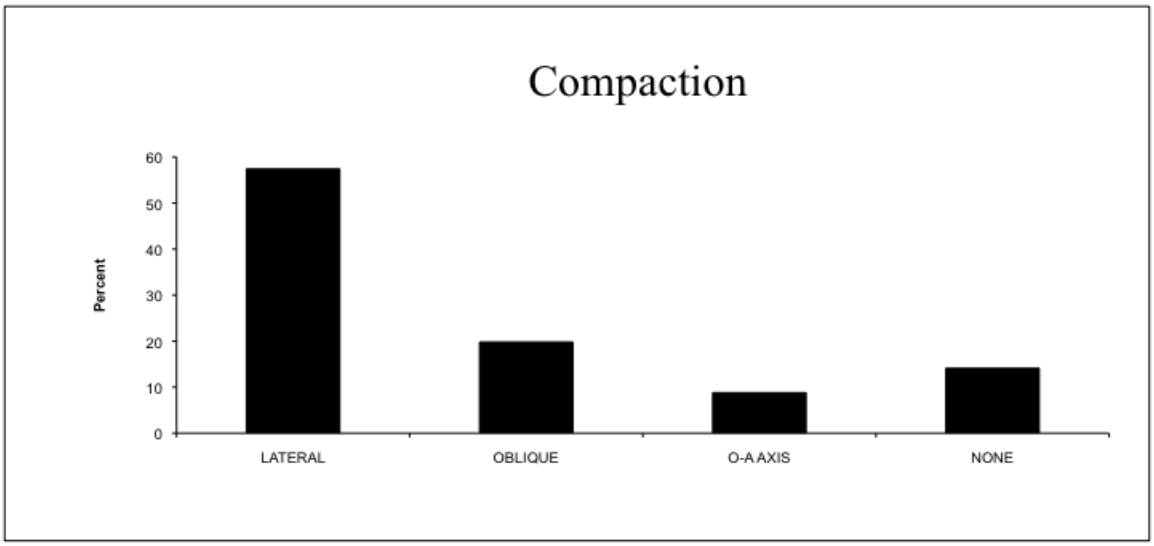

FIGURE 30—Summary compaction data for UNSM crinoid collection.

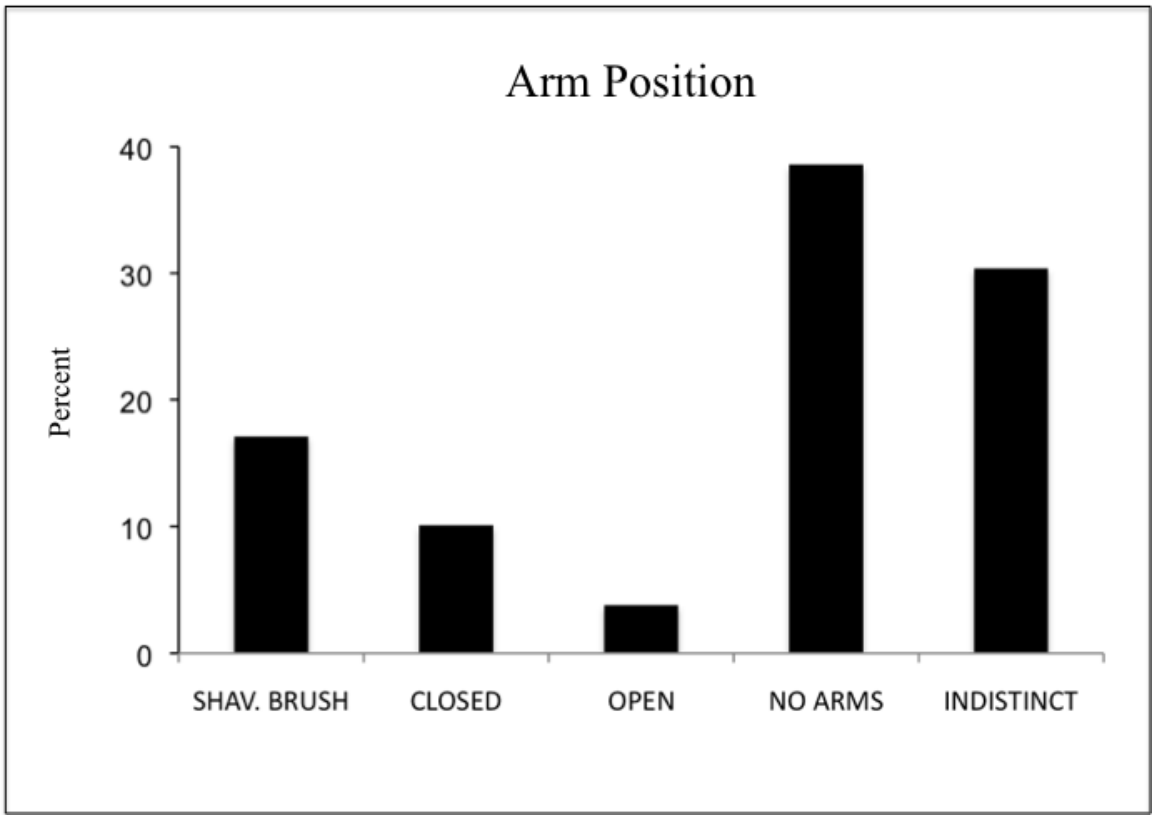

FIGURE 31—Summary of arm position data for UNSM crinoid collection.

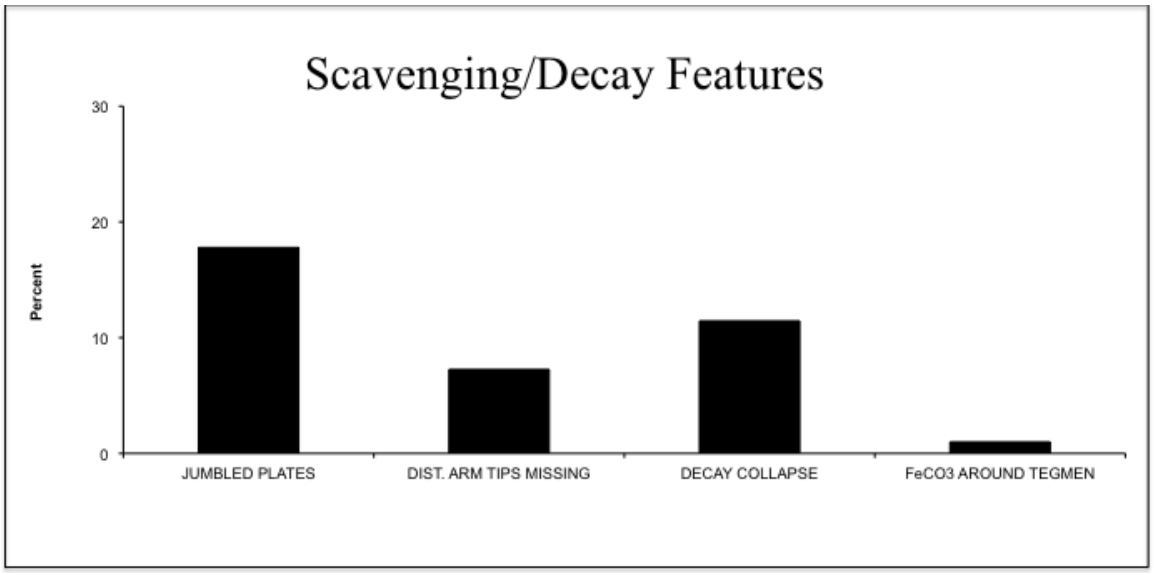

FIGURE 32—Summary of scavenging- or decay-related features on crinoids from the UNSM collection. See text for explanation of features.

technique of Mosher, made necessary by the poorly indurated sediment, which is likely to result in a single skeleton being recovered in several pieces; and (3) autotomy, where crinoids voluntarily cast off portions of their body as a stress response. This last possible causal mechanism is interesting, as recent work by Baumiller and Ausich (1992) and Baumiller et al. (1995) has indicated that identification of unambiguous autotomy in Paleozoic crinoids is nearly impossible, as the "hard part" skeletal morphology necessary for autotomy was present by the early Mississippian, but the configuration of (non-preserved) ligaments dictates whether crinoids were capable of autotomy; furthermore, even if the ligaments were properly configured to permit autotomy, the behavior of autotomy as a stress response may not have evolved yet.

Copan specimens are predominantly compacted laterally, with relatively few specimens exhibiting oblique or no compaction, and even fewer exhibiting oral-aboral compaction (Fig. 30). There is considerable variation in arm position, although many specimens lacked arms or had only a few brachials and were grouped into the absent and indistinct classes, respectively, giving these two categories a majority. The common occurrence of the shaving-brush position (Fig. 31) indicates a consistent stress response by the crinoid fauna, most likely to the event responsible for crinoid mortality. The number of crinoid individuals that actually adopted the shaving-brush position is greater than the number of specimens displaying this arm position, as the occurrence of numerous specimens in the closed arm position suggests that at least some crinoids underwent partial decay prior to final burial, allowing for relaxation of the shaving-brush posture producing the closed posture. The relative rarity of specimens with open arms (Fig. 31) suggests that very few crinoids were buried so rapidly that they could not

respond by adopting a trauma position. Other taphonomic features (i.e., jumbling of plates, loss of distal arm tips, concavities at the base of arms, development of localized siderite concretions) were relatively rare, but distributed very unevenly among taxa (Fig. 32).

Indeed, the most significant discovery is the degree of taphonomic variability expressed within this assemblage of crinoids, collected from the same source horizon and overwhelmingly belonging to the same subclass (Table 1). Such taphonomic heterogeneity within a taxonomically similar assemblage is rarely reported; this may be because most taphonomic grade studies on lower Paleozoic assemblages contain crinoid assemblages that are diverse at the subclass and/or order level but contain relatively low diversity at the genus level. In addition, the holistic treatment of crinoid specimens, as previously discussed, may make detection of subtle taphonomic differences more difficult than separate assessment of individual crinoid parts. However, the fundamental controls on crinoid preservation may be expressed through differential preservation of fairly closely related taxa; analysis of the causes of this taphonomic diversity has the potential for revealing paleoenvironmental information that might not be detected through interpretation of the entire assemblage. The taxa selected for taphonomic comparison were those represented by a minimum of twenty specimens each, and included the cladids *Exocrinus multirami*, *Apographiocrinus typicalis*, *Erisocrinus typus*, *Stenopecrinus planus*, *Galateacrinus ornatus*, and *Stellarocrinus virgilensis*, as well as the disparid microcrinoid *Kallimorphocrinus copani*.

The taphonomic grade data for the seven selected genera, shown in Figure 33, reflect considerable variation in specimen completeness. In general, *E. multirami*, *A.*

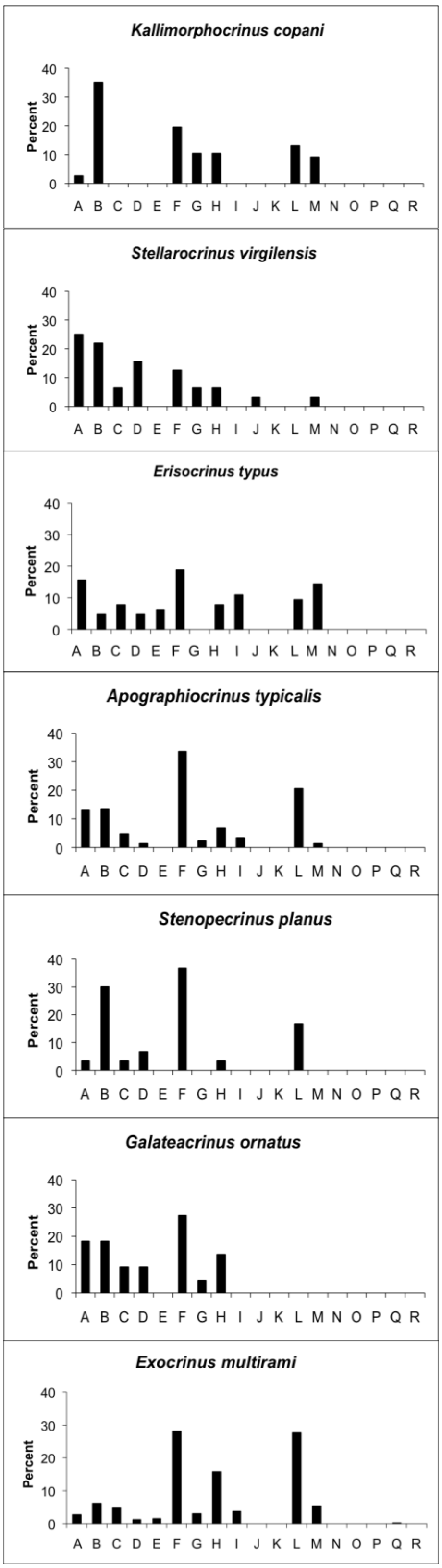

FIGURE 33—Comparison of taphonomic grade data for crinoid genera with a minimum of 20 specimens. See Table 2 and Figure 25 for definitions of taphonomic grades.

typicalis, *S. planus*, and particularly *E. typus* are more complete than the other genera. This pattern parallels trends observed in compaction data (Fig. 34), where those taxa that are most complete are also dominated by lateral compaction, with few specimens exhibiting oblique or oral-aboral compaction. Seemingly, orientation of compaction is a more important control on preservation than whether or not a specimen undergoes compaction at all (i.e., *E. multirami*, which is characterized by a large number of fairly complete specimens despite lacking a single uncompacted specimen).

The ultimate reason for this may have more to do with the integrity of the cup than anything else: taxa with a large number of oblique-compacted specimens, despite their generally poorer preservation, have a large number of specimens with complete cups (e.g., *S. virgilensis*), in contrast to taxa like *E. typus*, which, despite being one of the most well preserved taxa, has a large number of specimens with incomplete cups. Based on observations made on specimens collected in matrix, this trend reflects the tendency of taxa with rigidly sutured cup plates to rotate slightly during compaction, resulting in the shearing and total loss of arms but the retention of a complete cup (which itself is commonly uncompacted), or the bending of arms to one side of the cup (i.e., oblique compaction; Fig. 35); those taxa with a weakly sutured cup simply flatten, resulting in the retention of arms but the increased likelihood of incomplete cups and dominance by lateral compaction (e.g., *E. typus*). Meyer et al. (1989) demonstrated that Mississippian inadunate crinoids occur as either complete crowns or as isolated ossicles; they interpreted this bimodal taphonomic distribution as evidence of weakly sutured cups not capable of withstanding the physical alteration responsible for the spectrum of taphonomic states observed in camerate crinoids. The results of the taphonomic

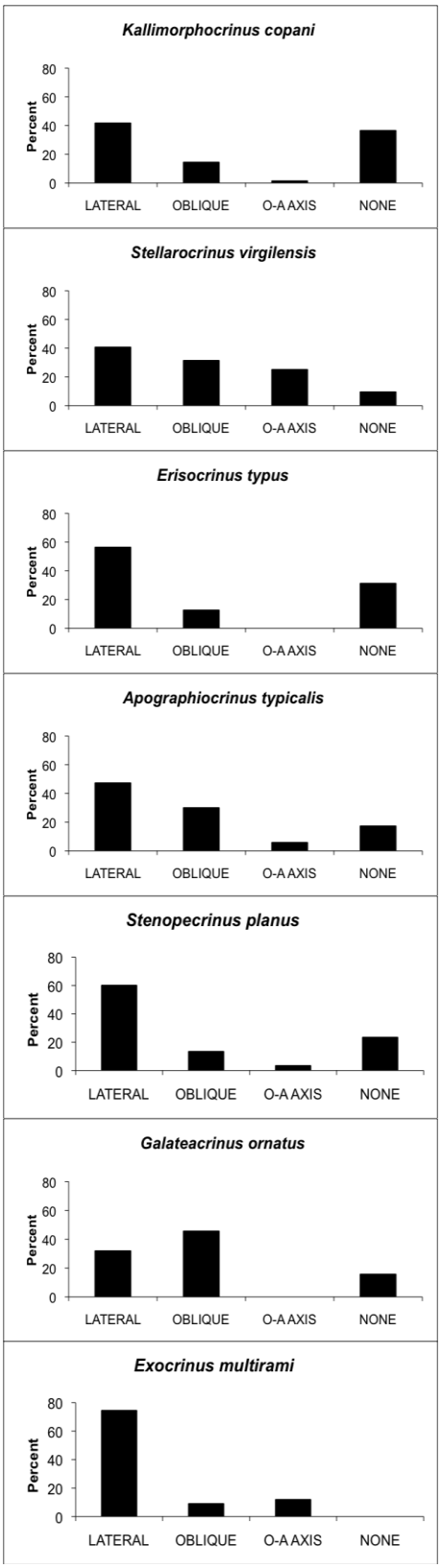

FIGURE 34—Comparison of compaction data for selected crinoid genera. See Figure 26 for definitions of compaction orientations.

FIGURE 35—Two *Apographiocrinus* crowns displaying oblique compaction. Note the "smearing" of arms to one side of the cup, which remains generally uncompacted. This reflects the rigidity of *Apographiocrinus* cups, which rotate during compaction. Note also the collapse of the infrabasal circlet into the cup of the specimen on the right. Arms of *Exocrinus* are visible in the upper part of the image. Scale bar = 1 cm.

assessment presented here indicates that a similar pattern is observed between different genera within the subclass Cladida, and that the strength of cup-plate sutures may be among the most important controls on the preservation of crinoids.

Genus-level trends in arm position, shown in Figure 36, are somewhat parallel to those of specimen completeness and compaction described above. Of course, taxa that are particularly poorly preserved will not have attached arms capable of displaying any recognizable posture (e.g., *G. ornatus*). Consequently, taxa with a large number of specimens exhibiting the shaving-brush posture are more complete than those with a large number of specimens exhibiting the open or closed posture (compare *E. typus* and *S. virgilensis*, although the unusual anatomy of *Stellarocrinus* may place some biomechanical constraints on arm position [Strimple and Moore, 1971]). This may indicate that the shaving-brush posture is more stable during compaction, that arms in the open position are easier to remove than arms in the shaving-brush configuration, or that crinoids that adopted the shaving-brush posture prior to burial were harder to scavenge than crinoids in other positions, leaving the arms of crinoids with a shaving-brush posture undisturbed. There also appears to be a positive correlation between the shaving-brush position and lateral compaction, although it is possible that this is the result of the influence of compaction on specimen completeness, with taxa not dominated by lateral compaction more likely to lack arms.

The comparative data for other taphonomic features is given in Figure 37. The first observation that must be made is that a sufficient number of relatively well-preserved specimens is required to recognize these taphonomic patterns. *G. ornatus*, for example, is represented primarily by specimens that lack considerable arm segments and

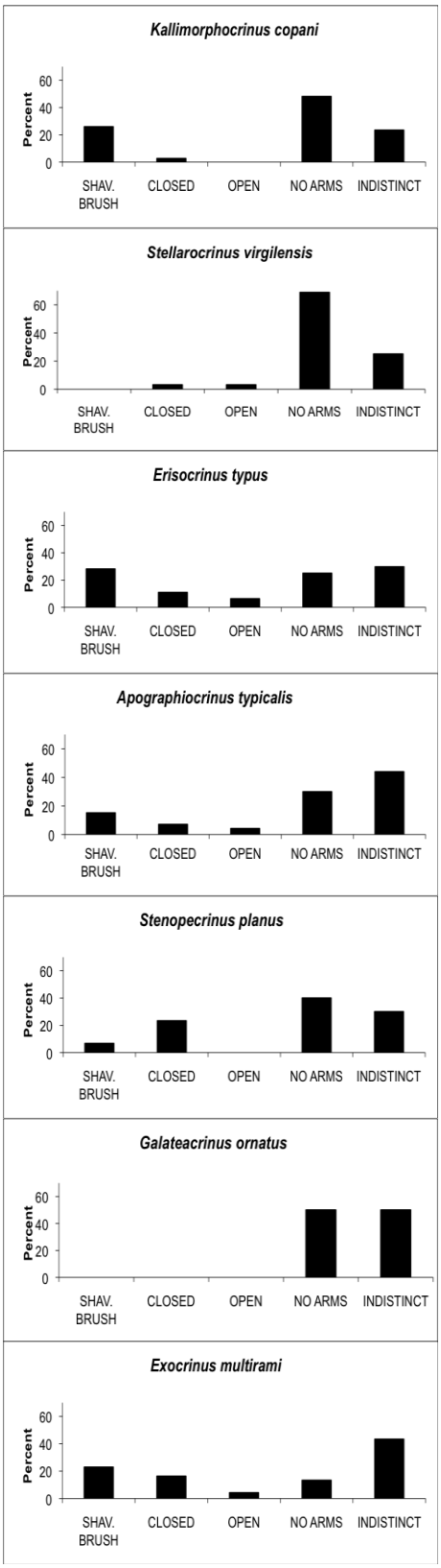

FIGURE 36—Comparison of arm positions for selected crinoid genera. See Figure 27 for examples of arm positions.

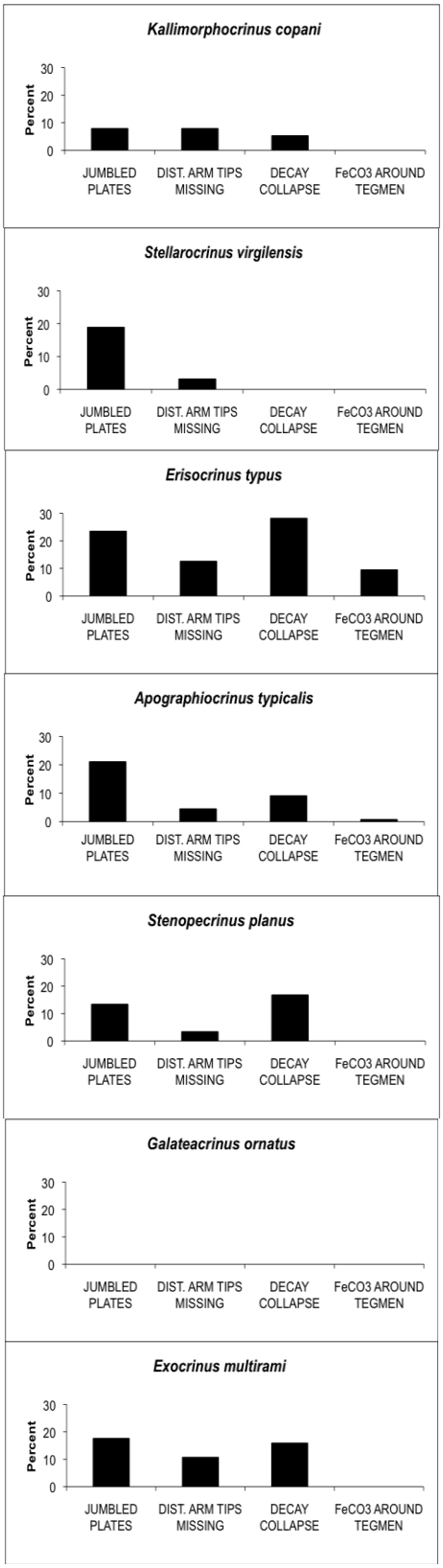

FIGURE 37—Comparison of scavenging- and decay-related taphonomic features for selected crinoid genera. See Figure 28 for examples of features.

are therefore, incapable of displaying any of the selected taphonomic features. Among those taxa with enough well-preserved specimens, the distribution of scavenging- and decay-related features appears heavily influenced by size, with many features occurring only in large taxa or large individuals within a population of typically smaller specimens. This is best exemplified by the development of localized siderite concretions only on *E. typus*, one of the largest common crinoid genera, and on particularly large specimens of *A. typicalis*. Seemingly, only these large individuals contained the large visceral mass necessary for the production of substantial decay gases required for generation of a siderite concretion nucleated on the site of soft tissue. The patterns of decay-induced collapse of proximal arm plates parallel this trend, presumably for the same reason; only those individuals with considerable viscera would create a cavity into which overlying plates could collapse. *E. typus* and, somewhat surprisingly, *S. planus* are the most affected by this feature, although large specimens belonging to *A. typicalis* and *E. multirami* also exhibit this attribute. The loss of distal arm tips is fairly ubiquitous, but most greatly affects *E. multirami* and *E. typus*. This loss suggests that some minor decay may have occurred prior to final burial of many specimens recovered from the Main Crinoid Bed. The jumbling of arm plates is the most common of noted taphonomic features, and occurs in most of the common taxa regardless of size. Although some of this jumbling may be the result of firm objects (e.g., siderite concretions, skeletal material) pushed into crinoid specimens during compaction, the consistent occurrence of disturbance at the proximal arms, while distal arms are left intact, strongly suggests the influence of scavenging activity.

Evidence indicates that scavenging occurred at the sediment-water interface in

many cases but after shallow burial in other cases. A number of crinoid crowns and arm segments are found with one side nearly perfectly intact, with the other side significantly jumbled (Fig. 38). This is interpreted as resulting from partial burial, where the exposed side underwent biostratinomic jumbling, leaving the buried side undisturbed. This indicates that some burial events were sufficiently thin to only partially bury crinoid skeletons. Meyer and Milsom (2001) attribute this mode of preservation almost exclusively to environments where a microbial mat can become established over crinoid remains; however, the thoroughly biotubated sediment, abundant endobenthic fauna, lack of mineralized or carbonaceous coating on crinoid specimens, and evidence for post-burial disturbance argues against the development of a microbial covering on Copan specimens.

Evidence for post-burial scavenging comes from several crowns with complete cups, extensive jumbling of arm plates, and long, randomly oriented tegminal spines (Fig. 39). Although these specimens may seem similar to dozens of other crinoid fossils, consideration of the highly porous nature of fresh crinoidal material (Savarese et al., 1997), especially the delicate and lightweight spines of pirasocrininds (R. D. Lewis, pers. comm., 2009), makes numerous long spines unlikely to remain in close association to a crown that had disarticulated at the sediment-water interface; at the very least, the spines would be likely to become somewhat aligned. Instead, this argues for scavenging below the sediment-water interface, where jumbling of arm plates and re-orientation of spines could occur, with the overlying sediment preventing entrainment of the delicate spines.

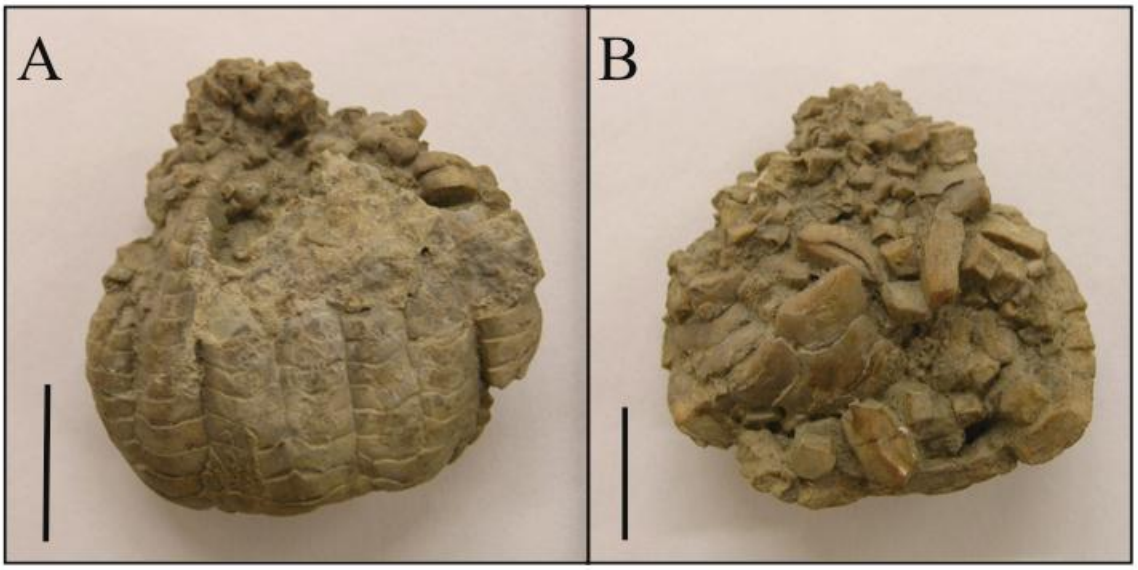

FIGURE 38—Example of crinoid (*Paramphricrinus*) material exhibiting contrasting taphonomic states on opposite sides of a single specimen. A is completely articulated, with arms intact, while B is jumbled and disarticulated. This is evidence of partial burial, in this case, with side A covered and side B exposed to physical and biological disruption. Scale bars = 1 cm.

FIGURE 39—Partially disarticulated pirasocrinid (likely *Polygonocrinus*) crown discovered in the Main Crinoid Bed. The cup is completely intact, as are a number of the long, extremely delicate spines (marked by arrows), while the rest of the crown is disarticulated. The occurrence of spines in such proximity to a (selectively) disarticulated crown, as well as their random orientation, indicate post-burial scavenging, as the spines would be prone to transportation or alignment if not covered by sediment. Scale bar = 1 cm. Photograph provided by R. D. Lewis.

MUDSTONE DISAGGREGATION

Methods

Mudstone samples that were too small to yield sedimentary fabric data, samples that provided unusable fabrics due to excessive fracturing, and completely unlithified samples were physically disaggregated in order to provide information on the amount and size distribution of skeletal material and crinoidal material present at various horizons, as well as the taphonomic character of completely disarticulated crinoids represented solely by isolated ossicles. Samples were dry-weighed and then immersed in kerosene for a period of one day, which served to break the electrostatic bonds between clay minerals. After this period, the solvent was drained off and an equal volume of water was immediately added, after which the sample was allowed to stand for another day. Allowing the material to remain immersed in water for a longer period resulted in more complete disaggregation. At this point, the samples had become thoroughly disaggregated and consisted of a dense slurry of clastic mud and fossil material. This material was passed through 3.0-, 2.0-, 1.0-, and 0.5-mm sieves, with all fossil material collected and weighed, thus providing a crude weight-based size distribution for skeletal material at each horizon within the sampled interval. This approach is utilized in favor of Mosher's processing technique due, in part at least, to recent studies by Kidwell et al. (2001) and Bush et al. (2007) demonstrating that the use of a series of size classes to recognize taphonomic patterns is more accurate than the use of a single minimum size

cutoff.

The fossil-rich residue for each size class from each sample was picked for crinoid material using a standard low-magnification optical microscope, with the crinoidal material weighed to provide information on the relative weight-distribution of crinoid ossicles. For the >3 mm and 2-3 mm size classes, all crinoid material was picked and identified as representing pluricolumnals, columnals, crown plates (brachials, cup plates, and elements of the tegmen), or arm segments. Individual ossicles were inspected for signs of breakage and encrustation (e.g., serpulid worm tubes, bryozoans). Fragments consisting of several articulated ossicles were counted and taphonomically categorized as showing signs of "minor articulation." Pluricolumnals were searched for any offset between adjacent component columnal plates, which may indicate incomplete decay of connective ligaments prior to compaction. Examples of these taphonomic features are shown in Figure 40. Material in the 1-2 mm and 0.5-1 mm size fractions was assessed using a similar methodology, although large samples utilized a sample splitter to create a sample size suitable for microscopic analysis. The crinoid component of these smaller size fractions was weighed, but underwent no taphonomic analysis or identification, primarily because the identity of individual ossicles became difficult with such minute specimens, and also because multi-ossicle elements (e.g., pluricolumnals, arm segments) might be "double-counted" with the majority component counted as part of the larger size class and the minority component counted as part of the smaller size class. The data from these disaggregations were standardized to allow comparisons between horizons, with skeletal material and crinoidal material weight given in grams per kilogram of sample (essentially per mil), and taphonomic attributes given in number of specimens (ossicles or

FIGURE 40—Examples of taphonomic attributes documented on crinoid material greater than 2 mm recovered from mudstone disaggregation. A) Exterior surface of *Apographiocrinus typicalis* radial plate encrusted by serpulid worm tubes; scale bar = 0.5 mm. B) Interior surface of ossicle in A, showing encrustation that could only have occurred after death and disarticulation of crinoid; scale bar = 0.5 mm. C) Columnal plate exhibiting breakage (and encrustation as well); scale bar = 1 mm. D) Examples of "minor" articulation in the form of pluricolumnals on the left and arm segments (*Apographiocrinus*?) on the right; scale bar = 2 mm. E) Pluricolumnals exhibiting offset between adjacent columnals; scale bar = 1 mm. See text for further explanation.

multi-ossicle segments) exhibiting each feature per kilogram of sample.

Results and Discussion

The raw data from mudstone disaggregation is in Appendix 1, and all values in this section represent averages obtained from multiple samples per sampled horizon. Figure 41 shows the relative abundance of skeletal material and crinoid material throughout the microstratigraphic section. Although there is some variability, the values are all within a fairly narrow range. Peaks in skeletal material are present at the Main Crinoid Bed and Bed 3; interestingly, Bed 1 is represented by relatively low fossil-material values, although this may be the result of one particularly fossil-poor sample. This seemingly reflects the increased stratigraphic condensation of the thinner units relative to the thicker units. The abundance of crinoid material is also variable but comparable between all horizons, with the highest values occurring within Bed 1, Bed 3, and lower Bed 4. The Main Crinoid Bed is represented by a relatively small amount of crinoid material. While this may seem surprising, it is likely the result of sampling bias, with blocks containing long lengths of column or partial crowns spared from disaggregation. The presence of similar values of skeletal and crinoidal material directly above and below the thinner units provides strong evidence that the Main Crinoid Bed, Bed 1, and Bed 3 do not represent allochthonous assemblages transported downslope and eventually buried by density currents or slides. Rather, they represent true shifts in faunal composition and taphonomic state within a single environment. In addition, these data provide further evidence that the thinner units are not simple shell concentrations

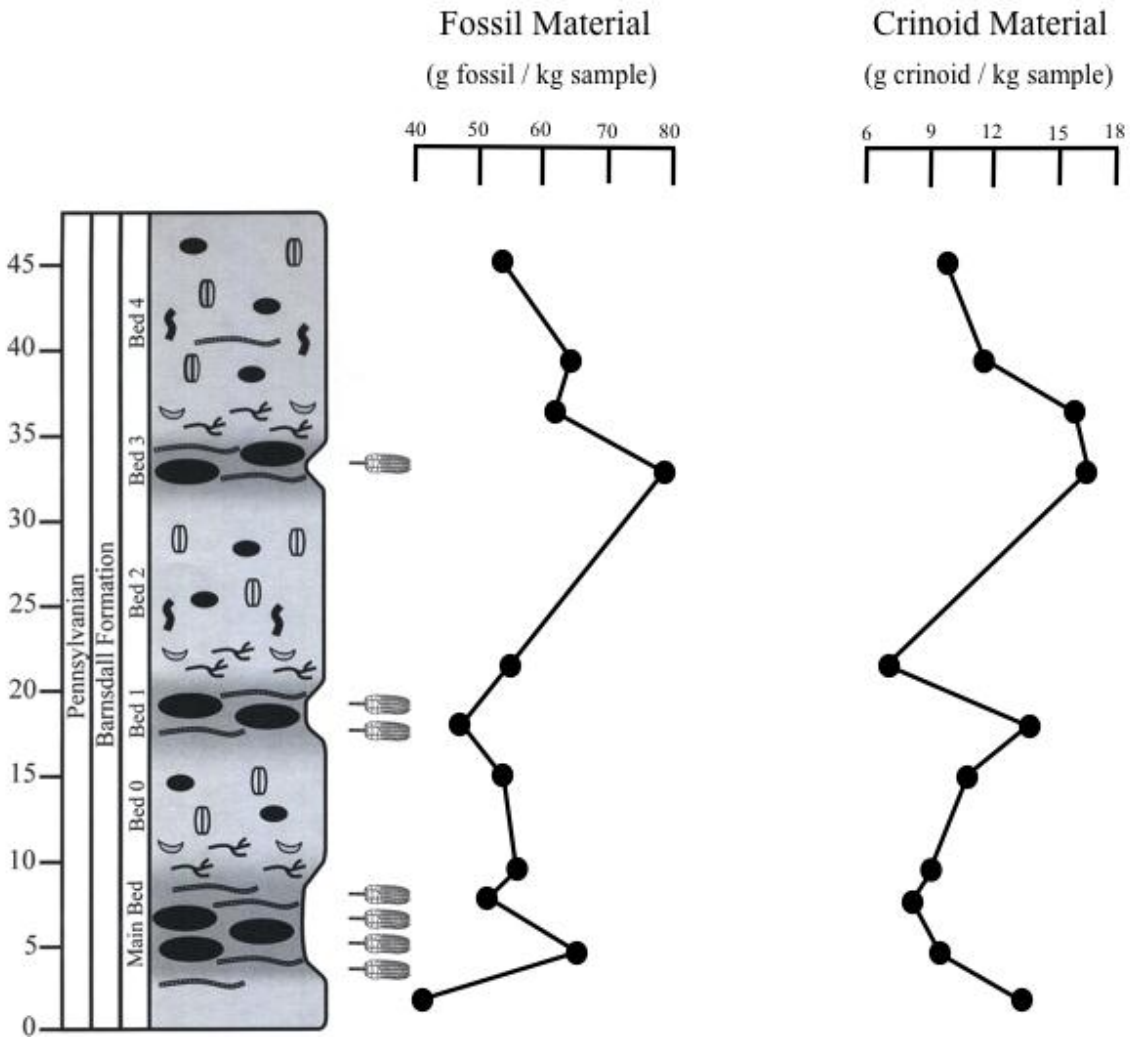

FIGURE 41—Values of skeletal material and crinoidal material at selected horizons within the microstratigraphic section. Note the different scales for each graph. Although there is variability in both graphs, values are generally comparable between all sampled horizons.

generated by winnowing of "normal" conditions represented by the thicker units.

Analysis of the size distribution of skeletal and crinoidal material, shown in Figure 42, reveals some interesting, if difficult to interpret, patterns.

It is clear that there is often a poor correspondence between the values of all fossil material and purely crinoidal material for a given size class. In fact, the values for crinoidal material from all size classes are fairly similar, while the corresponding values for all fossil material tend to vary greatly, indicating that shifts in the size distribution of non-crinoid skeletal grains (i.e., large productid brachiopod valves, small fenestrate bryozoan debris) holds greater control over the size distribution and general fossil density for a given horizon. For example, the transition from the top of the Main Crinoid Bed to the bottom of Bed 0 and the transition from Bed 1 to the bottom of Bed 2 are characterized by a drastic increase in fossil material greater than 3 mm, while the crinoid component undergoes a decrease (Fig. 42). This reflects the increase in large tubular sponge fragments and productid brachiopod shell material associated with the intervals directly overlying the thinner units (see discussion of fabric analysis above). Why this pattern is not observed above Bed 3 is unclear.

In addition, there is an absence of grading within any units; in fact, the >3 mm class and 0.5-1 mm class are most often very similar. The poorly sorted and ungraded nature of this sediment argues against interpretation of the thinner units as single event deposits, although the effects of bioturbation must also be taken into account. Poorly sorted crinoid-rich debris has been reported from the living site of deep water crinoids by Améziane-Cominardi and Roux (1987), Fujita et al. (1987), Messing et al. (1990), Llewellyn and Messing (1993), Messing and Rankin (1995), and Messing (1997),

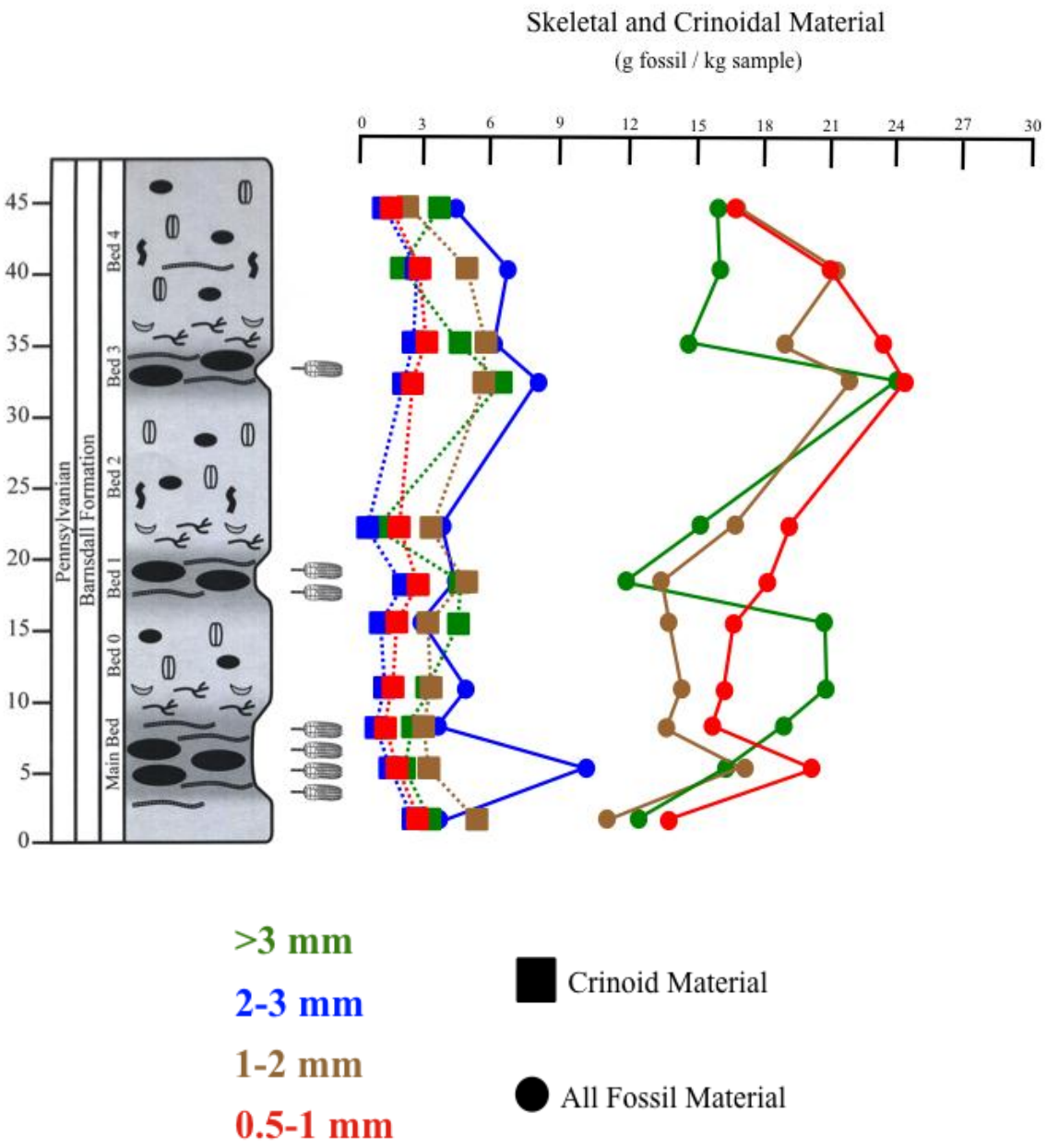

FIGURE 42—Size distribution of all fossil material and crinoid material throughout the microstratigraphic section. Note the general similarity of crinoid material values compared to the disparity of the overall fossil values, as well as the absence of complete agreement between shifts in crinoid values and overall fossil values.

indicating that the Copan deposit bears the sedimentologic signature of autochthony (or parautochthony) derived from modern analogs. In general, however, little other information of interpretive value can be extracted from analysis of the size distribution of bioclasts without consideration of other factors, such as taxonomic identity and taphonomic state of skeletal grains.

The stratigraphic distribution of crinoid bioclasts greater than 2 mm, given in Figure 43, may help to explain at least some of the patterns observed in Figure 42. Of particular interest is the interaction between the abundance of pluricolumnals and columnals, which display nearly identical trends. This suggests that the thinner units are not necessarily enriched in pluricolumnals relative to columnals, contrary to preliminary results presented by Thomka et al. (2010), who reported an increased in pluricolumnals and a decrease in individual columnals within the thinner units. Instead, the dominance of both pluricolumnals and columnals in the thinner units may simply indicate the overall enhanced abundance of crinoid columns, which have disarticulated to different degrees under different burial processes (i.e., some completely disarticulated under background conditions, some partially disarticulated before burial). The increase in pluricolumnals throughout Bed 4 is unusual, and is only detected in the crinoidal material greater than 3 mm data in Figure 42. Perhaps a solitary partially articulated column was within one of the disaggregated blocks from this typically poorly fossiliferous interval.

The distribution of arm segments is also unusual, in that all horizons are relatively poor in arm segments except for the upper Main Crinoid Bed, which contains nearly five times as many as the next highest unit. This may reflect rapid burial of crinoids shortly before the increase in sedimentation rate, leaving them undisturbed.

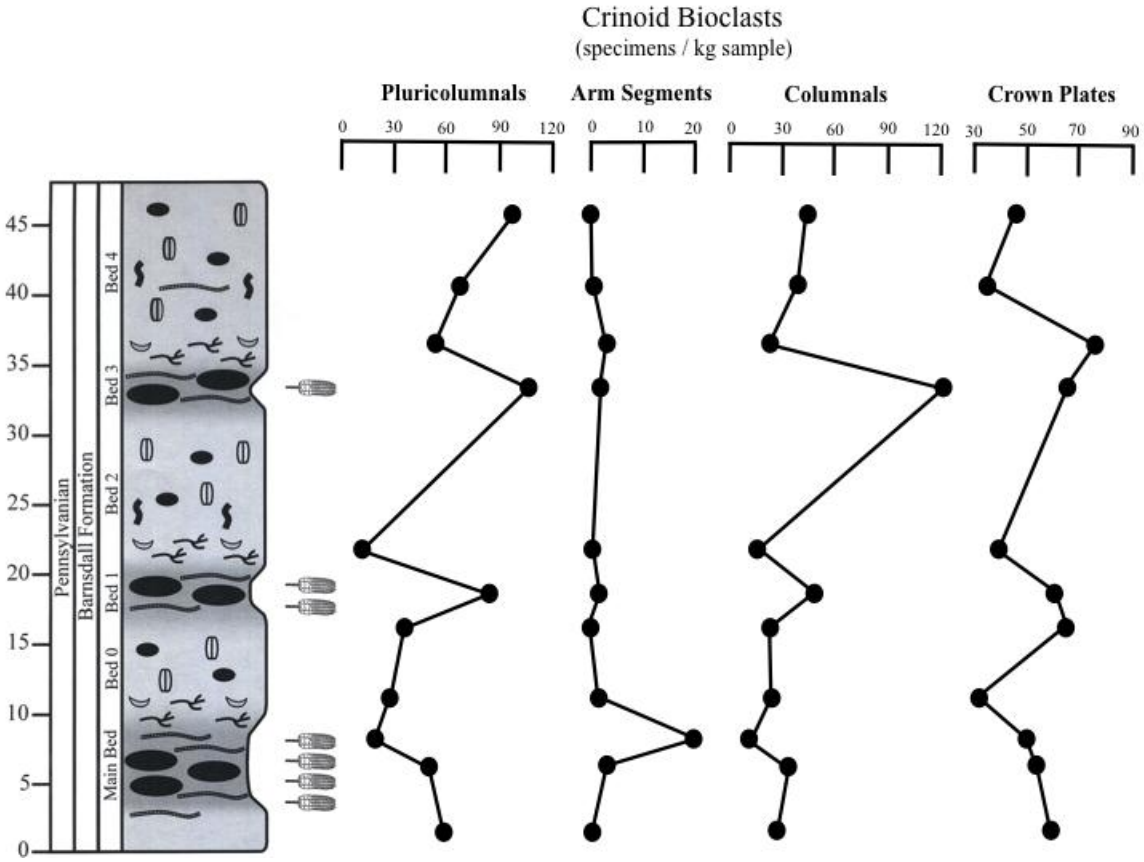

FIGURE 43—Distribution of crinoid bioclasts within the microstratigraphic section. Note the different scales for each category.

Consequently, the increase in arm segments occurred at the same horizon as a somewhat unexpected decrease in pluricolumnals, resulting in the lack of a peak in crinoid material greater than 3 mm (Fig. 42). Again, sampling must be taken into account here, as blocks known to contain crinoid crowns were not disaggregated, making the values for arm segments within the thinner units gross underestimates.

Data on the distribution of crown plates is particularly unusual, as peaks are absent from all three of the thinner units, in sharp contrast to practically all other attributes documented for disaggregated samples. Instead, peaks are present beneath the Main Crinoid Bed and Bed 1 and in lower Bed 4. The reason for this is unclear, but it likely reflects the dominance in the thinner units of small crinoid taxa (most notably *Kallimorphocrinus*, *Exocrinus*, and *Apographiocrinus*), whose crowns would disarticulate into ossicles smaller than the 2-mm minimum for identification and counting, but would still contribute to overall crinoid abundance. Indeed, Figure 42 shows that the 1-2 mm size fraction of crinoidal material increases dramatically from upper Bed 0 to Bed 1, and from Bed 2 to Bed 3.

The distribution of taphonomic attributes of crinoidal material greater than 2 mm, given in Figure 44, produces several interesting results. Encrustation appears to have been a significant process throughout deposition of the entire section, perhaps due to the possibility of encrustation prior to death of the host organism; nevertheless, pronounced peaks are present at all three of the thinner units. This provides further strong evidence that these units accumulated over a long period of time, in an environment characterized by low turbidity, low sedimentation rates, and oxygenated conditions (e.g., Parsons and Brett, 1991). Furthermore, in an actualistic study of echinoid comparative taphonomy,

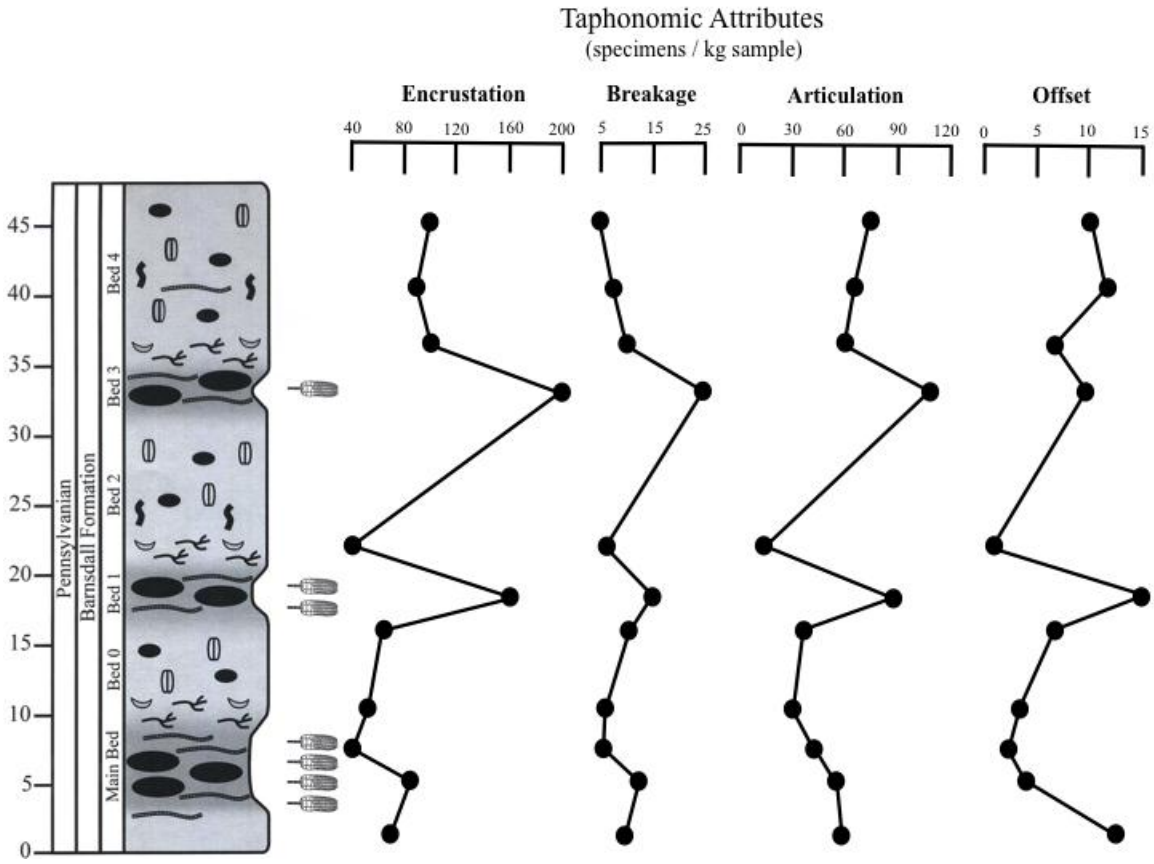

FIGURE 44—Distribution of taphonomic features throughout the microstratigraphic section. Note the different scales for each attribute, and that only bioclasts larger than 2 mm were counted.

Nebelsick (1999; see also Nebelsick et al., 1997) found that the only taphofacies dominated by encrustation of tests was a sediment-starved marine shelf environment.

Although values of breakage were consistently low throughout the section, there are minor peaks at the thinner units. This may seem at odds with the numerous indicators of these units as low energy environments. However, ossicle breakage does not necessarily have to result from physical reworking or turbulent events; instead, this may reflect the long-term destructive influence of biological activity (e.g., microboring) on skeletal material exposed at the sediment-water interface (Brett and Baird, 1986). Another possible explanation is that the large amount of fossil material and siderite in the thinner units, coupled with intense post-depositional compaction, led to increased breakage by skeletal grain-to-skeletal grain and skeletal grain-to-siderite concretion contact in the subsurface.

Trends in articulation parallel those of many of the other attributes documented in that distinct peaks are present at Bed 1 and Bed 3. This apparently reflects the abundance of pluricolumnals in these units shown in Figure 43. Interestingly, the previously discussed, unexplained increase in pluricolumnals in upper Bed 4 is evident in the articulation data, as Bed 4 is characterized by a relatively steady rise in articulated multi-plate crinoid fossils. Also of interest is the apparent lack of influence by the greatly increased number of arm segments in the upper Main Crinoid Bed (Fig. 43) on overall articulation value. The lack of a peak in articulation within the Main Crinoid Bed is consistent with previous results, although in this attribute, there is not a distinct valley either.

Evaluation of trends in offset skeletal material is intimately tied to patterns of

articulation, as only articulated material can exhibit offset between adjacent ossicles. As a result, the values of crinoidal material displaying offset must be interpreted with caution. While there is a distinct peak in offset at Bed 1, this likely reflects the abundance of pluricolumnals relative to surrounding units. A more informative approach is to compare the abundance of offset material between Bed 1 and Bed 3, which have been shown to be taphonomically and compositionally comparable (Figs. 41-44). The lack of a peak in Bed 3 may suggest that Bed 1 has indeed experienced greater compaction than at least some of the other sampled units. The greater number of crinoid remains that underwent partial disarticulation prior to or concurrent with shallow burial, and then were disrupted such that adjacent ossicles were shifted out of alignment, provides the evidence. Why Bed 3 did not experience similar values of offset, or even greater numbers, given its decreased thickness relative to Bed 1, is unclear. It may be related in some way to the increase in pluricolumnals in Bed 4, although this is purely speculative (Fig. 43).

SIDERITE CONCRETION ANALYSIS

Background and Methods

Siderite ($FeCO_3$) within the stratigraphic section near Copan is present as abundant concretions of various sizes and shapes, present in all horizons but generally concentrated in the three horizons containing articulated crinoid fossils. The term concretion is favored over nodule, following Sellés-Martínez (1996), who defined a concretion as an authigenic precipitate that incorporates clastic material during growth and stands out from its host sediment.

Studies of modern marine sediments (e.g., Presley and Kaplan, 1968; Nissenbaum et al., 1972; Claypool and Kaplan, 1974; Sayles and Manheim, 1975; Froelich et al., 1979) show that, in a typical setting, aerobic oxidation occurs in the uppermost few centimeters of sediment, with porewater anoxia and reducing conditions occurring deeper in the sediment profile. Within the zone of anoxia, microbes utilize a series of alternative oxidants to break down organic matter in the absence of porewater oxygen, resulting in a layering of subsurface redox zones, each of which is defined by a unique community of microbes that produce a unique set of products, in addition to the ubiquitous production of bicarbonate (Coleman, 1993). The vertical sequence of redox zones is controlled by Gibb's free energy yield, with those oxidants that are most efficient at shallower depths, and those that are less efficient at greater depths beneath the sediment-water interface and utilized only after more efficient oxidants are completely depleted (Claypool and Kaplan,

1974; Froelich et al., 1979). The descending redox zonation in an ideal setting consists of manganese reduction, nitrate reduction, ferric iron reduction, sulphate reduction, methanogenesis, and, at relatively great depths, thermal decarboxylation (Coleman, 1993; Fig. 45). Precipitation of siderite requires (1) abundant carbonate, accomplished by production of bicarbonate, (2) ferrous iron ions, produced by direct reduction of ferric iron by anaerobic bacteria or inorganic reduction by reaction with hydrogen sulfide, and (3) alkalinity, produced by bicarbonate generation (Coleman, 1993), and also by ammonia given off during decay of organic matter (Berner, 1968; Allison, 1988a). Therefore, siderite can only be precipitated in a narrow subsurface zone where ferric iron reduction, sulphate reduction, or methanogenesis can operate (Fig. 45).

In both modern and ancient deposits, siderite is most commonly precipitated in environments characterized by fresh or brackish water because the low values of dissolved sulphate in these waters limit sulfide mineral precipitation. In these settings, the zones of ferric iron reduction and methanogenesis are most important to siderite precipitation, with sulphate reduction of less significance (e.g., Fritz et al., 1971; Baird et al., 1986; Fisher et al., 1998; Choi et al., 2003). In contrast, anoxic marine sediment is dominated by sulphate reduction due to the large amount of sulphate in seawater and, in some cases, a lack of reducible iron minerals. In modern marine environments ferric iron reduction plays only a minor role in authigenesis (Martin and Sayles, 2004), leading to precipitation of pyrite over other ferrous minerals, including siderite. The occurrence of siderite in undeniably marine environments is, therefore, an unusual occurrence.

Despite the predicted exclusion of ferroan carbonates in the presence of sulfides (Curtis and Spears, 1968; Berner, 1981b; Maynard, 1982), siderite concretions are often

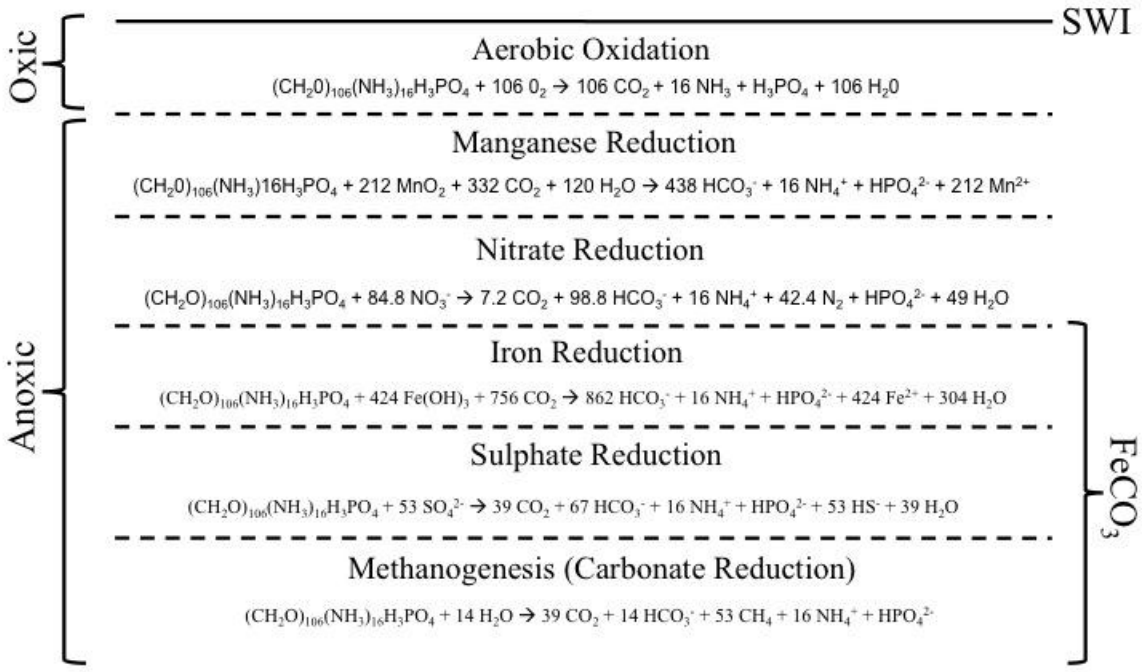

FIGURE 45—Subsurface redox facies in an idealized sediment profile. Note the relatively narrow zone in which siderite can be precipitated; in fresh or brackish water settings, iron reduction and methanogenesis are the dominant processes and in marine settings, sulphate reduction is the dominant process in siderite genesis. SWI = sediment-water interface. After Allison (1988b) with formulas from Berner (1981a).

intimately associated with pyrite (e.g., Sellwood, 1971; Coleman and Raiswell, 1981; Curtis et al., 1986; Carpenter et al., 1988; Coleman, 1993; Laenen and De Craen, 2003; and others), indicating that sulphate reduction may play an important role in siderite precipitation, but only under specific conditions. Sellwood (1971; see also Shannon, 1977) developed a model for the precipitation of marine siderite bands within the zone of sulphate reduction based on work with Jurassic strata of England. In this model, low sedimentation rates and oxidizing shallow substrates lead to organic-poor sediment and concentration of iron, most likely in the form of iron oxy-hydroxides (Berner, 1984; Coleman et al., 1993). Subsequent increases in sedimentation effectively formed a seal between buried sediments and the sediment-water interface, preventing exchange of sulphate-rich seawater with porewater. This resulted in porewater that was enriched in ferrous iron and lacking in sulphate (and, hence, sulfide). Sulphate reduction operating on the limited amount of porewater sulphate yielded small volumes of sulfide, which reacted to form minor amounts of disseminated pyrite; once the sulphate was depleted, the ferrous iron was able to react with carbonate to form considerable amounts of siderite.

The model of Sellwood (1971) explains the co-occurrence of siderite and pyrite, as well as the common volumetric dominance by siderite over pyrite and the sequence of mineral precipitation (i.e., pyrite first, siderite after). However, an alternative mechanism for marine siderite precipitation was identified through work with modern siderite-dominated concretions forming in the tidal marshes of North Norfolk, England (Pye, 1981; Pye et al., 1990; Coleman et al., 1993; Allison and Pye, 1994; Duan et al., 1996), where it has been shown that particular species of marine sulphate-reducing bacteria are directly reducing ferric iron enzymatically, rather than through indirect reaction with

hydrogen sulfide. The implication of this discovery is that the poorly understood preferences of archaic anaerobic bacteria may lead to precipitation of unexpected minerals or mineral assemblages; indeed, in this setting, pyrite should be forming and siderite should be excluded. Why the sulphate-reducing bacteria are not using their typical chemical substrates is a source of ongoing research, but it is possible that the occurrence of marine siderite in at least some ancient deposits may have resulted from an alteration of the behavior of sulphate-reducing bacteria, rather than variations in inorganic processes.

A third mechanism for marine siderite genesis involves competitive inhibition of sulphate-reducing bacteria by metal oxide-reducing bacteria, more specifically iron-reducing bacteria. Work by Lovley and Phillips (1987) and Chapelle and Lovley (1992) has shown that microbial iron reduction can dominate and actually drastically decrease sulphate reduction in environments characterized by oxygenated bottom water, low organic matter contents, high iron oxide contents, and intense bioturbation. Work with modern sediments by Aller et al. (1986) and Canfield et al. (1993) provides support for this model: apparently, biogenic reworking of the substrate serves to continually reintroduce oxygenated waters, thereby re-oxidizing iron that had been reduced. In this way, oxidants (iron, in the form of iron oxy-hydroxides) are replenished, while organic carbon and hydrogen sulfide are depleted. This may lead to actual exclusion of communities of sulphate-reducing bacteria (favored by Lovley and Phillips [1987] and Chapelle and Lovley [1992]), or it may allow sulphate-reducing bacteria to remain, but continued (re)oxidation of sulfide minerals, over significant periods of time, may lead to their exclusion from the sedimentary deposit (favored by Aller et al. [1986]).

In summary, the precipitation of siderite in marine deposits, although unusual and relatively rare, becomes possible as a result of bacteria operating in an anoxic, but nonsulfidic, environment (Berner, 1981b, Maynard, 1982). More specifically, marine siderite can form through (1) restriction of dissolved sulphate within the zone of sulphate reduction, (2) altering the behavior of (sulphate-reducing?) bacterial communities, or (3) competitive inhibition of sulphate-reducing bacteria by ferric iron-reducing bacteria. Which of these mechanisms is responsible for the early diagenetic siderite in the Copan deposit is unknown, making an increased understanding of this atypical mineral occurrence an important, if somewhat indirect, goal of this study.

The genesis of siderite has the potential to provide evidence of unique environmental parameters that may have influenced crinoid paleoecology and taphonomy. Since the siderite was formed prior to significant sediment compaction, the fabric preserved in concretions may be a more accurate source of data than the matrix sediment, which has undergone considerable compaction. Therefore, concretions that had been collected during previous field investigations, including some that had been cut perpendicular to bedding, were examined with a binocular microscope for any surface or internal features that may provide information on depositional history, including evidence for post-formational exposure and reworking (e.g., borings, encrusting organisms, holdfast structures) and any discrete physical or biogenic sedimentary structures not preserved in mudstone samples. Siderite samples were inspected for associated minerals, as the occurrence of pyrite may shed light on timing of concretion precipitation and, more importantly, may allow elucidation of the mechanism responsible for genesis. In addition, siderite concretion morphology was documented as part of the

microstratigraphic analysis (see above), with special attention paid to understanding the sedimentary processes responsible for each morphology.

Results and Discussion

Despite the ubiquitous occurrence of siderite in the Copan section (Fig. 9), concretion morphologies are variable and are distributed nonrandomly throughout the microstratigraphic section. Four morphologies of siderite concretions are recognized in this study: (1) large concretions lacking a distinct fossil nucleus; (2) small concretions, commonly enclosing a single fossil; (3) large-diameter sideritized burrows; and (4) small concretions nucleated around the sites of soft tissue on macrofossils. Each morphology reflects a different process or parameter, and the distribution of these morphologies allows temporal shifts in paleoenvironmental setting to be recognized.

Large siderite concretions occur within the thinner units and are, in fact, essential to locating these horizons in the field (Lewis et al., 1998). Estimating the average diameter of these concretions is difficult, as several smaller concretions may coalesce to form a larger concretionary body; likewise, a single (or coalesced) concretion may weather into several smaller portions. Although the horizons bearing these large concretions are readily visible due to the enrichment in iron staining and a nodular texture, concretions do not coalesce to the point of forming a well-cemented carbonate layer, and are always contained within a mudstone matrix. Diameters of up to 25 cm for single concretions are observed relatively commonly (Fig. 46A). Concretions are rarely, if ever, spherical, and have a long axis parallel to bedding, a feature which has typically been interpreted to indicate minor compaction during concretion formation (Seilacher,

2001).

Inspection of concretion exteriors reveals a total absence of bioerosion structures and encrusting organisms, including the serpulid worm tubes that are so abundant on disarticulated crinoidal material (Fig. 44). Furthermore, abrasion or signs of erosion are absent from concretion exteriors, and reworked siderite clasts are not found incorporated into the surrounding mudstone. Collectively, these observations indicate that the siderite concretions were not exposed at the sediment-water interface after precipitation. Inspection of concretion interiors on slabbed samples provided strong evidence of an early diagenetic origin, confirming interpretations by Lewis et al. (1998). This evidence includes abundant brachiopod fossils preserved uncrushed and articulated (Fig. 46B), in sharp contrast to the same fossils found severely compacted and/or disarticulated within the associated mudstone, as well as partially articulated crinoid crowns, some with splayed arms. This indicates that siderite precipitation began shortly after burial of the organisms and occurred in the still fluid-rich upper layers of sediment. Concretions are generally fossiliferous and contain a fossil assemblage identical to that of the surrounding mudstone. Interestingly, despite containing abundant skeletal material, large concretions do not appear to contain a distinct skeletal nucleus that initiated siderite precipitation; instead, fossils are scattered throughout the concretion and appear to have been preserved incidentally (sensu Hall and Savrda, 2008) as the concretion grew and incorporated surrounding sediment (Fig. 46C). This may mean that all or most of the enclosed fossils collectively served as a nucleus, or that the fossil material collectively served to concentrate anaerobic bacteria, leading to siderite precipitation. The latter interpretation appears to be supported by work by Raiswell (1976) and Canfield and Raiswell (1991),

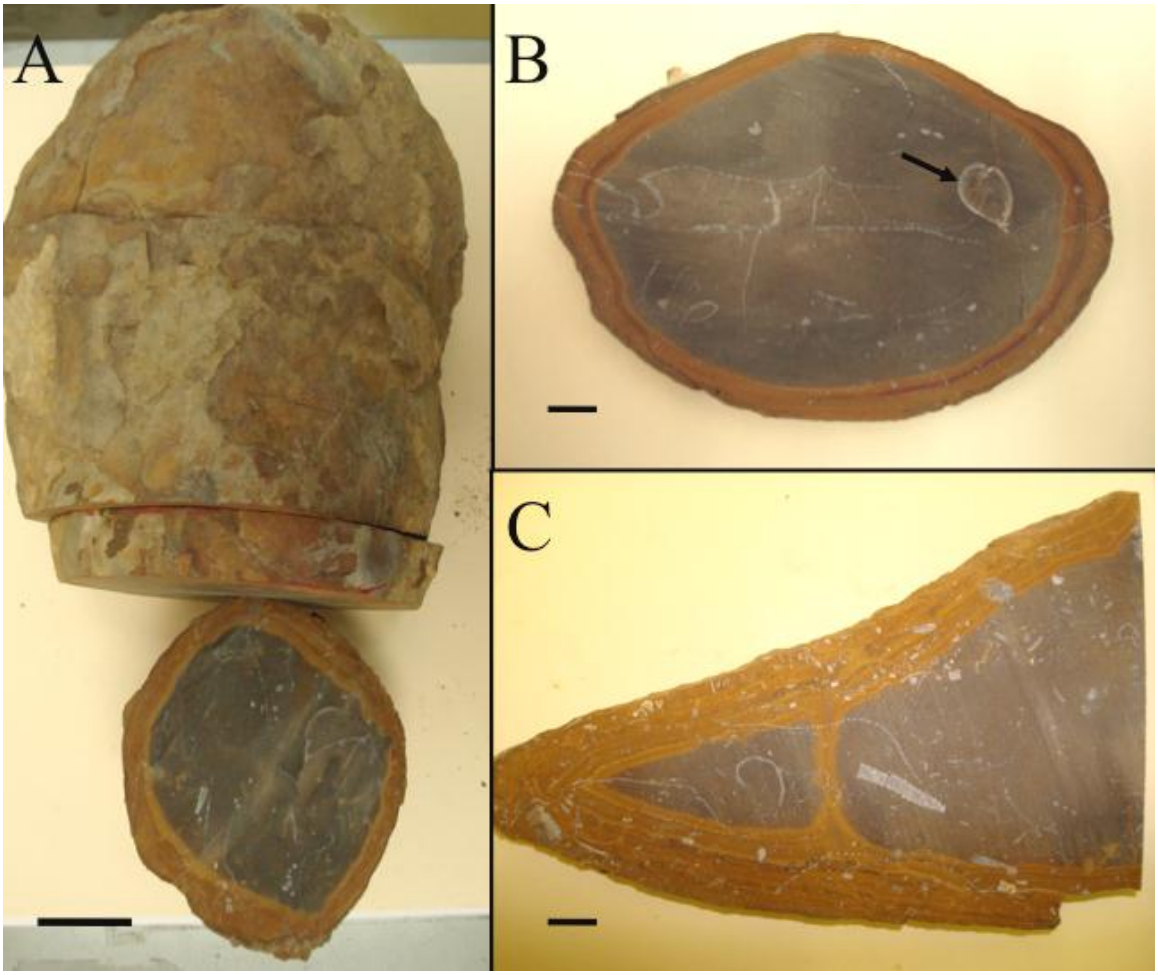

FIGURE 46—Attributes of large siderite concretions found within the the Main Crinoid Bed, Bed 1, and Bed 3. All pictured samples are from the Main Crinoid Bed. A) Partially slabbed concretion demonstrating exceptional size and bedding-parallel long axis; scale bar = 5 cm. B) Cross-section through concretion exposing an articulated and uncompacted brachiopod that would likely be found crushed if not preserved within an early diagenetic concretion; scale bar = 1 cm. C) Partial cross-section through concretion containing abundant scattered skeletal grains, but lacking a single fossil nucleus; scale bar = 1 cm.

who calculated that the amount of bicarbonate produced by the decay of most marine invertebrates is insufficient to produce average-sized concretions, and that bacterial concentration is the most critical step in concretion genesis. Inspection of concretion interiors under a binocular microscope did not reveal any discrete physical or biogenic sedimentary structures preserved as a result of early diagenesis. Seemingly, biogenic homogenization of sedimentary fabric was pervasive enough or substrates were so fluid-rich that there was simply nothing to preserve.

The most significant aspect of the large siderite concretions is simply their large size. Because concretions need time to grow, precipitation of large concretions requires considerable time within a stabilized zone of alkalinity enriched in ferrous iron and bicarbonate. Such requirements exist only in a narrow subsurface zone (Fig. 45), and since methanogenesis was not involved in concretion formation (Lewis et al., 1998), the zone is restricted even further. Since redox boundaries migrate upwards with vertical sediment accretion or erosion, siderite concretions of this size require static and stable redox boundaries for an extended period of time, likely hundreds to a few thousand years (Raiswell, 1987), reflecting little net sediment accumulation or removal. Thus, the occurrence of such large siderite concretions, and their restriction to only the three units bearing articulated crinoids, can only result from sediment starvation operating during deposition of the thinner units.

Smaller siderite concretions are found concentrated within the thicker units. Typical diameters range from 3 to 6 cm, and shapes are generally similar to those of the large concretions, although the smaller concretions are commonly more strongly compacted, resulting in a thickly discoidal shape. As with the larger concretions, no

evidence of post-formational exposure was detected in these concretions despite their co-occurrence with evidence of occasional winnowing and erosion (i.e., lags, sideritized burrows). Smaller concretions frequently contain a skeletal nucleus, most commonly endobenthic bivalves (Fig. 47). Unfortunately, very few concretions of this variety were collected in place, so the orientation of the bivalve fossils (in living position or not) is unknown. Fossil nuclei are generally well preserved, and bivalves always contain both articulated valves (Fig. 47B), again providing evidence that these are early diagenetic in origin. In fact, the occurrence of articulated bivalves at the center of small concretions indicates that the decay of soft tissue generated the ionically reactive, reducing microenvironment required for concretion formation and, therefore, serves as evidence of rapid, thick burial (Allison, 1988a, b). Otherwise, the decaying bivalve would be subjected to aerobic decay and the activity of scavenging organisms.

More importantly, the size of these concretions indicates that insufficient time was spent within the zone of siderite-forming conditions to produce concretions as large as those within the thinner beds. This indicates more transient redox boundaries, reflecting relatively rapid changes in the position of the sediment-water interface as a result of deposition or erosion. Coupled with paleontologic evidence discussed previously, the stratigraphic occurrence of this siderite morpohology indicates considerably higher sedimentation rates in the thicker units relative to the thinner units. Additionally, the more highly flattened shape of smaller concretions may be the result of higher sedimentation rates serving to increase compaction throughout concretion growth.

It is important to note here that no pyrite was observed in association with either the large or small concretions. In environments with oxygenated bottom waters, organic

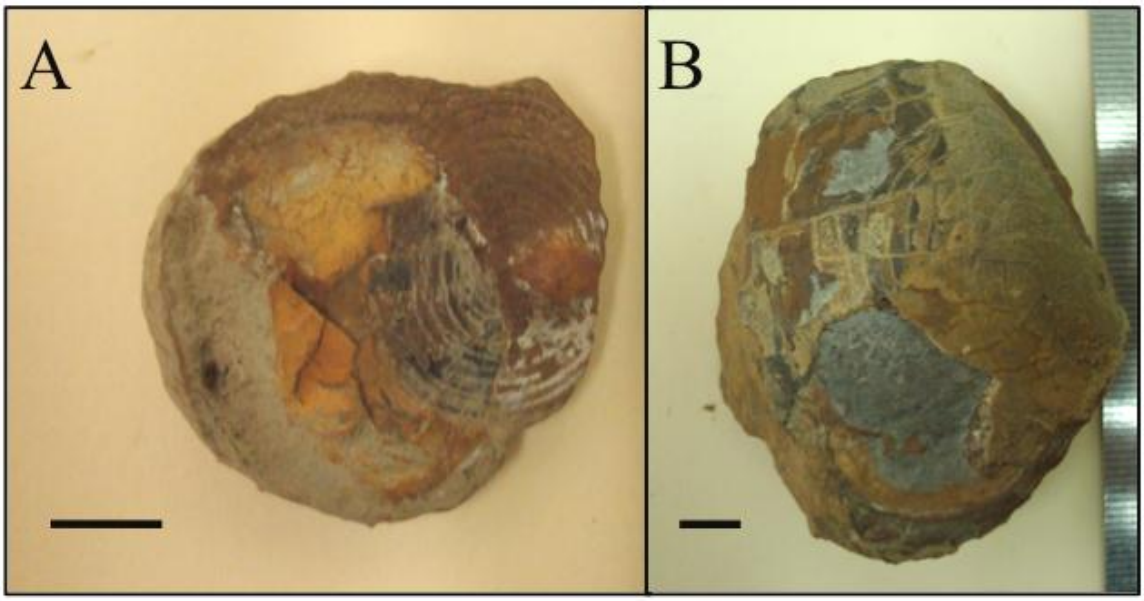

FIGURE 47—Small siderite concretions typical of those abundant within the thicker units. A) Concretion broken to reveal inarticulate brachiopod (orbiculoidid?) nucleus; scale bar = 1 cm. B) Concretion nucleated around a fairly large endobenthic bivalve preserved with both valves present and articulated; scale bar = 1 cm.

matter is rapidly degraded and is distributed unevenly throughout the sediment, resulting in a lack of organic matter concentrations upon entering the diagenetic environment (Berner, 1981). Sulphate reduction in the presence of this irregularly distributed organic matter may precipitate disseminated and scattered pyrite framboids and crystallites, resulting in the eventual precipitation of other ferrous minerals (e.g., siderite) in considerably greater volumes once the sulfide has been depleted, as theorized in the Sellwood (1971) model. One might interpret this as a reason for the absence of pyrite in association with the large concretions, as these may have formed after precipitation of scattered, microscopic pyrite in such a model. However, rapidly buried, generally undegraded carcasses, like those observed serving as nuclei for small siderite concretions, represent concentrations of organic matter. Sulphate reduction, operating within the reducing microenvironment created by the decay of this carcass, will serve to produce appreciable pyrite to the exclusion of siderite, but only in direct association with the localized organic matter concentration—thus, even in deposits where siderite is more dominant, well preserved fossils, steinkerns, and/or burrow fills (representing reducing microenvironments) are often pyritized (Brett and Allison, 1998). The absence of pyrite in association with the endobenthic bivalves within small siderite concretions provides strong evidence that precipitation of marine siderite after depletion of porewater sulfide generated by sulphate reduction is an insufficient explanation for the genesis of siderite in this section.

The occurrence and significance of large sideritized burrows (Fig. 17) have been discussed previously, but the stratigraphic occurrence is worth re-emphasizing: these structures, which indicate minor erosive events, occur only in the thicker units

(specifically, Bed 2 and Bed 4). These units seemingly represent environments where episodic events were energetic enough to remove at least some of the uppermost, fluid-rich sediment.

The fourth siderite morphology occurring within the section under study is directly tied to a fossil nucleus; more specifically, these concretions do not completely enclose fossils, but rather are nucleated only around the sites of soft tissue. Localized concretion development commonly occurs around the proximal arms of articulated crinoid crowns, reflecting decay of the tegmen (Fig. 12D), and as infill of productid brachiopod shells, reflecting the decay of viscera (Fig. 19A). While this may seem similar to the small, commonly bivalve-nucleated concretions described above, there is a considerable difference. In the previously described concretions, siderite completely encloses the fossil, indicating that although decay may have initiated concretion development, concretion growth seemingly continued for some time after the soft tissues had completely decayed. Furthermore, bivalves contain a fairly large volume of soft tissue, making them excellent candidates for sites of reducing microenvironments. Crinoids and brachiopods, however, are noted for their general shortage of visceral mass, making it far more likely that what little soft tissue was present on an individual would be lost to aerobic degradation and/or scavenging before concretion development could begin. Indeed, the results of comparative crinoid taphonomy analysis show that localized concretion development occurs only in large individuals (see above), indicating that few crinoids were capable of generating any siderite through soft tissue decay at all. Likewise, only productid brachiopods, which are the largest of brachiopod taxa within this assemblage, showcase siderite infilling. Those crinoids and brachiopods that did

produce siderite did so only during the period of soft tissue degradation, and thus must have had nearly all of their viscera intact prior to entry into the diagenetic environment. This is interpreted to indicate live burial of some crinoids and brachiopods; only through live burial could the small volume of viscera avoid destruction long enough to generate an extremely localized siderite concretion. This concretion morphology is generally concentrated within the thinner beds, due primarily to the dominance of crinoids and productid brachopods. Where present, however, brachiopods are occasionally found infilled with siderite in thicker units as well.

DEPOSITIONAL HISTORY

Depositional Environment and Pre-Event Paleoecology

Previous investigations have interpreted the depositional environment of the Copan Lagerstätte as a low energy, low turbidity distal shelf environment characterized by muddy substrates and low sedimentation rates (e.g., Holterhoff, 1997a; Lewis et al., 1998). Based on its transitional relationship with underlying dysaerobic facies, Holterhoff (1988, 1997a) interpreted the Copan deposit as being continually or intermittently oxygen-stressed. However, the high diversity macrobenthic assemblage, consisting of both epibenthic and endobenthic organisms, as well as the complete biogenic homogenization of sediment, supports a well-oxygenated seafloor capable of supporting abundant life. The small size of the crinoid taxa within the assemblage, as argued by Pabian and Strimple (1970, 1979, 1985, 1993) and Heckel and Pabian (1981), likely reflects colder bottom water, rather than decreased oxygen levels. Likewise, the apparent dominance of the ichnological assemblage by *Chondrites* reflects depth of burrow emplacement, rather than poor benthic oxygenation. In fact, the presence of *Chondrites* superimposed upon a thoroughly mixed fabric typically argues for oxygenated conditions (Bromley and Ekdale, 1984). Finally, the large number of encrusted skeletal grains within the section suggests well-oxygenated conditions, as epibionts would not be abundant in oxygen-stressed environments.

Despite the somewhat common occurrence of *Chondrites*, presumably made by

organisms occupying the deepest endobenthic tier and the relatively rare large sideritized burrows, the absence of other discrete biogenic structures, including intermediate-tier traces or deep-tier traces other than *Chondrites*, makes the depth of bioturbation unclear. It is possible that numerous other biogenic structures were produced in deep tiers, but infilling sediment does not contrast with host sediment, resulting in poor trace fossil visibility. Consequently, only those structures that were fortuitously infilled with sediment that contrasts in some way with surrounding sediment can be recognized, as is fairly common in muddy shelf deposits (Savrda, 2007; see also Wetzel and Uchmann, 1998). Another possibility involves the excavation of many deep burrows, but their subsequent transformation into a mottled texture following intense compaction, as has been observed with modern micritic sediments (Shinn and Robbin, 1983). Alternatively, the abundance of shell material within these densely fossiliferous units might have precluded deep bioturbation of any kind (inhibitory taphonomic feedback of Kidwell and Jablonski, 1983), although this may depend on how long skeletal remains have had to accumulate on the seafloor, and must also account for pre-compaction sediment thickness and its effects on the concentration of fossil material. Speyer and Brett (1986), in a study of a Devonian shell-rich, muddy facies, concluded that bioturbation in such environments is dominated by scavengers, and that thorough bioturbation is the result of the migration of a shallow mixed layer only. Regardless, the depth and nature of bioturbation within this environment remains an unanswered paleoecological question.

There is abundant evidence that the thinner units (Main Crinoid Bed, Bed 1, and Bed 3) represent periods of sediment starvation punctuated by rapid burial events. This evidence includes (1) the dominance of the fossil assemblage by epibenthic suspension

feeders (i.e., crinoids, articulate brachiopods, bryozoans), which require low turbidity and low sedimentation rates; (2) the prominent background assemblage, representing individuals that lived, died, disarticulated, and contributed their skeletal remains to the seafloor sediment over a long period of time; (3) the thorough biogenic mixing of sediment such that nearly no distinct physical or biogenic sedimentary structures remain; (4) the enrichment in fossil material relative to considerably thicker units without any evidence of transportation or deposition as a single event; (5) the abundance of encrusted skeletal grains, which indicate periods of exposure of skeletal material at the sediment-water interface under conditions of low sedimentation; (6) the high number of broken skeletal grains, which may represent biological degradation of hard substrates; and (7) the presence of very large siderite concretions, which can only form through considerable residence time within a narrowly defined subsurface redox zone. Such findings are in agreement with a shift in interpretation of deposits consisting of alternating thin shell-rich units and thicker mud-rich units. Previously interpreted as storm-winnowed lags alternating with quiet background sediments (the "storm-winnowing model"), taphonomic evidence has convincingly demonstrated that the thinner, more fossiliferous units in these deposits are more time-rich and represent the end result of numerous depositional, erosional, and/or biological events operating under sediment-starved conditions (the "episodic starvation model"). A comprehensive comparative review of these two models is presented in Dattilo et al. (2008).

Temporal resolution within mud-dominated deposits is notoriously difficult to obtain (Brett and Baird, 1993; Brett and Allison, 1998). In many cases, subtle evidence must be utilized, and explanations achieved through careful scrutiny of this evidence are

decidedly counter-intuitive. One of the most counter-intuitive of results is that the well-preserved crinoids in the Main Crinoid Bed (and to a lesser extent the other beds) do not represent a single event-buried assemblage. Intuitively, one might interpret these distinctive fossil occurrences, which are restricted to thin horizons and are associated with fauna that contrast, to some degree, with fauna from overlying and underlying horizons, as transported in single-event deposits. However, evidence of autochthony or parauthochthony comes from the discovery of distal crinoid stems apparently preserved in place (Fig. 8); productid brachiopods preserved in living position and with articulated valves; possible spatial patchiness in crinoid fossils, suggesting living distributions; skeletal grain-size distributions similar to those observed in association with modern crinoid assemblages; and consideration of the articulated nature of the crinoid fossils themselves (but see Allison, 1986; Kidwell and Baumiller, 1990). Furthermore, there is a total absence of (1) vertical size grading within the units; (2) size sorting of crinoid, overall skeletal, or siliciclastic grains; (3) current alignment, despite an interesting pattern in Figure 27D, which considers only crinoid stems and is based on a low sample number; (4) sedimentary structures associated with transport (e.g., tool marks, gutter casts); (5) refolded crinoid stems or bryozoan fronds that can't be explained by compaction; (6) functional morphological evidence of adaptation for life under widely different environmental regimes; and (7) remains of other, more clearly exotic fauna. In addition to the evidence described above, work by Westrop (1986) and Zuschin et al., (2005) has shown that transportation of exotic taxa in offshore environments is rare and typically easy to detect.

Consequently, the incredibly abundant and diverse crinoid fauna of the Main

Crinoid Bed (and other thinner units) does not represent a single community that was rapidly buried, but instead represents the amalgamation of several less diverse and less abundant communities that were rapidly buried individually, with periods of normal sedimentation in between burial events. Although the concept of "time-averaged event assemblages" seems impossible, evidence from fabric analysis of mudstones, including the sample in Figure 17, supports this interpretation, as does the sheer number of articulated crinoid cups and crowns. If the approximately 1300 articulated or partially articulated individuals recovered from the Main Crinoid Bed constitute a single community buried by a single depositional event, then the background assemblage, representing multiple generations of this community, would have to consist of tens of thousands of individuals (or more, given the long time span represented by the Main Crinoid Bed) that lived and died prior to burial of the event assemblage. This means that the sediment would have to contain hundreds of thousands to tens of millions of crinoid ossicles, excluding any articulated specimens. The occurrence of articulated crowns and columns at several levels within and directly above the Main Crinoid Bed, consideration of pre-compaction unit thickness and the amount of time represented by the thinner units, and the taphonomic evidence for thin individual burial layers all combine to indicate that during deposition of the thinner layers, multiple rapid deposition events each preserved an assemblage of generally articulated crinoids, which were then telescoped together as a result of stratigraphic condensation and intense compaction.

This makes sense in light of work with modern marine environments, where time-averaging was shown to increase alpha diversity in molluskan assemblages, while emphasizing the abundance-based dominance of taxa that were common over a longer

span of time (Staff et al., 1986; Kidwell, 2002). This may explain the incredible crinoid alpha diversity, in that the long span of time allowed taxa that may have only been present temporarily to be preserved, albeit as rare specimens, while those taxa that were common throughout the entire interval of deposition were allowed to become numerically dominant in terms of abundance (e.g., *Exocrinus multirami*, *Apographiocrinus typicalis*). Rather than a crinoid community that is both exceedingly diverse at the species level and dominated by only a few taxa, the Copan Lagerstätte may represent an environment where a few taxa truly were dominant, but enough rapid burial events occurred to preserve a variety of rare taxa that may have been insignificant members of the paleocommunity or only entered the environment temporarily.

The thicker units, in contrast, show evidence of being deposited under higher sedimentation rates and energy conditions and possibly slightly firmer substrates. Evidence for this interpretation includes: (1) dominance by endobenthic deposit feeders (i.e., bivalves), which are more tolerant of turbidity and require a steady influence of organic matter to be brought into the environment through deposition; (2) numerous endobenthic bivalves preserved articulated, sometimes in living position or within a siderite concretion, indicative of much thicker individual burial events relative to the thinner units; (3) large-diameter sideritized burrows, which provide evidence of occasional erosive events to expose firmer substrates; (4) thin winnowed shell lags, produced by episodic reworking of the seafloor; (5) decreased abundance of skeletal material despite increased stratigraphic thickness; (6) decreased numbers of encrusted and broken skeletal grains, suggesting decreased exposure time at the seafloor; and (7) small siderite concretions, indicating transient redox boundaries and, therefore, enhanced

migration of the sediment-water interface.

Although both the thinner and thicker units reflect relatively deep-water, low-energy environments on a regional scale, there is clearly a marked difference between the two units that influenced biofacies, taphofacies, ichnofabrics, lithologic properties, and siderite concretion morphology. While it may be problematic to interpret the thicker units as shallower, the higher background sedimentation rate, increased event-bed thickness, and increased frequency of physical seafloor disturbance at least argues for a slightly more proximal environment. Both units are prodeltaic, influenced by delta complexes to the south and fed by the uplifted Ouachita highlands. The stratigraphic alternation between more proximal and more distal prodelta facies is here interpreted to reflect periods of delta progradation and inundation, respectively. It must be stressed again, however, that the differences between the thicker and thinner units are detected only through detailed microstratigraphic analysis, and reflect admittedly subtle shifts in environmental parameters; both units are undeniably considered prodeltaic distal shelf deposits on anything other than outcrop to local scales.

While the shift from the Main Crinoid Bed to Bed 0 represents a single episode of deltaic progradation and its resultant modulation of the tempestite proximality gradient, the transition from Bed 0 to Bed 1 and return to conditions similar to those of the Main Crinoid Bed may be more significant. This shift represents an episode of transgression, with the consequences for sequence stratigraphy discussed below. What is relevant to this discussion of paleoecology and non-event deposition, is why a localized environment containing abundant, well-preserved crinoid fossils becomes re-established. The geographic limits of the area containing articulated crinoid remains were tested during

fieldwork, resulting in the tentative conclusion that the crinoid-bearing facies appears to be laterally restricted at all horizons (Lewis et al., 1998) and regional stratigraphic studies by Holterhoff (1996, 1997a) have failed to locate similar Lagerstätten in correlative portions of the Barnsdall Formation. Following the first episode of deltaic progradation and the destruction of the crinoid-rich environment represented by the Main Crinoid Bed, why, then, was the same environment re-established twice in the same laterally restricted zone when it could have migrated anywhere else once sediment starvation resumed? A possible, although speculative, explanation might involve some sort of submarine topographic low which served to funnel nutrients and promote steady current flow, but also funnel sediment during storm events, leading to repeated burial followed by rapid re-colonization. Such a scenario was documented by Ausich et al. (1979) and Kammer (1985) in the Mississippian Borden Delta complex; in addition to promoting rapid re-establishment of crinoid communities following individual burial events, the diversity of prodeltaic crinoid communities was increased by the ready availability of nutrients. Although no evidence for such a feature has been detected within the Barnsdall Formation, it may help explain aspects of crinoid paleoecology (i.e., the high diversity of arm morphologies and, therefore, methods of feeding, within a single local environment) and taphonomy (i.e., why well-preserved crinoids are restricted to the same ~12 square meter area at three separate stratigraphic horizons).

Nature of Burial Events in the Main Crinoid Bed and Similar Units

The rapid burial events that punctuated the long spans of low sedimentation are worthy of special attention, as they are responsible for the excellent preservation of

crinoid fossils. The fine grain size of all sediment within the thinner units seems to preclude rapid burial, but flocculation of clay grains permits clay to behave hydrodynamically like coarser particles. Scanning electron microscopy can be used to detect a flocculated fabric by allowing the orientation of individual clay particles to be evaluated (O'Brien, 1987); however, both the intense bioturbation and strong compaction in the Barnsdall Formation preclude such microfabric analysis. In this case, the taphonomic evidence for rapid burial is sufficient to conclude that a mixture of quartz-silt and clay flocculates must have entombed the well-preserved epibenthos (compare O'Brien et al., 1994).

The lack of any recognizable differences in sediment composition between different units of the microstratigraphic section or between event layers and background sediment indicates that the event-deposited sediment may have been resuspended local sediment, or that the dominant components of the mudstone facies of the Barnsdall Formation, namely quartz, illite, chlorite, and kaolinite (Bellis and Rowland, 1976), are so ubiquitous in shelf sediments that the sediment may have been derived from slightly upslope but is indistinguishable from local sediment.

The lack of any mobile fauna within the event assemblage indicates that burial events were quite thin, and the occurrence of cross-cutting stems and an absence of strong current alignment indicates the influence of shifting paleocurrent directions. These attributes are typical of distal tempestites. During storm activity, shelf environments are affected by stirring of the seafloor by oscillatory currents and by seaward-flowing gradient currents carrying entrained fine-grained material (Aigner, 1985). Distal environments are far from the sources of coarse sediment, making

development of many of the typical features of tempestites (e.g., hummocky cross stratification) impossible. In addition, gradient currents generated by storm events flow primarily under the influence of gravity in distal environments, making them less capable of eroding muddy sediment and creating high-velocity blow-down deposits than current-driven flows. The net result of distal tempestite deposition may be a muddy plume that asphyxiates sessile organisms before settling into what may eventually be only millimeters of sediment.

Since both the frequency and thickness of storm layers decrease with water depth, along with an increase in the intensity of bioturbation, recognition of individual storm-generated event layers becomes difficult in offshore environments (Kreisa and Bambach, 1982; Aigner, 1985; Brett and Seilacher, 1991, and others). Wheatcroft (1990) and Pemberton and MacEachern (1997) reviewed the conditions necessary for preservation of event layers in marine strata, noting such important variables as thickness of the event bed, depth of bioturbation, rate of background sedimentation, ethology of bioturbating organisms, size of bioturbating organisms, time available for bioturbation, and physical properties of event-deposited sediment. A cursory glance at these variables reveals that there is practically no chance of preserving event layers responsible for rapid burial of crinoids.

Although burial events are interpreted here as resulting from storm deposition, it should be noted that in this environment, distal tempestites would be virtually indistinguishable sedimentologically from silty turbidites or gradient currents generated by seismic disturbance upslope. Lehman and Pope (1989) used pre-event oxygenation levels to distinguish turbidites from distal tempestites, with the former occurring in

dysaerobic environments and the latter preserving diverse benthic assemblages. Near Copan, abundant turbidites are associated with low-oxygen, lower core shale faces in a paleotopographic low near the Kansas-Oklahoma border (P. F. Holterhoff, pers. comm., 2010), so tempestites appear to be more likely agents of sedimentation to the south. Rascoe (1975) reports deformation in sedimentary strata near Copan that resulted from tectonic activity associated with uplift during the final stages in the formation of Pangea, including some features within the Barnsdall Formation. Although the sedimentary properties of the depositional environment containing the Lagerstätte were not conducive to liquefaction or other processes that might suspend sediment (McLaughlin and Brett, 2004), coeval environments in the proximal shelf likely were; i.e., disruption in these settings might generate gradient currents that would periodically flow downslope and bury benthic assemblages. This mechanism was actually favored by some investigators of the Copan deposit (P. F. Holterhoff, pers. comm., 2010). An interpretation of tempestites is preferred here, however, based on the frequency of burial events. Since the thinner units are composed of several thin burial events, and the thicker units are composed of numerous thick burial events, the burial mechanism must be frequent and vary along a proximality gradient. Storms meet both criteria, while the evidence for repeated soft-sediment deformation cited by Rascoe (1975) does not appear to occur with the frequency necessary to be responsible for crinoid preservation.

The effects of tempestite deposition on crinoid preservation appear to be quite variable, as evidenced by the genus-level taphonomic variability of crinoids recovered from the Main Crinoid Bed. Perhaps most interesting are patterns concerning crinoid mortality relative to burial. Several observations suggest that crinoid mortality occurred

very slightly prior to rapid burial: (1) the loss of distal arm tips on some otherwise intact specimens, (2) the relaxation of the shaving-brush posture, and (3) predominantly articulated, but slightly imperfect crowns. Although seemingly unlikely, this observation is not unique, as many deposits featuring articulated echinoderms that were once cited as evidence of live burial are increasingly showing signs of organism mortality hours to a few days before actual deposition of sediment (C. E. Brett, pers. comm., 2010). Although the exact reasons for this are currently being debated, it has been hypothesized that some chemical disturbance (e.g., fluctuation of salinity or temperature), likely generated by the same event responsible for rapid burial, slightly preceded deposition. Despite the evidence for mortality before burial, there is also evidence for live burial of crinoids, including: (1) the genesis of extremely localized siderite concretions around the site of soft tissue in crinoids, (2) perfectly preserved crowns, and (3) crowns with splayed arms oriented obliquely in the sediment, possibly representing an individual that was embedded mouth-down in rapidly deposited sediment.

In addition to variations in the apparent timing of crinoid mortality relative to sediment burial, there are inconsistencies in the depth of burial of crinoid remains. The specimen shown in Figure 38 indicates a sediment blanket so thin that it could not cover the crinoid; yet, there are specimens preserved perfectly intact, without evidence of any disturbance and indicating deep burial. The specimens displaying evidence of infaunal scavenging (Fig. 39) represent an intermediate burial depth, where the sediment blanket was thick enough to cover the individual but insufficiently thin to prevent bioturbating scavengers from detecting and disrupting the carcass.

These heterogeneities likely reflect variations in sediment blanket thickness,

perhaps related to seafloor topography; variations in crinoid size, as smaller taxa may be completely covered by thinner sediment blankets and/or crinoids elevated higher off the seafloor might experience turbidity or respond to chemical stress to a greater or lesser degree; and possibly temporal variations in sediment blanket thickness and chemical precursors.

Post-Event Taphonomic History

Following rapid burial, a number of other taphonomic processes operated to produce the taphonomically variable fossil assemblages characteristic of the Copan deposit. Decay began, either at the sediment-water interface, in the very shallow subsurface, or deeper within the sediment profile. Once deposition and suspension fallout ceased, scavenging of partially buried and fully buried crinoid carcasses occurred. This scavenging activity seemingly served to create much of the observed disruption in crinoid specimens, and likely contributed to the low number of crinoid crowns capable of generating a localized siderite concretion. Formation of large siderite concretions began shortly after burial and occurred in the shallow subsurface as the sudden input of dead organisms initiated porewater anoxia and siderite precipitation. Scavenging was apparently limited in duration, as even specimens that had undergone infaunal scavenging were not so biogenically mixed as to completely disarticulate. This is an interesting and poorly understood phase in multi-element skeleton taphonomy, as recent studies of Devonian trilobite taphonomy (Brett et al., 2009b) have also revealed a scenario where scavenging in bioturbated sediments was halted for some reason prior to early diagenetic mineralization. As mentioned above, perhaps the mass decay of buried organisms at

several levels induced anoxia in typically oxidized environments where scavenging had been occurring.

As the sediment-starved conditions persisted at the sediment-water interface, the siderite concretions continued to grow within the shallow subsurface. The surface was rapidly repopulated and bioturbation likely resumed, at least within the very shallow subsurface. During this period of sediment starvation, organisms died, decayed, and disarticulated, leaving their skeletal grains exposed at the surface, where they became encrusted by serpulid worm tubes, small bryozoan colonies, and/or larval crinoids. At some point, another rapid burial event occurred, introducing more material to the subsurface, and the process just described would begin again. Because the siderite concretions are not present as a series of distinct individual layers, it is possible, if not likely, that successive event-buried organisms contributed to the growth of siderite concretions that had been initiated by previous burial events. After siderite precipitation, the sediments underwent dewatering and extreme compaction resulting from the pressure of overlying sediments. This served to crush many of the brachiopods, disarticulate and separate portions of crinoid skeletons, break some crinoid ossicles, and force together fossils from stratigraphic horizons formerly separated by millimeters or centimeters of sediment. Bed 1 and Bed 3 may have experienced greater compaction-related temporal condensation due to their decreased thickness, which likely reflects a decrease in the number of burial events occurring during deposition of these units.

During continued deltaic progradation, sedimentation rates would increase to the exclusion of many of the crinoids, who likely tracked their preferred habitat to more offshore environments, while endobenthic mollusks dominated the formerly sediment-

starved environment. The rate of this transition is difficult to determine, and the microstratigraphic signature is ambiguous; perhaps the sponge-rich bed and/or the sponge- and productid brachiopod-rich beds consistently overlying the thinner units represent some form of transitional community more tolerant of the increased turbidity than the biofacies characteristic of the Main Crinoid Bed and similar horizons.

The taphonomic history of the thicker beds is very similar to that of the thinner beds described above, except that individual burial events are thicker in the thicker units, leading to decreased scavenging of event-buried organisms. In addition, precipitation of siderite occurred over a considerably shorter duration, and compaction may have played a role sooner after burial in the thicker beds than in the thinner beds as a result of increased weight of overlying sediment due to more rapid deposition. This compaction of the thicker beds may even have further increased the compaction in underlying thinner units.

IMPLICATIONS AND SIGNIFICANCE

Implications for Crinoid Taphonomy

Previous studies of crinoid taphonomy have convincingly demonstrated that processes and rates of disarticulation are variable, and controlled by a variety of factors that differ with depositional environment and crinoid constructional morphology (Meyer et al., 1989; Ausich and Sevastopulo, 1994; Taylor and Brett, 1996; Webster, 1997; Gahn and Baumiller, 2004; Wetzel and Meyer, 2006), as previously noted. These studies have, with one exception (Wezel and Meyer, 2006), focused on recognizing the differences in relative propensity for disarticulation at fairly coarse taxonomic levels—primarily the subclass or order. For example, monobathrid camerates have consistently been found to be the most resistant to disarticulation, with flexibles the least resistant; cladids and articulates are less prone to disarticulation than flexibles, but are rarely found as articulated crowns (see Ausich, 2001). As research on echinoderm taphonomy has progressed, the need for understanding of taphonomic patterns at more precise levels has become more apparent. Indeed, following the decrease in subclass-level diversity after the Mississippian, and the eventual reduction to a single subclass following the Permian, knowledge of genus-level disarticulation patterns is necessary in order to assess deposits containing crinoid assemblages that are diverse at the genus or species level, but homogenous (or practically so) at the subclass level.

The results of this study demonstrate that taphonomic variability extends at least

to the genus level for the subclass Cladida, which dominates the Copan assemblage (Thomka et al., 2009). Patterns of specimen completeness, compaction orientation, and arm position are strongly inter-related, and reflect variations that cannot be the result of subclass-level differences in skeletal construction or preservation in different facies. Furthermore, several of the taphonomic patterns observed in this assemblage appear to be based on the size of the individual, making them intraspecific. Early work on the Copan crinoids by Mosher comparing the number of specimens of each genus represented by articulated individuals to the number represented by isolated ossicles showed that certain taxa are more prone to total disarticulation than others (see Thomka et al., 2010). These findings are also consistent with decay studies of modern echinoderms by Lewis (1986; see also Lewis, 1987) and Allison (1990), which stress that emphasis on taphonomic variation on a coarse scale can be potentially dangerous, as interpretations concerning residence time in the taphonomically active zone, patterns of time-averaging, and degree of environmental energy, for example, can be strongly biased by preconceptions about the propensity for disarticulation of a large taxonomic group when, in some cases, it is taphonomic variation at the level of individual genera or species within that group that determine the taphonomic character of a fossil assemblage.

Inclusion of scavenging-related features as part of the genus-level comparative taphonomic study provided important insights into the post-mortem history of the Copan crinoid assemblage. Interestingly, this is the first taphonomic grade study to document such features, as previous studies purposely excluded any specimens exhibiting signs of disarticulation not related to purely physical processes. Even the actualistic study of Allison (1990) considered only decay-induced disintegration. This is surprising, given

the tremendously important roles that bioturbation and scavenging play in determining the taphonomic state of multi-element skeletons (Plotnick, 1986; Allison, 1988a). Preferential scavenging of certain crinoid species or individuals over others, observed in modern crinoids in the early studies of Meyer (1971) and Liddell (1975), have the potential to shed light on problematic taphonomic patterns, including anomalously high or low numbers of articulated specimens of a given taxon. Species-level variations in soft tissue biochemistry, for example, would be otherwise undetectable in fossil crinoids, but may be manifest in the taphonomic signature of preferential scavenging, as certain taxa may contain noxious compounds within soft tissues that would inhibit scavenging. Likewise, currently unexplained trends in parasitism and commensalism may be related to soft tissue properties potentially evident in scavenging patterns. Finally, exclusion of specimens displaying signs of scavenging may be dangerous to taphonomic grade studies by biasing the dataset: scavenging within the Copan assemblage is evident nearly exclusively in large taxa or large individuals. Removal of all of these specimens might lead to taphonomic characterization of a large genus based solely on the properties of small specimens.

In a larger sense, this study provided a unique opportunity to identify the factors that are most significant in controlling preservation within a generally well-preserved crinoid assemblage. Previous investigations dealt with units containing perfect or nearly perfect specimens, where single crinoid individuals are often found intact, from distal arm tips to holdfasts. The less pristine state of the Copan fauna, resulting from thinner burial layers and more intense bioturbation, permits causes of taphonomic diversity to be assessed. These controls are summarized in Table 3. The most important control on

crinoid preservation within the Copan assemblage is rate of burial, with rapidly buried individuals defining the event assemblage and slowly buried individuals defining the background assemblage. Consequently, the background assemblage consists nearly entirely of isolated ossicles or short pluricolumnals, whereas the event assemblage consists of more articulated specimens preserved in a variety of states. Within the event assemblage, specimens exhibit both interspecific variability and intraspecific variability. Interspecific variability, discussed in greater detail in the section on crinoid taphonomy, appears to be controlled by (1) morphology (i.e., size and thickness of plates, rigidity of cup, muscular vs. ligamentary articulations), (2) scavenger preferences, and (3) behavior (i.e., willingness or capacity to close arms). Taphonomic variability within a single species (intraspecific variability) appears to be controlled by (1) size (i.e., visceral mass, appeal to scavengers, predators, or parasites), (2) lateral variations in sediment blanket thickness during a single burial event (i.e., some individuals deeply buried, others partially buried), and possibly (3) temporal variations in sediment thickness during successive burial events.

Extension of this style of analysis into other crinoid-bearing deposits opens up the possibility of determining the fundamental controls on crinoid taphonomy through geologic time and in all depositional settings. Preliminary results indicate three main factors: morphological controls, ecological controls, and environmental controls (Table 4). Within the arena of morphological controls, size (individual and genus), nature of connective tissues (strength and composition), and plate size and thickness are significant, especially in Early Paleozoic assemblages where connective tissues in

TABLE 3—Factors responsible for taphonomic variability within the Copan crinoid fauna.

1. Slow Burial (Background Assemblage)
2. Rapid Burial (Event Assemblage)
    - 2a. Interspecific Variation
        - 2aI. Morphology
        - 2aII. Scavenger Preferences
        - 2aIII. Crinoid Ethology
    - 2b. Intraspecific Variation
        - 2bI. Size
        - 2bII. Lateral Variation in Sediment Cover Thickness
        - 2bIII. Temporal Variation in Sediment Cover Thickness

TABLE 4—Generalized controls on crinoid preservation (compare with Table 3, which only deals with taphonomic variability within the Copan assemblage). These attributes, when recognized in a variety of crinoid-bearing deposits, provide the basis for understanding the taphonomic state of crinoid assemblages, regardless of specimen articulation and degree of taphonomic variability.

1. Morphological Controls
    - 1a. Size
        - 1aI. Species
        - 1aII. Individual
    - 1b. Connective Tissue
        - 1bI. Composition (Ligament vs. Muscle)
        - 1bII. Relative Strength
    - 1c. Size and Thickness of Ossicles
2. Ecological Controls
    - 2a. Capacity/Willingness to Adopt Trauma Posture
    - 2b. Scavenger Preferences
    - 2c. Extent of Bioturbation
        - 2cI. Depth of Burrow Excavation
        - 2cII. Intensity of Bioturbation
3. Sedimentological Controls
    - 3a. Background Sedimentation Rate
    - 3b. Nature of Episodic Burial Events
        - 3bI. Frequency
        - 3bII. Thickness of Sediment Blanket
        - 3bIII. Associated Increase in Energy (Scouring, Transport, etc.)
    - 3c. Heterogeneity in Sediment Blanket
    - 3d. Early Diagenetic Mineralization Regime

crinoids were not ubiquitous (compare Ausich and Baumiller 1993, 1998). Ecological controls include both autecological and synecological attributes: the relative willingness and ability to adopt a trauma response, possibly related to connective tissues in the arms, serves as an autecological property, while the preferences of scavengers and extent of bioturbation serve as important synecologic properties. Environmental controls include the rate of normal (background) sedimentation, the frequency and magnitude of rapid burial events (in terms of thickness of sediment cover and energy), the geochemical setting, as it pertains to diagenetic mineralization, and the degree of heterogeneity within individual burial events (related to seafloor topography and mechanism for deposition). Development of a comprehensive model for crinoid taphonomy, based on comparative taphonomic studies, is truly an exciting initiative in echinoderm research.

Implications for Sequence Stratigraphy

The relationships between fossil occurrence and preservation and sequence stratigraphic concepts are numerous, significant, and a major source of current research (sensu Holland, 1995, 1999; Harries, 2003). Detailed and convincing reviews by Kidwell (1991) and Brett (1995, 1998) show that paleocommunities and taphonomic features are distributed nonrandomly throughout stratigraphic sequences, and that consistent and recurrent taphofacies reflect the interplay between relative sea level, storm dynamics, sediment supply, and environmentally controlled organismal influences. Indeed, understanding of the relationships between fossil preservation and sequence stratigraphic setting has progressed to the point that the stratigraphic occurrence of Lagerstätten can be accurately predicted and discovered based only on their position relative to key surfaces

or systems tracts (see Brett et al., 2009a for a particularly thorough study).

Such models show that Lagerstätten similar to the Copan deposit are fairly common in offshore settings during initial periods of sea-level fall; however, since sedimentation rates increase with continued regression, environmental conditions necessary for crinoids become increasingly scarce. Furthermore, increased sedimentation rates through time cause these thin horizons to experience a dilution effect, where Lagerstätten representing laterally and temporally limited refugia from turbidity and sedimentation become separated from each other by many meters of less fossiliferous strata representing more typical conditions. Hence, the laterally and vertically restricted nature of the Copan deposit makes sense, but represents an ephemeral and geographically localized occurrence made possible by its unique paleogeographic position between a dysaerobic, turbidite-fed submarine valley to the north and delta complexes and an isolated carbonate platform to the south (P. F. Holterhoff, pers. comm., 2010), which seemingly served to prolong oxygenated and low-sedimentation conditions. It is likely that other similar occurrences exist within the Barnsdall Formation but are scattered throughout a considerable volume of homogenous sediment and, therefore, may never be discovered. In addition, the increase in energy with continued regression increases the likelihood of erosional exhumation and subsequent destruction of Lagerstätten formed during late highstand/early regressive phases (Brett, 1995).

The cyclicity observed within the microstratigraphic section, expressed as alternations between thin units containing articulated crinoids with large siderite concretions and thick units containing an endobenthic molluskan assemblage, may have important sequence stratigraphic implications. An individual cycle, approximately 15 cm

in thickness, records an initial period of sediment starvation punctuated by thin, rapid burial events, which is then overlain by sediments representing deposition under higher sedimentation rates and punctuated by thicker rapid burial events associated with higher energy. This thicker unit is fairly abruptly overlain by another thinner unit. Thus, the overall pattern represented by each cycle is one of gradual shallowing, followed by rapid flooding. There are three such cycles observed within the Copan deposit, and the stacking pattern of these cycles appears to represent a longer-term pattern. The stratigraphic thickness, crinoid diversity, and crinoid specimen abundance decreases successively from the Main Crinoid Bed to Bed 1, and from Bed 1 to Bed 3. Likewise, bed thickness increases upsection within the thicker units, and sideritized burrows (indicating minor erosive episodes) are observed in Bed 2 and Bed 4, but not in Bed 0. Collectively, these trends suggest that less time is spent in the more distal facies of each successive cycle, with more time, and possibly increasing energy conditions, in the more proximal portion of successive cycles. This distinctly progradational pattern of cycle stacking indicates that regression occurred not in a single episode, but rather in several phases interrupted by minor flooding events (i.e., phased regression). Such a pattern has been documented by Felton and Heckel (1996) in the regressive limestone member of the Dennis cyclothem. The extension of phased regression into the upper core shale facies provides further evidence that the dynamics of glacio-eustatic sea-level fluctuations in the late Pennsylvanian are comparable to that of the Pleistocene (see also Fielding et al., 2008).

Based on this evidence, an interpretation of the cycles as parasequences, or sixth-order cycles, becomes possible. Although the concept of a 15-cm parasequence is

currently undocumented and admittedly controversial, there is abundant evidence that each cycle was deposited over a considerable period of time, and that the relative thinness is a consequence of sediment starvation. Each cycle meets the criteria for parasequences as defined by Van Wagoner et al. (1990): they are generally conformably, genetically related, and bounded (conformably) by evidence of relative deepening. In this case, the "deepening" may be difficult to prove absolutely, but is represented by a return to more distal conditions, characterized by lower sedimentation rates, thinner storm event layers, and a decrease in erosive episodes. The bases of thinner units are herein designated as marine flooding surfaces.

In a study of the stratigraphic distribution of authigenic minerals, Taylor and Macquaker (2000) found carbonate concretions in association with marine flooding surfaces, in partial agreement with the model proposed here, but placed the parasequence boundary above the concretionary layer. In this model, flooding events concurrently created minor erosional disconformities and sediment-starved conditions; in this setting, the sediment-water interface is represented by the disconformity while concretions grow beneath it in the shallow subsurface (Taylor and Macquaker, 2000). In contrast, the placement of marine flooding surfaces below concretionary layers in the Copan deposit is necessary because the concretions occur with the fossil assemblage and taphofacies indicative of sediment starvation, rather than below them. Thus, flooding must have occurred, allowing the epibenthic biofacies to become established, with concretion growth beginning after minor sediment accumulation. Although Posamentier and Allen (1999, p. 186) argue that the term parasequence should be restricted to those settings shallow enough for true marine flooding surfaces to form through erosion or prolonged

nondeposition, most other workers (e.g., Van Wagoner et al., 1988, 1990; Miall, 2000) are comfortable with a definition of parasequence that can be recognized on the basis of evidence for relative deepening, regardless of depositional setting.

Based on the thinness of cycles, one might interpret these units as representing beds or, more likely, bedsets of Van Wagoner et al. (1990). However, there are a number of arguments against this interpretation: (1) bedsets typically represent a considerably shorter span of time than that interpreted for the Copan cycles; (2) bedsets are typically simple internally, and recognized by such features as normal grading (e.g., Taylor and Macquaker, 2000), while these cycles are more complex and represent entire facies shifts; and (3) the parasequence is, above all else, an architectural element, and should be recognized in the context of its relationship to the sequence, rather than more variable or arbitrary factors like stratigraphic thickness (as eloquently argued in Holland et al., 1997). Furthermore, sub-meter, mud-dominated parasequences have been recognized in other deposits with greater outcrop availability. In a study presenting results that closely parallel those obtained here, Brett and Baird (1986b, 1996) describe parasequences from the Devonian of New York that are 0.5 to 1 m in thickness and consist of alternating fossil-rich, concretionary, argillaceous limestone (analogous to the thinner, siderite-bearing units of this study) and thicker, more barren mudstone. Individual cycles of this type, deposited in offshore, intermittently sediment-starved environments, have been correlated to thicker cycles more typical of "classic" parasequences deposited in more proximal environments (e.g., Van Wagoner et al., 1990; see also Elder et al., 1994).

Jennette and Pryor (1993; see also Holland et al., 1997), in an investigation of storm processes in the Upper Ordovician of the Cincinnati area, conclude that meter- to

sub-meter cycles consisting of offshore deposits containing well-preserved fossils buried in thin, distal tempestites, alternating with higher energy, amalgamated proximal storm deposits represent parasequences. They argue that the evidence for relative deepening between cycles justifies interpretation of the cycles as parasequences despite their thinness and the absence of unconformable marine flooding surfaces. Continued work on these well-studied units by Holland et al. (2001) revealed the striking degree to which subtle changes in faunal assemblages highlight shifts in sea-level that are otherwise unrecognizable lithologically; these authors supported many of the stratigraphic interpretations of Jennette and Pryor (1993), and further stress that recognition of parasequences in mud-dominated sequences is nearly impossible without detailed paleontologic analyses. In a study dealing entirely with homogenous mudstone strata, Macquaker et al. (1998) identified decimeter- to meter-scale parasequences in the Jurassic of eastern England. Although identified primarily on the basis of sedimentologic, rather than paleontologic, analysis, that study demonstrated that in distal environments, parasequences can be quite thin, and their expression subtle.

Implications for Authigenesis

The occurrence of siderite played an important role in the study of the Copan deposit both in the field and as evidence for the paleoenvironmental conditions. The implications of early diagenetic siderite that is associated with crinoid fossils and its various morphologies has been discussed above; what remains unresolved is the mechanism responsible for precipitation of marine siderite in such quantities and within thin layers of mudstone. Sediment starvation can account for the timespan necessary for

growth of large concretions, but the prevailing redox zone where precipitation occurred and the role of sulphate reduction must be addressed.

Based on the absence of early diagenetic pyrite associated with reducing microenvironments represented by rapidly buried organisms, strict application of the model of Sellwood (1971) is rejected as an explanation for Copan siderite. In addition to the lack of early diagenetic pyrite, the low sedimentation rates, thin burial events, and thorough bioturbation would make sealing off the shallow subsurface porewater from seawater nearly impossible. These factors seem to support siderite precipitation within the zone of ferric iron reduction through competitive exclusion of sulphate-reducing bacteria, although alteration of the preferences of sulphate-reducing bacteria can be neither ruled out nor proven.

Seemingly, initial sediment starvation and consequent thorough bioturbation resulted in a concentration of iron oxy-hydroxides (through repeated oxidation of iron-rich porewater and ferroan minerals produced in subsurface redox zones) within the oxidizing zone at and immediately below the sediment-water interface. The continued concentration of iron allowed abundant siderite to be precipitated after one or more rapid burial events and during continued sediment starvation, by serving to either enhance the community of ferric iron-reducing bacteria to the point of excluding sulphate-reducing bacteria, or by forcing sulphate-reducing bacteria to alter their chemical substrates in the presence of abundant iron and low organic matter. Thus, both the large size of siderite concretions and the large amount of iron necessary for their growth serve as evidence of sediment starvation of the distal shelf. Although this model fails to explain how porewater sulphate is excluded from the diagenetic environment, in contrast to Sellwood

(1971), it better fits the paleoenvironmental parameters of the Copan deposit; perhaps more importantly, it appears to fit with studies based on modern sediments (Lovley and Phillips, 1987; Chapelle and Lovley, 1992), allowing for further clarification as research continues.

Comparisons to Other Lagerstätten

Recent research focusing on the genesis, stratigraphic distribution, and taphonomic signatures of marine Lagerstätten has resulted in a shift in interpretation of these unusual and rare deposits. Formerly thought to result from relatively simple processes such as stagnation or thick, rapid burial of living organisms (compare Seilacher et al., 1985), many Lagerstätten have now been shown to result from complex interactions between physical, chemical, and organismal processes, each operating at different rates and varying temporally as well as spatially (Brett et al., 1997a). Consequently, Lagerstätten are extraordinarily diverse, as variations in depositional regime, stage in the history of life, and paleogeographic setting, among other factors, serve to make no two exceptional deposits identical. Despite such tremendous heterogeneity in Lagerstätten, certain deposits can be grouped together as similar, either in terms of genesis, taphonomic state of fossils, or taxonomic identity of fossils. Brett and Seilacher (1991) produced a preliminary genetic classification of Lagerstätten created by obrution, often using the presence of intact echinoderms as a significant diagnostic feature, and Brett et al. (1997b) created a classification scheme for echinoderm-bearing Lagerstätten based on depositional setting and taphonomic attributes. These two classification schemes can be used to identify deposits most similar to the Copan

Lagerstätte, and investigate the causes of variation between them.

Hamilton Group (Middle Devonian)

Using the classification of Brett and Seilacher (1991), the Copan assemblage generally falls under the Hamilton-type deposit, named for the Middle Devonian Hamilton Group of New York. Hamilton-type deposits are defined by a diverse and well-preserved faunal content, the absence of strong alignment or other current indicators, and a fine-grained matrix (Brett and Seilacher, 1991). The Hamilton Group, and more specifically, the echinoderm-bearing Windom Shale Member, represents repeated storm-generated mud suspensions that blanketed a distal shelf environment featuring a muddy substrate, well-oxygenated waters, and a diverse benthic fauna dominated by crinoids, trilobites, brachiopods, and bryozoans (Parsons et al., 1988; Miller et al., 1988; Seilacher and Brett, 1991; Brett, 1999). Taphonomic evidence suggests that certain organisms died slightly prior to burial, resulting in minor disarticulation due to scavenging or incipient decay at the seafloor. Other organisms within the same layers show evidence of death concurrent with burial. The effects on the fossil assemblage include (1) very well-preserved (but not perfect) crinoids and trilobites; (2) occasional indicators of trauma prior to death, including enrolled trilobites (Speyer and Brett, 1986; Brett and Seilacher, 1991); and (3) alternating concretionary layers and barren mudstones (Parsons et al., 1988; Miller et al., 1988; Brett, 1999). Such taphonomic and sedimentologic features are quite similar to those documented in the present study of the Copan assemblage, particularly in terms of crinoid taphonomy and the occurrence of repeated concretion-bearing horizons, which represent very low

sedimentation rates.

Yet, the Copan deposit differs from the Hamilton Group in several ways. Brett and Seilacher (1991) noted that a significant faunal constituent of the mudrocks of the Hamilton Group are trilobites, often in low diversity clusters and comprising a narrow size range; the genetic classification places great emphasis on the presence of trilobites, citing their presence as a criterion for recognition of Hamilton-type deposits. Trilobites underwent a considerable decline throughout the late Paleozoic, and were no longer dominant constituents of shelf environments in the Pennsylvanian. Consequently, the Copan deposit has thus far yielded very few trilobite fossils, making taphonomic comparisons between multi-element skeletons other than crinoids impossible. Moreover, the Copan fauna is notably lacking in well-preserved mobile benthos, indicating that burial events were capable of smothering or choking sessile crinoids, brachiopods, and bryozoans, but sufficiently thin to allow vagile organisms to escape burial or burrow upwards through the event layer. Individual event layers in the Hamilton Group can be up to 10 cm thick, making any rapidly buried organisms unlikely to escape (Miller et al., 1988).

Seemingly, the shellbeds represent sediment-starved conditions, but there are no thin, rapid-burial event layers as are seen in the Copan deposit; the mudstones of the Hamilton Group represent one or a few very thick rapid-burial events that completely covered the seafloor during particularly strong storm events. Evidence for this comes from Parsons et al. (1988) and Brett (1999), who documented the regional-scale lateral persistence of crinoid-bearing beds, allowing the mudstones to serve as isochronous markers over a large area and indicating that the storms responsible for the obrution

horizons deposited sediment over a broad geographic area. The thicker units within the Copan section represent overall higher sedimentation rates and thicker burial events, but were still deposited over a considerable period of time. The Hamilton Group is recognized within large outcrop belt throughout upstate New York, which allows for lateral depositional facies to be recognized, including shoreward deposits that show evidence of storm winnowing (Parsons et al., 1988) and provide a easily recognizable mechanism for the burial of fauna.

Other important paleoecological differences include the significant effects of intense bioturbation on the Copan fauna, whereas burrowing organisms have not played as much of a disruptive role in the Hamilton Group. The amount of information loss in offshore Upper Pennsylvanian strata, coupled with the smaller outcrop area, decreases the level of confidence in identifying sedimentary processes with any precision. The crinoid paleoecology also makes the Hamilton Group an imperfect model for the genesis of the Copan Lagerstätte, as Devonian crinoids required hard substrates, while Pennsylvanian crinoids could exist on muddy, fluid-rich substrates. As a result, crinoids recovered from the Hamilton Group are only associated with winnowed shell lags, with a completely different biofacies associated with the post-burial softground substrate; interactions between the two biofacies create a great deal of complexity within horizons that had experienced repeated burial and winnowing (Miller et al., 1988).

Rochester Shale (Silurian)

Using the classification scheme of Brett et al. (1997b), the Copan deposit falls under the Waldron category, named after the Waldron Shale of southern Indiana. Despite

being the type for this particular mode of echinoderm preservation, little recent taphonomic work on the Waldron Shale has been undertaken since the work of Feldman (1989), which focused primarily on diagenesis. Well-studied echinoderm assemblages exhibiting Waldron-type preservation are best exemplified by the Silurian Rochester Shale of New York and Ontario, Canada. This deposit contains a diverse invertebrate fauna including crinoids, trilobites, ophiuroids, cystoids, and brachiopods; the fauna is generally well-preserved, but also contains fossils exhibiting moderate to complete disarticulation (Taylor and Brett, 1996; 1999). This taphonomic state is similar to that of the Copan deposit, and is attributable to the rapid burial of fauna (resulting in well-preserved fossils) superimposed on the accumulation of skeletal material representing normal "background" disarticulation on the seafloor (Speyer and Brett, 1991; O'Brien et al., 1994; Taylor and Brett, 1996), as well as death and decay slightly prior to burial. The depositional environment of the Rochester Shale is interpreted as a muddy offshore shelf or marginal basin with well-oxygenated waters (Taylor and Brett, 1996; 1999). Burial was due to storm-generated suspensions of carbonate silt and clay that flocculated to rapidly and deeply entomb the epifauna (O'Brien et al., 1994; Taylor and Brett, 1999).

In sediment-starved offshore shelf environments such as those interpreted for the Copan Lagerstätte and facies of the Rochester Shale, it has been shown that (practically) the only sediment that accumulated was deposited by distal tempestites. This results in a bundling of thin obrution deposits directly above marine flooding surfaces. Following flooding and the resulting shift to a more offshore facies, distal storm events occasionally smothered benthic communities, under thin sediment layers; this model is nearly identical to that proposed herein for the genesis of the thinner units of the Copan section. Due to

the drastic difference in bioturbation intensity between the Rochester Shale and the Copan deposit, however, a series of individual burial events are preserved within the former, while these beds are biogenically homogenized in the latter. This provides further, although indirect, evidence for the placement of marine flooding surfaces at the base of the thinner units.

Although some elements of the taphonomy of the Rochester Shale are similar to that of the Copan Lagerstätte, several significant differences exist; many of these differences are shared with the Hamilton Group, as discussed above. First, the presence of obvious bedding planes in the Rochester Shale allow for bed-by-bed biostratinomic analysis, made impossible by extensive bioturbation in the Copan deposit. In addition, the requirement of hard substrates for crinoids, also discussed above, makes recognition of different biofacies more straightforward. The Rochester Shale crops out in a broad, laterally extensive facies belt, including thin fossil horizons that can be correlated over tens of kilometers (Brett, 1983). Within this facies belt, lithologic heterogeneity is pronounced, with clastic, carbonate, and mixed clastic-carbonate sediments dominant at different locations. The sediment that rapidly buried benthic organisms in the Rochester Shale was transported from a carbonate environment and into a siliciclastic setting. The homogeneous lithology of the Barnsdall Formation as a whole differs greatly from the Rochester Shale and makes any form of provenance analysis impossible. On a smaller scale, recognition of distinct physical sedimentary structures in the carbonate silt, including hummocky cross-stratification and basal scour marks, unambiguously suggest a storm origin in the Rochester Shale (Taylor and Brett, 1999). This is further supported by patterns of current alignment in trilobite and crinoid fossils (Taylor and Brett, 1996;

Brett and Taylor, 1997). Neither identifiable sedimentary structures nor evidence of strong current have been documented from the Copan unit to date (e.g., Lewis et al., 1998), indicating a less energetic environment and more intense post-depositional bioturbation.

LaSalle Limestone (Upper Pennsylvanian)

The fauna of the LaSalle Member of the Bond Formation as exposed in central Illinois represents one of only a few well-studied Pennsylvanian crinoid-bearing Lagerstätten (Strimple and Moore, 1971; Ausich, 1999). Occurring within the Missourian Stage, the LaSalle assemblage is nearly equivalent in age with the Copan deposit, but represents a shallower, carbonate-dominated facies northward of the terrigenous detrital facies belt. There is much overlap between crinoid taxa in both units at the genus level, with 22 genera in common, including the four genera most common within the Copan assemblage: *Apographiocrinus*, *Erisocrinus*, *Kallimorphocrinus*, and *Exocrinus* (Strimple and Moore, 1971). Crinoids are preserved as articulated crowns with long lengths of articulated column commonly attached. Many crinoid taxa appear to have morphological adaptations to life in a soft substrate, as documented within the Copan crinoids, and several specimens featuring a runner-type holdfast structure have been recovered from the LaSalle deposit.

The Copan deposit differs from the LaSalle occurrence in depositional environment and taphonomic state of crinoid specimens. The LaSalle crinoids occur within minor depressions at the top of a marine limestone unit representing a shallower, higher-energy carbonate shelf where diverse crinoid assemblages were most commonly

preserved in the early and middle Paleozoic. In contrast, the Copan Lagerstätte is a low-energy, offshore, siliciclastic-dominated muddy shelf where a diverse crinoid fauna is more likely to be found in the late Paleozoic. While many of the same taxa are present in both assemblages, the relative abundances are disparate. This results from the difference in depositional environment between the two deposits and its effects on crinoid paleoecology: the higher energy, warmer water faunas of the Pennsylvanian carbonate shelves are richer in flexibles (although cladids are still numerically greater) and contain larger, more robust taxa than the offshore deposits (i.e., Copan), which are utterly dominated by small, unornamented cladids (Holterhoff, 1988, 1997a).

In addition to an environmental discrepancy, many of the crinoid fossils from the LaSalle deposit exhibit excellent to perfect preservation, including intact crowns with splayed arms and articulated pinnules, frequently attached to long lengths of stem (Strimple and Moore, 1971; Ausich, 1999), indicating deeper burial and possibly less intense compaction. Where imperfect crowns are found, disarticulation is much more commonly found to be the result of compaction, rather than decay or scavenging.

More importantly, taphonomic and sedimentologic evidence indicates that the articulated crinoids were preserved through a single rapid burial event, and therefore provide a snapshot of a benthic community with minimal time-averaging. Despite representing an environment conducive to a diverse crinoid assemblage (Ausich, 1999), the LaSalle deposits are considerably lower in crinoid alpha diversity (33 genera represented; Strimple and Moore, 1971) than the Copan deposit. This appears to provide indirect evidence that the tremendous crinoid diversity within the Copan Lagerstätte is due, at least in part, to the amalgamation of multiple communities.

CONCLUSIONS

Setting

The Copan crinoid Lagerstätte occurs in sediment representing a low-energy, oxygenated, muddy, prodeltaic distal shelf setting bordered to the north by shallower, carbonate-dominated environments, and to the south by deltaic wedges fed by the Ouachitas. The abundant and diverse macrofaunal assemblage characteristic of this environment is made possible by the breakdown of water column stratification following initial regression; therefore the Lagerstätte is located stratigraphically above dysoxic gray shale facies representing highstand and below poorly fossiliferous mudrocks and sandstones representing shallower facies formed by deltaic progradation. These fluctuations in relative sea level are likely glacio-eustatic, rather than tectonic, in origin.

Genesis of Lagerstätte

Abundant articulated crinoids are restricted to three thin (3-8 cm) horizons separated from each other by thicker (10-15 cm) units that contain very few articulated crinoid remains and are instead dominated by endobenthic bivalves commonly preserved in living position. The thin units also contain abundant large siderite concretions, while the thicker units contain siderite concretions of considerably smaller size. In addition, the thicker units contain discrete sideritized burrows and winnowed shell lags, both of which

are absent from the thinner units.

The thinner units are dominated by sessile epibenthic suspension feeders, indicating a low turbidity environment with low net sedimentation rates. An interpretation of sediment-starved conditions for the thinner beds is supported by the occurrence of a background assemblage of fossil material, large siderite concretions, the high proportion of encrusted skeletal grains, thorough biogenic homogenization of sediment, and the increase in skeletal material relative to thicker units. Paleoecologic, taphonomic, and sedimentologic evidence indicates that thinner units contain an autochthonous to parautochthonous faunal assemblage. The articulated crinoids, productid brachiopods in living position, and intact fenestrate bryozoan fronds indicate episodic rapid burial, although individual burial layers were very thin. Further, each thin unit represents multiple rapid burial events, with successive communities of event-buried organisms amalgamated through biogenic mixing and low rates of net sediment accumulation.

The thicker units are dominated by vagile endobenthic deposit feeders, indicating increased sedimentation rates relative to the thinner units. The faunal assemblage of thicker units is also interpreted as autochthonous to parautochthonous, and the occurrence of endobenthic bivalves preserved with articulated valves and in living position indicates episodic rapid burial, but with much thicker individual burial layers relative to the thinner units.

Rapid burial events in both the thicker and thinner units are interpreted as tempestites. Storm deposition in the thicker units is accompanied by minor erosive events, winnowing, and thicker burial layers; in contrast, the thinner units appear to have

experienced only thin sediment blanketing and multi-directional paleocurrents. Thus, burial events in the thinner units evidently represent more distal storm events than those in the thicker units.

The upward shift in biofacies, taphofacies, and tempestite character from thinner to thicker units, equated with a shift to a more proximal position along the tempestite proximality gradient, indicates shoaling-upward resulting from deltaic progradation during regressive periods. During subsequent transgression, deltaic complexes are inundated, the tempestite proximality gradient shifts landward, and the more distal, sediment-starved facies is re-established. The three cycles recognized within the microstratigraphic section represent a progradational stacking pattern, with less time and fewer burial events occurring in the distal portion of successive cycles. Consequently, these cycles represent phased regression and indicate that the regression observed in the upper portion of the Stanton Cyclothem occurred through a series of minor regressions punctuated by minor flooding episodes. Furthermore, these thin cycles may be the distal expression of parasequences, preserved as remarkably thin (~15 cm) cycles representing long spans of time as a consequence of sediment-starvation.

The high abundance and diversity of crinoids recovered from the Main Crinoid Bed results from the amalgamation of multiple, successive communities smothered individually by tempestites, rather than from the rapid burial of a single diverse community of co-existing individuals. Thus, the most common crinoid genera represent occupants of the environment for spans of time long enough to become buried in multiple events, rather than genera that were present in large numbers in this localized area at any one time. However, the majority of crinoid genera are represented by very few

individuals each. These taxa are interpreted as having been present in this environment only for a short time, resulting in their burial by only one (or few) tempestite(s). Bed 1 and Bed 3 represent the same environment as the Main Crinoid Bed, but experienced progressively fewer burial events; as a result, the diversity of crinoidal material recovered from these units decreases upsection, while bed thickness decreases, and encrustation and compaction-related damage increase.

Crinoid Taphonomy

The crinoid fauna recovered from the Main Crinoid Bed displays significant variability in taphonomic state, which is detected even at the genus level. Such taphonomic differences among taxonomically similar organisms highlight the potential danger of generalizing about the taphonomy of large taxonomic units when based on limited genus-level data. Furthermore, several taphonomic trends appear to be dependent on the size of the individual, resulting in intraspecific taphonomic diversity.

Numerous interrelated factors account for the taphonomic state of articulated and partially articulated crinoid specimens recovered from the Copan Lagerstätte and include rate of burial, differences in skeletal morphology between genera, preferences of scavenging organisms, behavioral differences between genera, size of individuals, and variations in the thickness of burial layers.

REFERENCES CITED

AIGNER, T., 1985, Storm depositional systems: Dynamic stratigraphy in Modern and ancient shallow-marine sequences: Lecture Notes in Earth Sciences, v. 3, 174 p.

AIGNER, T., and REINECK, H.-E., 1982, Proximality trends in modern storm sands from the Helgoland Bight (North Sea) and their implications for basin analysis: Senckenbergiana Maritima, v. 14, p. 183-215.

ALGEO, T.J., and HECKEL, P.H., 2008, The Late Pennsylvanian Midcontinent Sea of North America: A review: Palaeogeography, Palaeoclimatology, Palaeoecology, v. 268, p. 205-221.

ALLER, R.C., MACKIN, J.E., and COX, R.T., Jr., 1986, Diagenesis of Fe and S in Amazon inner shelf muds: Apparent dominance of Fe reduction and implications for the genesis of ironstones: Continental Shelf Research, v. 6, p. 263-289.

ALLISON, P.A., 1986, Soft-bodied animals in the fossil record: The role of decay in fragmentation during transport: Geology, v. 14, p. 979-981.

ALLISON, P.A., 1988a, The role of anoxia in the decay and mineralization of proteinaceous macro-fossils: Paleobiology, v. 14, p. 139-154.

ALLISON, P.A., 1988b, *Konservat-Lagerstätten*: Cause and classification: Paleobiology, v. 14, p. 331-344.

ALLISON, P.A., 1990, Variation in rates of decay and disarticulation of Echinodermata: Implications for the application of actualistic data: PALAIOS, v. 5, p. 423-440.

ALLISON, P.A., and PYE, K., 1994, Early diagenetic mineralization and fossil preservation in modern carbonate concretions: PALAIOS, v. 9, p. 561-575.

ALLMON, R.A., 1985, "Butterflied" bivalves as paleoenvironmental indicators: Geological Society of America Abstracts with Program, v. 17, p. 512.

AMÉZIANE-COMINARDI, N., and ROUX, M., 1987, Biocorrosion et micritisation des ossicules d'Echinodermes en milieu bathyal au large de la Nouvelle-Calédonie: Comptes-Rendus de l'Académie des Sciences, Paris, Serie II, v. 305, p. 701-705.

AUSICH, W.I., 1999, Upper Pennsylvanian LaSalle Member, Bond Formation of central

Illinois, USA: *in* Hess, H., Ausich, W.I., Brett, C.E., and Simms, M.J., eds., Fossil Crinoids: Cambridge University Press, Cambridge, UK, p. 155-159.

AUSICH, W.I., 2001, Echinoderm taphonomy: *in* Jangoux, M., and Lawrence, J.M., eds., Echinoderm Studies, v. 6: A. A. Balkema, Rotterdam, p. 171-227.

AUSICH, W.I., and BAUMILLER, T.K., 1993, Taphonomic method for determining muscular articulations in fossil crinoids: PALAIOS, v. 8, p. 477-483.

AUSICH, W.I, and BAUMILLER, T.K., 1998, Disarticulation patterns in Ordovician crinoids: Implications for the evolutionary history of connective tissue in the Crinoidea: Lethaia, v. 31, p. 113-123.

AUSICH, W.I., and SEVASTOPULO, G.D., 1994, Taphonomy of Lower Carboniferous crinoids from the Hook Head Formation, Ireland: Lethaia, v. 27, p. 245-256.

AUSICH, W.I., KAMMER, T.W., and LANE, N.G., 1979, Fossil communities of the Borden (Mississippian) delta in Indiana and northern Kentucky: Journal of Paleontology, v. 53, p. 1182-1196.

BAIRD, G.C., SROKA, S.D., SHABICA, C.W., and KUECHER, G.J., 1986, Taphonomy of Middle Pennsylvanian Mazon Creek area fossil localities, northeastern Illinois: Significance of exceptional fossil preservation in syngenetic concretions: PALAIOS, v. 1, p. 271-285.

BAUMILLER, T.K., 1994, Implications of stress induced shedding body parts in crinoids: Geological Society of America Abstracts with Program, v. 26, p. 428.

BAUMILLER, T.K., 2003, Experimental and biostratinomic disarticulation of crinoids: Taphonomic implications: *in* Feral, J.P., and David, B., eds., Echinoderm Research 2001: Balkema, Rotterdam, p. 243-248.

BAUMILLER, T.K., and AUSICH, W.I., 1992, The broken-stick model as a null hypothesis for crinoid stalk taphonomy and as a guide to the distribution of connective tissue in fossils: Paleobiology, v. 18, p. 288-298.

BAUMILLER, T.K., and AUSICH, W.I., 1996, Crinoid stalk flexibility: Theoretical predictions and fossil stalk postures: Lethaia, v. 29, p. 47-59.

BAUMILLER, T.K., LLEWELLYN, G., MESSING, C.G., and AUSICH, W.I., 1995, Taphonomy of isocrinid stalks: Influence of decay and autotomy: PALAIOS, v. 10, p. 87-95.

BAUMILLER, T.K., GAHN, F.J., HESS, H., and MESSING, C.G., 2008, Taphonomy as an indicator of behavior among fossil crinoids: *in* Ausich, W.I., and Webster, G.D., eds., Echinoderm Paleobiology: Indiana University Press, Bloomington, p. 7-20.

BELLIS, W.H., and ROWLAND, T.L., 1976, Shale and carbonate-rock resources of Osage County, Oklahoma: Oklahoma Geological Survey Bulletin 76, 50 p.

BERNER, R.A., 1968, Calcium carbonate concretions formed by the decomposition of organic matter: Science, v. 159, p. 195-197.

BERNER, R.A., 1981a, Authigenic mineral formation resulting from organic matter decomposition in modern sediments: Fortschritte der Mineralogie, v. 59, p. 117-135.

BERNER, R.A., 1981b, A new geochemical classification of sedimentary environments: Journal of Sedimentary Petrology, v. 51, p. 359-365.

BERNER, R.A., 1984, Sedimentary pyrite: An update: Geochimica et Cosmochimica Acta, v. 48, p. 605-615.

BLYTH CAIN, J.D., 1968, Aspects of the depositional environment and palaeoecology of crinoidal limesones: Scottish Journal of Geology, v. 4, p. 191-208.

BOARDMAN, D.R., II, and HECKEL, P.H., 1989, Glacial-eustatic sea-level curve for early Late Pennsylvanian sequence in north-central Texas and biostratigraphic correlation with curve for midcontinent North America: Geology, v. 17, p. 802-805.

BOARDMAN, D.R., II, MAPES, R.H., YANCEY, T.E., and MALINKY, J.M., 1984, A new model for the depth-related allogenic community succession within North American Pennsylvanian cyclothems and implications for the black shale problem: *in* Hyne, N.J., ed., Limestones of the Mid-Continent: Tulsa Geological Society Special Publication 2, p. 141-182.

BRANDT, D.S., 1989, Taphonomic grades as a classification for fossiliferous assemblages and implications for paleoecology: PALAIOS, v. 4, p. 303-309.

BRENCHLEY, P.J., and NEWALL, G., 1970, Flume experiments on the orientation and transport of models and shell valves: Palaeogeography, Palaeoclimatology, Palaeoecology, v. 7, p. 185-220.

BRETT, C.E., 1983, Sedimentology, facies and depositional environments of the Rochester Shale (Silurian; Wenlockian) in western New York and Ontario: Journal of Sedimentary Petrology, v. 53, p. 947-971.

BRETT, C.E., 1995, Sequence stratigraphy, biostratigraphy, and taphonomy in shallow marine environments: PALAIOS, v. 10, p. 597-616.

BRETT, C.E., 1998, Sequence stratigraphy, paleoecology, and evolution: Biotic clues and responses to sea-level fluctuations: PALAIOS, v. 13, p. 241-262.

BRETT, C.E., 1999, Middle Devonian Windom Shale of Vincent, New York, USA: *in* Hess, H., Ausich, W., Brett, C.E., and Simms, M.J., eds., Fossil Crinoids: Cambridge University Press, Cambridge, UK, p. 122-128.

BRETT, C. E., and ALLISON, P.A., 1998, Paleontological approaches to the environmental interpretation of marine mudrocks: *in* Schieber, J., Zimmerle, W., and Sethi, P.S., eds., Shales and Mudstones I: Basin Studies, Sedimentology, and Paleontology: E. Schweizerbart'sche Verlagsbuchhandlung, Stuttgart, p. 301-349.

BRETT, C.E., and BAIRD, G.C., 1986a, Comparative taphonomy: A key to paleoenvironmental interpretation based on fossil preservation: PALAIOS, v. 1, p. 207-227.

BRETT, C.E., and BAIRD, G.C., 1986b, Symmetrical and upward shallowing cycles in the Middle Devonian of New York state and their implications for the punctuated aggradational cycle hypothesis: Paleoceanography, v. 1, p. 431-445.

BRETT, C.E., and BAIRD, G.C., 1993, Taphonomic approaches to temporal resolution in stratigraphy: Examples from Paleozoic marine mudrocks: *in* Kidwell, S.M., and Behrensmeyer, A.K., eds., Taphonomic Approaches to Time Resolution in Fossil Assemblages: Paleontological Society Short Courses in Paleontology, v. 6, p. 250-274.

BRETT, C.E., and BAIRD, G.C., 1996, Middle Devonian sedimentary cycles and sequences in the northern Appalachian Basin: *in* Witzke, B.J., Ludvigson, G.A., and Day, J., eds., Paleozoic Sequence Stratigraphy: Views from the North American Craton: Geological Society of America Special Paper 306, p. 213-241.

BRETT, C.E., and SEILACHER, A., 1991, Fossil Lagerstätten: A taphonomic consequence of event sedimentation: *in* Einsele, G., Ricken, W., and Seilacher, A., eds., Cycles and Events in Stratigraphy: Springer-Verlag, Berlin, p. 283-297.

BRETT, C.E., and TAYLOR, W.L., 1997, The *Homocrinus* beds: Silurian crinoid Lagerstätten of western New York and southern Ontario: *in* Brett, C.E., and Baird, G.C., eds., Paleontological Events: Stratigraphic, Ecological, and Evolutionary Implications: Columbia University Press, New York, p. 181-223.

BRETT, C.E., ALLISON, P.A., DESANTIS, M.K., LIDDELL, W.D., and KRAMER, A., 2009a, Sequence stratigraphy, cyclic facies, and *lagerstätten* in the Middle Cambrian Wheeler and Marjum Formations, Great Basin, Utah: Palaeogeography, Palaeoclimatology, Palaeoecology, v. 277, p. 9-33.

BRETT, C.E., BAIRD, G.C., and SPEYER, S.E., 1997a, Fossil Lagerstätten: Stratigraphic records of palentologic and taphonomic events: *in* Brett, C.E., and Baird, G.C., eds., Paleontological Events: Stratigraphic, Ecological, and Evolutionary

Implications: Columbia University Press, New York, p. 3-40.

BRETT, C.E., MOFFAT, H.A., and TAYLOR, W.L., 1997b, Echinoderm taphonomy, taphofacies and Lagerstätten: *in* Waters, J.A., and Maples, C.G., eds., Geobiology of Echinoderms: Paleontological Society Papers, v. 3, p. 147-190.

BRETT, C.E., ZAMBITO, J.J., HUNDA, B.R., KOLBE, S.E., and SCHINDLER, E., 2009b, Taphonomic analysis of Devonian rhythmic trilobite beds: Event sedimentation and cyclic cementation: Geological Society of America Abstracts with Program, v. 41, p. 31.

BROMLEY, R.G., and EKDALE, A.A., 1984, *Chondrites*: A trace fossil indicator of anoxia I n sediments: Science, v. 224, p. 872-874.

BUSH, A.M., KOWALEWSKI, M., HOFFMEISTER, A.P., BAMBACH, R.K., and DALEY, G.M., 2007, Potential paleoecologic biases from size-filtering of fossils: Strategies for sieving: PALAIOS, v. 22, p. 612-622.

CANFIELD, D.E., and RAISWELL, R., 1991, Carbonate precipitation and dissolution: Its relevance to fossil preservation: *in* Allison, P.A., and Briggs, D.E.G., eds., Taphonomy: Releasing the Data Locked in the Fossil Record: Plenum Press, New York, p. 411-463.

CANFIELD, D.E., THAMDRUP, B., and HANSEN, J.W., 1993, The anaerobic degradation of organic matter in Danish coastal sediments: Iron reduction, manganese reduction, and sulfate reduction: Geochimica et Cosmochimica Acta, v. 57, p. 3867-3883.

CARPENTER, S.J., ERICKSON, J.M., LOHMANN, K.C., and OWEN, M.R., 1988, Diagenesis of fossiliferous concretions from the Upper Cretaceous Fox Hills Formation, North Dakota: Journal of Sedimentary Petrology, v. 58, p. 706-723.

CHAPELLE, F.H., and LOVLEY, D.R., 1992, Competitive exclusion of sulfate reduction by Fe(III)-reducing bacteria: A mechanism for producing discrete zones of high-iron ground water: Ground Water, v. 30, p. 29-36.

CHOI, K.S., KHIM, B.K., and WOO, K.S., 2003, Spherulitic siderites in the Holocene coastal deposits of Korea (eastern Yellow Sea): Elemental and isotopic composition and depositional environment: Marine Geology, v. 202, p. 17-31.

CLAYPOOL, G.E., and KAPLAN, I.R., 1974, The origin and distribution of methane in marine sediments: *in* Kaplan, I.R., ed., Natural Gases in Marine Sediments: Plenum Press, New York, p. 99-139.

COLEMAN, M.L., 1993, Microbial processes: Controls on the shape and composition of carbonate concretions: Marine Geology, v. 113, p. 127-140.

COLEMAN, M.L., and RAISWELL, R., 1981, Carbon, oxygen, and sulphur isotope variations in concretions from the Upper Lias of N. E. England: Geochimica et Cosmochimica Acta, v. 45, p. 329-340.

COLEMAN, M.L., HEDRICK, D.B., LOVLEY, D.R., WHITE, D.C., and PYE, K., 1993, Reduction of Fe (III) in sediments by sulphate-reducing bacteria: Nature, v. 361, p. 436-438.

CROWELL, J.C., 1978, Gondwanan glaciation, cyclothems, continental positioning, and climate change: American Journal of Science, v. 278, p. 1345-1372.

CURTIS, C.D., and SPEARS, D.A., 1968, The formation of sedimentary iron minerals: Economic Geology, v. 63, p. 257-270.

CURTIS, C.D., COLEMAN, M.L., and LOVE, L.G., 1986, Pore water evolution during sediment burial from isotopic and mineral chemistry of calcite, dolomite and siderite concretions: Geochimica et Cosmochimica Acta, v. 50, p. 2321-2334.

DATTILO, B.F., BRETT, C.E., TSUJITA, C.J., and FAIRHURST, C., 2008, Sediment supply versus storm winnowing in the development of muddy and shelly interbeds from the Upper Ordovician of the Cincinnati region, USA: Canadian Journal of Earth Sciences, v. 45, p. 243-265.

DONOVAN, S.K., 1991, The taphonomy of echinoderms: Calcareous multi-element skeletons in the marine environment: *in* Donovan, S.K., ed., The Processes of Fossilization: Columbia University Press, New York, p. 241-269.

DUAN, W.M., HEDRICK, D.B., PYE, K., COLEMAN, M.L., and WHITE, D.C., 1996, A preliminary study of the geochemical and microbiological characteristics of modern sedimentary concretions: Limnology and Oceanography, v. 7, p. 1404-1414.

ELDER, W.P., GUSTASON, E.R., and SAGEMAN, B.B., 1994, Correlation of basinal carbonate cycles to nearshore parasequences in the Late Cretaceous Greenhorn seaway, Western Interior U.S.A.: Geological Society of America Bulletin, v. 106, p. 892-902.

FELDMAN, H.R., 1989, Taphonomic processes in the Waldron Shale, Silurian, southern Indiana: PALAIOS, v. 4, p. 144-156.

FELTON, R.M., and HECKEL, P.H., 1996, Small-scale cycles in Winterset Limestone Member (Dennis Formation, Pennsylvanian of northern Midcontinent) represent 'phased regression': *in* Witzke, B.J., Ludvigson, G.A., and Day, J., eds., Paleozoic Sequence Stratigraphy: Views from the North American Craton: Geological Society of America Special Paper 306, p. 389-397.

FIELDING, C.R., FRANK, T.D., and ISBELL, J.L., eds., 2008, Resolving the Late Paleozoic Ice Age in Time and Space: Geological Society of America Special Paper 441, 354 p.

FISHER, Q.J., RAISWELL, R., and MARSHALL, J.D., 1998, Siderite concretions from nonmarine shales (Westphalian A) of the Pennines, England: Controls on their growth and composition: Journal of Sedimentary Research, v. 68, p. 1034-1045.

FRITZ, P., BINDA, P.L., FOLINSBEE, F.E., and KROUSE, H.R., 1971, Isotopic composition of diagenetic siderites from Cretaceous sediments in western Canada: Journal of Sedimentary Petrology, v. 41, p. 282-288.

FROELICH, P.H., KLINKHAMMER, G.P., BENDER, M.L., LUEDKE, N.A., HEATH, G.R., CULLEN, D., DAUPHIN, P., HAMMOND, D., HARTMAN, B., and MAYNARD, V., 1979, Early oxidation of organic matter in pelagic sediments of the eastern equatorial Atlantic: Suboxic diagenesis: Geochimica et Cosmochimica Acta, v. 43, p. 1075-1090.

FUJITA, T., OHTA, S., and OJI, T., 1987, Photographic observations of the stalked crinoid *Metacrinus rotundus* Carpenter in Suruga Bay, central Japan: Journal of the Oceanographic Society of Japan, v. 43, p. 333-343.

GAHN, F.J., and BAUMILLER, T.K., 2004, A bootstrap analysis for comparative taphonomy applied to Early Mississippian (Kinderhookian) crinoids from the Wassonville cycle of Iowa: PALAIOS, v. 19, p. 17-38.

GOULD, S.J., 1989, Wonderful Life: The Burgess Shale and the Nature of History: Norton, New York, 347 p.

GRAY, D.I., and BENTON, M.J., 1982, Multidirectional paleocurrents as indicators of shelf storm beds: *in* Einsele, G., and Seilacher, A., eds., Cyclic and Event Stratification: Springer-Verlag, Berlin, p. 350-353.

HALL, J.T., and SAVRDA, C.E., 2008, Ichnofossils and ichnofabrics in syngenetic phosphatic concretions in siliciclastic shelf deposits, Ripley Formation, Cretaceous, Alabama: PALAIOS, v. 23, p. 233-245.

HARRIES, P.J., ed., 2003, High-Resolution Approaches in Stratigraphic Paleontology: Kluwer Academic Publishers, Dordrecht, 474 p.

HECKEL, P.H., 1977, Origin of phosphatic black shale facies in Pennsylvanian cyclothems of midcontinent North America: American Association of Petroleum Geologists Bulletin, v. 61, p. 1045-1068.

HECKEL, P.H., 1978, Field guide to Upper Pennsylvanian cyclothemic limestone facies in eastern Kansas: Kansas Geological Survey Guidebook Series 2, 79 p.

HECKEL, P.H., 1980, Paleogeography of eustatic model for deposition of midcontinent Upper Paleozoic cyclothems: *in* Fouch, T.D., and Magathan, E.R., eds., Paleozoic Paleogeography of the west-central United States: Society of Economic Paleontologists and Mineralogists, Rocky Mountain Section, West-Central United States Paleogeography Symposium 1, p. 197-215.

HECKEL, P.H., 1984, Changing concepts of midcontinent Pennsylvanian cyclothems, North America: *in* Congrès International de Stratigraphie et de Géologie du Carbonifere, 9th, 1979, Compte Redu, Volume 3, pt. 3: Southern Illinois University Press, Carbondale, Illinois, p. 535-553.

HECKEL, P.H., 1986, Sea-level curve for Pennsylvanian eustatic marine transgressive-regressive depositional cycles along midcontinent outcrop belt, North America: Geology, v. 14, p. 330-334.

HECKEL, P.H., 1994, Evaluation of evidence for glacio-eustatic control over marine Pennsylvanian cyclothems in North America and consideration of possible tectonic effects: *in* Dennison, J.M., and Ettensohn, F.R., eds., Tectonic and Eustatic Controls on Sedimentary Cycles: Society of Economic Paleontologists and Mineralogists Concepts in Sedimentology and Paleontology 4, p. 65-87.

HOLLAND, S.M., 1988, Taphonomic effects of seafloor exposure on an Ordovician brachiopod assemblage: PALAIOS, v. 3, p. 588-597.

HOLLAND, S.M., 1995, The stratigraphic distribution of fossils: Paleobiology, v. 21, p. 109-121.

HOLLAND, S.M., 1999, The New Stratigraphy and its promise for paleobiology: Paleobiology, v. 25, p. 409-416.

HOLLAND, S.M., MILLER, A.I., DATTILO, B.F., MEYER, D.L., and DIEKMEYER, S.L., 1997, Cycle anatomy and variability in the storm-dominated type Cincinnatian (Upper Ordovician): Coming to grips with cycle delineation and genesis: Journal of Geology, v. 105, p. 135-152.

HOLLAND, S.M., MILLER, A.I., MEYER, D.L., and DATTILO, B.F., 2001, The detection and importance of subtle biofacies within a single lithofacies: The Upper Ordovician Kope Formation of the Cincinnati, Ohio region: PALAIOS, v. 16, p. 205-217.

HOLTERHOFF, P.F., 1988, Paleobiology and paleoecology of crinoids from the Lower Stanton Formation (Late Pennsylvanian, Missourian) of the mid-continent United States: Unpublished M. S. thesis, University of Nebraska, Lincoln, 137 p.

HOLTERHOFF, P.F., 1996, Crinoid biofacies in Upper Carboniferous cyclothems, midcontinent North America: Faunal tracking and the role of regional processes

in biofacies recurrence: Palaeogeography, Palaeoclimatology, Palaeoecology, v. 127, p. 47-81.

HOLTERHOFF, P.F., 1997a, Filtration models, guilds, and biofacies: Crinoid paleoecology of the Stanton Formation (Upper Pennsylvanian), midcontinent, North America: Palaeogeography, Palaeoclimatology, Palaeoecology, v. 130, p. 177-208.

HOLTERHOFF, P.F., 1997b, Paleocommunity and evolutionary ecology of Paleozoic crinoids: *in* Waters, J.A., and Maples, C.G., eds., Geobiology of Echinoderms: Paleontological Society Papers, v. 3, p. 69-106.

JENNETTE, D.C., and PRYOR, W.A., 1993, Cyclic alternation of proximal and distal storm facies: Kope and Fairview Formations (Upper Ordovician), Ohio and Kentucky: Journal of Sedimentary Petrology, v. 63, p. 183-203.

KAMMER, T.W., 1985, Basinal and prodeltaic communities of the Early Carboniferous Borden Formation in northern Kentucky and southern Indiana (U.S.A.): Palaeogeography, Palaeoclimatology, Palaeoecology, v. 49, p. 79-121.

KAMMER, T.W., BRETT, C.E., BOARDMAN, D.R., II, and MAPES, R.H., 1986, Ecologic stability of the dysaerobic biofacies during the late Paleozoic: Lethaia, v. 19, p. 109-121.

KIDWELL, S.M., 1991, The stratigraphy of shell concentrations: *in* Allison, P.A., and Briggs, D.E.G., eds., Taphonomy: Releasing the Data Locked in the Fossil Record: Plenum Press, New York, p. 211-290.

KIDWELL, S.M., 2002, Time-averaged molluscan death assemblages: Palimpsests of richness, snapshots of abundance: Geology, v. 30, p. 803-806.

KIDWELL, S.M., and BAUMILLER, T.K., 1990, Experiment disintegration of regular echinoids: Roles of temperature, oxygen, and decay thresholds: Paleobiology, v. 16, p. 247-271.

KIDWELL, S.M., and JABLONSKI, D., 1983, Taphonomic feedback: Ecological consequences of shell accumulation: *in* Tevesz, M.J.S., and McCall, P.L., eds., Biotic Interactions in Recent and Fossil Benthic Communitites: Plenum Press, New York, p. 195-248.

KIDWELL, S.M., ROTHFUS, T.A., and BEST, M.M.R., 2001, Sensitivity of taphonomic signatures to sample size, sieve size, damage scoring system, and target taxa: PALAIOS, v. 16, p. 26-52.

KLEIN, G.D., 1990, Comments on sedimentary-stratigraphic verification of some geodynamic basin models: Example from a cratonic and associated foreland basins: *in* Cross, A.T., ed., Quantitative Dynamic Stratigraphy: Prentice Hall,

Englewood Cliffs, New Jersey, p. 503-518.

KLEIN, G.D., and KUPPERMAN, J.B., 1992, Pennsylvanian cyclothems: Methods of distinguishing tectonically induced changes in sea level from climatically induced changes: Geological Society of America Bulletin, v. 104, p. 166-175.

KLEIN, G.D., and WILLARD, D.A., 1989, Origin of the Pennsylvanian coal-bearing cyclothems of North America: Geology, v. 17, p. 152-155.

KRANZ, P.M., 1974, The anastrophic burial of bivalves and its paleoecological significance: Journal of Geology, v. 82, p. 237-265.

KREISA, R.D., 1981, Storm-generated sedimentary structures in subtidal marine facies with examples from the Middle and Upper Ordovician of southwestern Virginia: Journal of Sedimentary Petrology, v. 51, p. 823-848.

KREISA, R.D., and BAMBACH, R.K., 1982, The role of storm processes in generating shell beds in Paleozoic shelf environments: *in* Einsele, G., and Seilacher, A., eds., Cyclic and Event Stratification: Springer-Verlag, Berlin, p. 200-207.

LAENEN, B., and DE CRAEN, M., 2004, Eogenetic siderite as an indicator for fluctuations in sedimentation rate in the Oligocene Boom Clay Formation (Belgium): Sedimentary Geology, v. 163, p. 165-174.

LANE, N.G., 1984, Predation and survival among inadunate crinoids: Paleobiology, v. 10, p. 453- 458.

LANE, N.G., and SEVASTOPULO, G.D., 1981, Functional morphology of a microcrinoid: *Kallimorphocrinus punctatus* n. sp.: Journal of Paleontology, v. 55, p. 13-28.

LANE, N.G., and SEVASTOPULO, G.D., 1982, Growth and systematic revision of *Kallimorphocrinus astrus*, a Pennsylvanian microcrinoid: Journal of Paleontology, v. 56, p. 244-259.

LEHMAN, D., and POPE, J.K., 1989, Upper Ordovician tempestites from Swatara Gap, Pennsylvania: Depositional processes affecting the sediments and paleoecology of the fossil faunas: PALAIOS, v. 4, p. 553-564.

LEWIS, R.D., 1980, Taphonomy: *in* Broadhead, T. W., and Waters, J. A., eds., Echinoderms: Notes for a Short Course: University of Tennessee Studies in Geology, v. 3, p. 27-39.

LEWIS, R.D., 1986, Relative rates of skeletal disarticulation in modern ophiuroids and Paleozoic crinoids: Geological Society of America Abstracts with Program, v. 18, p. 672.

LEWIS, R.D., 1987, Post-mortem decomposition of ophiuroids from the Mississippi Sound: Geological Society of America Abstracts with Program, v. 19, p. 94-95.

LEWIS, R.D., and STRIMPLE, H.L., 1990, *Sciadiocrinus*, convergence on the family Pirasocrinidae (Crinoidea: Echinodermata): Journal of Paleontology, v. 64, p. 293-300.

LEWIS, R.D., CHAMBERS, C.R., and PEEBLES, M.W., 1990, Grain morphologies and surface textures of Recent and Pleistocene crinoid ossicles, San Salvador, Bahamas: PALAIOS, v. 5, p. 570-579.

LEWIS, R.D., HOLTERHOFF, P.F., MOSHER, D., and PABIAN, R.K., 1998, Taphonomy of a crinoid Lagerstätte deposit, Barnsdall Formation (Upper Pennsylvanian), northeastern Oklahoma: Geological Society of America Abstracts with Progam, v. 30, p. 31.

LIDDELL, W.D., 1975, Recent crinoid biostratinomy: Geological Society of America Abstracts with Program, v. 7, p. 1169.

LLEWELLYN, G., and BAUMILLER, T.K., 1993, Stem growth strategies for two Western Atlantic isocrinid species: Geological Society of America Abstracts with Program, v. 25, p. 104-105.

LLEWELLYN, G., and MESSING, C.G., 1993, Compositional and taphonomic variations in modern crinoid-rich sediments from the deep-water margin of a carbonate bank: PALAIOS, v. 8, p. 554-573.

LOVLEY, D.R., and PHILLIPS, E.J.P., 1987, Competitive mechanisms for inhibition of sulfate reduction and methane production in the zone of ferric iron reduction in sediments: Applied and Environmental Microbiology, v. 53, p. 2636-2641.

MACQUAKER, J.H.S., GAWTHORPE, R.L., TAYLOR, K.G., and OATES, M.J., 1998, Heterogeneity, stacking patterns, and sequence stratigraphic interpretation in distal mudstone successions: Examples from the Kimmeridge Clay Formation, U. K.: *in* Schieber, J., Zimmerle, W., and Sethi, P., eds., Shales and Mudstones I: Basin Studies, Sedimentology, and Paleontology: E. Schweizerbart'sche Verlagsbuchhandlung, Stuttgart, p. 163-186.

MALINKY, J.M., and HECKEL, P.H., 1998, Paleoecology and taphonomy of faunal assemblages in gray "core" (offshore) shales in midcontinent Pennsylvanian cyclothems: PALAIOS, v. 13, p. 311-334.

MAPLES, C.G., 1986, Enhanced paleoecological and paleoenvironmental interpretations result from analysis of early diagenetic concretions in Pennsylvanian shales: PALAIOS, v. 1, p. 512-516.

MAPLES, C.G., and ARCHER, A.W., 1989, Paleoecological and sedimentological significance of bioturbated crinoid calyxes: PALAIOS, v. 4, p. 379-383.

MARTIN, W.R., and SAYLES, F.L., 2004, The recycling of biogenic material at the seafloor: *in* Mackenzie, F.T., ed., Treatise of Geochemistry: Sediments, Diagenesis, and Sedimentary Rocks: Elsevier, Amsterdam, p. 37-66.

MAYNARD, J.B., 1982, Extension of Berner's "New geochemical classifcation of sedimentary environments" to ancient sediments: Journal of Sedimentary Petrology, v. 52, p. 1325-1331.

MCLAUGHLIN, P.I., and BRETT, C.E., 2004, Eustatic and tectonic controls on the distribution of marine seismites: Examples from the Upper Ordovician of Kentucky, USA: Sedimentary Geology, v. 168, p. 165-192.

MESSING, C.G., 1997, Living comatulids: *in* Waters, J.A., and Maples, C.G., eds., Geobiology of Echinoderms: Paleontological Society Papers, v. 3, p. 3-30.

MESSING, C.G., and RANKIN, D., 1995, Local variations in skeletal contribution to sediment by a modern stalked crinoid (*Chladocrinus decorus*) (Echinodermata) relative to distribution of a living population: Geological Society of America Abstracts with Program, v. 27, p. 136.

MESSING, C.G., NEUMANN, A.C., and LANG, D.J.C., 1990, Biozonation of deep-water limestone lithoherms and associated hardgrounds in the northeastern Straits of Florida: PALAIOS, v. 5, p. 15-33.

MEYER, D.L., 1971, Post-mortem disarticulation of Recent crinoids and ophiuroids under natural conditions: Geological Society of America Abstracts with Programs, v. 3, p. 645.

MEYER, D.L., 1997, Implications of research on living stalked crinoids for paleobiology: *in* Waters, J.A., and Maples, C.G., eds., Geobiology of Echinoderms: Paleontological Society Papers, v. 3, p. 31-43.

MEYER, D.L., and AUSICH, W.I., 1983, Biotic interactions among Recent and among fossil crinoids: *in* Tevesz, M.J.S., and McCall, P.L., eds., Biotic Interactions in Recent and Fossil Benthic Communities: Plenum Press, New York, p. 377-427.

MEYER, D.L., and MEYER, K.B., 1986, Biostratinomy of Recent crinoids (Echinodermata) at Lizard Island, Great Barrier Reef, Australia: PALAIOS, v. 1, p. 294-302.

MEYER, D.L., and MILSON, C.V., 2001, Microbial sealing in the biostratinomy of *Uintacrinus* Lagerstätten in the Upper Cretaceous of Kansas and Colorado, USA: PALAIOS, v. 16, p. 535-546.

MEYER, D.L., AUSICH, W.I., and TERRY, R.E., 1989, Comparative taphonomy of echinoderms in carbonate facies: Fort Payne Formation (Lower Mississippian) of Kentucky and Tennessee: PALAIOS, v. 4, p. 533-552.

MIALL, A.D., 2000, Principles of Sedimentary Basin Analysis, 3rd ed.: Springer-Verlag, Berlin, 616 p.

MILLER, K.B., BRETT, C.E., and PARSONS, K.M., 1988, The paleoecologic significance of storm-generated disturbance within a Middle Devonian muddy epeiric sea: PALAIOS, v. 3, p. 35-52.

MOORE, R.C., and TEICHERT, C., eds., 1978, Treatise on Invertebrate Paleontology, Part T, Echinodermata 2, Crinoidea: Geological Society of America and University of Kansas, Boulder, CO and Lawrence, KS, 1027 p.

MOORE, R.C., and STRIMPLE, H L., 1969, Explosive evolutionary differentiation of a unique group of Mississippian-Pennsylvanian camerate crinoids (Acrocrindae): University of Kansas Paleontological Contributions Paper 39, 44 p.

NAGLE, J.S., 1967, Wave and current orientation of shells: Journal of Sedimentary Petrology, v. 37, p. 1124-1138.

NEBELSICK, J.H., 1999, Taphonomy of *Clypeaster* fragments: Preservation and taphofacies: Lethaia, v. 32, p. 241-252.

NEBELSICK, J.H., SCHMID, B., and STACHOWITSCH, M., 1997, The encrustation of fossil and recent sea-urchin tests: Ecological and taphonomic significance: Lethaia, v. 30, p. 271-284.

NISSENBAUM, A., PRESLEY, B.J., and KAPLAN, I.R., 1972, Early diagenesis in a reducing fjord, Saanich Inlet, British Columbia, I, chemical and isotopic changes in major components of interstitial water: Geochimica et Cosmochimica Acta, v. 36, p. 1007-1027.

NITECKI, M.H., 1979, Mazon Creek Fossils: Academic Press, New York, New York, 581 p.

OAKES, M.C., 1940, Geology and mineral resources of Washington County, Oklahoma: Oklahoma Geological Survey Bulletin 62, 208 p.

O'BRIEN, N.R., 1987, The effects of bioturbation on the fabric of shale: Journal of Sedimentary Research, v. 57, p. 449-455.

O'BRIEN, N.R., BRETT, C.E., and TAYLOR, W.L., 1994, The significance of microfabric and taphonomic analysis in determining sedimentary processes in marine

mudrocks: Journal of Sedimentary Research, v. A64, p. 847-852.

PABIAN, R.K., 1987, A Late Pennsylvanian (Missourian) echinoderm fauna from northeastern Oklahoma: Proceedings of the Nebraska Academy of Sciences, v. 97, p. 48.

PABIAN, R.K., 2003, Taphonomic analysis of crinoids from the Stanton Formation (Late Pennsylvanian, Missourian) of the North American midcontinent: Evidence for predation, parasitism, and commensalism: Geological Society of America Abstracts with Program, v. 35, p. 7-8.

PABIAN, R.K., and STRIMPLE, H.L., 1970, Paleoecology of Pennsylvanian crinoids from southeastern Nebraska and southwestern Iowa: Proceedings of the Nebraska Academy of Sciences, v. 80, 36 p.

PABIAN, R.K., and STRIMPLE, H.L., 1979, Notes on biometrics, paleoecology, and biostratigraphy of *Cibolocrinus conicus* Strimple from Oklahoma, Kansas, and Nebraska: Journal of Paleontology, v. 53, p. 421-437.

PABIAN, R.K., and STRIMPLE, H.L., 1985, Classification, paleoecology, and biostratigraphy of crinoids from the Stull Shale (Late Pennsylvanian) of Nebraska, Kansas, and Iowa: Bulletin of the University of Nebraska State Museum, v. 11, 81 p.

PABIAN, R.K., and STRIMPLE, H.L., 1993, Taxonomy, paleoecology and biostratigraphy of the crinoids of the South Bend Limestone (Late Pennsylvanian—Missourian, ?Virgilian) in southeastern Nebraska and southeastern Kansas: Nebraska Geological Survey Professional Publication 1, 55 p.

PABIAN, R.K., MOSHER, D., LEWIS, R.D., and HOLTERHOFF, P.F., 1995, Crinoid assemblage from the Barnsdall Formation, Late Pennsylvanian (Missourian), Washington County, Oklahoma: Geological Society of America Abstracts with Program, v. 27, p. 78.

PABIAN, R.K., MOSHER, D., LEWIS, R.D., and HOLTERHOFF, P.F., 1997, Prey-predator, parasitic, and commensal relationships with Late Pennsylvanian crinoids and associated fauna from the Barnsdall Formation (Late Pennsylvanian, Missourian/Virgilian) of northeastern Oklahoma: Proceedings of the Nebraska Academy of Sciences, v. 107, p. 49.

PARSONS, K.M., and BRETT, C.E., 1991, Taphonomic processes and biases in modern marine environments: An actualistic perspective on fossil assemblage preservation: *in* Donovan, S. K., ed., The Processes of Fossilization: Columbia University Press, New York, p. 22-65.

PARSONS, K.M., BRETT, C.E., and MILLER, K.B., 1988, Taphonomy and depositional

dynamics of Devonian shell-rich mudstones: Palaeogeography, Palaeoclimatology, Palaeoecology, v. 63, p. 109-139.

PEMBERTON, S.G., and MACEACHERN, J.A., 1997, The ichnological signature of storm deposits: The use of trace fossils in event stratigraphy: *in* Brett, C.E., and Baird, G.C., eds., Paleontological Events: Stratigraphic, Ecological, and Evolutionary Implications: Columia University Press, New York, p. 73-109.

PETERSON, C.H., 1985, Patterns of lagoonal bivalve mortality after heavy sedimentation and their paleoecological significance: Paleobiology, v. 11, p. 139-153.

PLOTNICK, R.E., 1986, Taphonomy of a modern shrimp: Implications for the arthropod fossil record: PALAIOS, v. 1, p. 286-293.

POSAMENTIER, H.W., and ALLEN, G.P., 1999, Siliciclastic Sequence Stratigraphy: Society of Economic Paleontologist and Mineralogists Concepts in Sedimentology and Paleontology, v.7, 191 p.

PRESLEY, B.J., and KAPLAN, I.R., 1968, Changes in dissolved sulphate calcium and carbonate from interstitial water of near-shore sediments: Geochimica et Cosmochimica Acta, v. 32, p. 1037-1049.

PYE, K., 1981, Marshrock formed by iron sulphide and siderite cementation in saltmarsh sediments: Nature, v. 294, p. 650-652.

PYE, K., DICKSON, J.A.D., SCHIAVON, N., COLEMAN, M.L., and COX, M., 1990, Formation of siderite-Mg calcite-iron sulfide concretions in intertidal marsh and sandflat sediments, north Norfolk, England: Sedimentology, v. 37, p. 325-343.

RAISWELL, R., 1976, The microbiological formation of carbonate concretions in the Upper Lias of NE England: Chemical Geology, v. 18, p. 227-244.

RAISWELL, R., 1987, Non-steady state microbiological diagenesis and the origin of concretions and nodular limestones: *in* Marshall, J.D., ed., Diagenesis of Sedimentary Sequences: Geological Society of London Special Publication 36, p. 41-54.

RASCOE, B., Jr., 1975, Tectonic origin of preconsolidation deformation in Upper Pennsylvanian rocks near Bartlesville, Oklahoma: AAPG Bulletin, v. 59, p. 1626-1638.

READ, W.A., and FORSYTH, I.H., 1989, Allocycles and autocycles in the upper part of the Limestone Coal Group (Pendlein E1) in the Glasgow-Stirling region of the Midland Valley of Scotland: Geological Journal, v. 24, p. 121-137.

ROSENKRANZ, D., 1971, Dur Sedimentologie und Okologie von Echinodermen-

Lagerstätten: Neues Jahrbuch für Geologie und Palaeontologie, Abh., 138, p. 221-258.

SAVARESE, M., DODD, J.R., and LANE, N.G., 1997, Taphonomic and sedimentologic implications of crinoid intraskeletal porosity: Lethaia, v. 29, p. 141-156.

SAVRDA, C.E., 1995, Ichnologic applications in paleoceanographic, paleoclimatic, and sea-level studies: PALAIOS, v. 10, p. 565-577.

SAVRDA, C.E., 2007, Taphonomy of trace fossils: *in* Miller, W., III, ed., Trace Fossils: Concepts, Problems, Prospects: Elsevier, Amsterdam, p. 92-109.

SAYLES, F.L., and MANHEIM, F.T., 1975, Interstitial solutions and diagenesis in deeply buried marine sediments: Results from the Deep Sea Drilling Project: Geochimica et Cosmochimica Acta, v. 39, p. 103-127.

SCHWARZACHER, W., 1963, Orientation of crinoids by current action: Journal of Sedimentary Petrology, v. 33, p. 580-586.

SEILACHER, A., 1970, Fossil-Lagerstätten, Nr. 1; begriff und Bedeutung der Fossil-Lagerstätten: Neues Jahrbuch für Geologie und Palaeontologie, v. 1, p. 34-39.

SEILACHER, A., 2001, Concretion morphologies reflecting diagenetic and epigenetic pathways: Sedimentary Geology, v. 143, p. 41-57.

SEILACHER, A., and MACCLINTOCK, C., 2005, Crinoid anchoring strategies for soft-bottom dwelling: PALAIOS, v. 20, p. 224-240.

SEILACHER, A., REIF, W.E., and WESTPHAL, F., 1985, Sedimentological, ecological, and temporal patterns of fossil Lagerstätten: Philosophical Transactions of the Royal Society of London, v. 311, p. 5-23.

SELLÉS-MARTÍNEZ, J., 1996, Concretion morphology, classification, and genesis: Earth Science Reviews, v. 41, p. 177-210.

SELLWOOD, B.W., 1971, The genesis of some sideritic beds in the Yorkshire Lias (England): Journal of Sedimentary Petrology, v. 41, p. 854-858.

SHANNON, P.M., 1977, Diagenetic concretions from the Ribband Group sediments of County Wexford, Ireland: Geological Magazine, v. 114, p. 127-132.

SEVASTOPULO, G.D., 2008, Paleobiology of Carboniferous microcrinoids: *in* Ausich, W.I., and Webster, G.D., eds., Echinoderm Paleobiology: Indiana University Press, Bloomington, Indiana, p. 55-69.

SHÄFER, W., 1972, Ecology and Palaeoecology of Marine Environments: University of

Chicago Press, Chicago, 568 p.

SIMMS, M.J., 1999, Systematics, phylogeny and evolutionary history: *in* Hess, H., Ausich, W.I., Brett, C.E., and Simms, M.J., eds., Fossil Crinoids: Cambridge University Press, Cambridge, United Kingdom, p. 31-40.

SPEYER, S.E., and BRETT, C.E., 1986, Trilobite taphonomy and Middle Devonian taphofacies: PALAIOS, v. 1, p. 312-327.

SPEYER, S.E., and BRETT, C.E., 1991, Taphofacies controls: Background and episodic processes in fossil assemblage preservation: *in* Allison, P.A., and Briggs, D.E G., eds., Taphonomy: Releasing the Data Locked in the Fossil Record: Plenum Press, New York, p. 502-541.

STAFF, G.M., STANTON, R.J., JR., POWELL, E.N., and CUMMINS, H., 1986, Time-averaging, taphonomy, and their impact on paleocommunity reconstruction: Death assemblages in Texas bays: Geological Society of America Bulletin, v. 97, p. 428-443.

STANLEY, S.M., 1970, Relation of shell form to life habits in the Bivalvia (Mollusca): Geological Society of America Memoir 125, 296 p.

STRIMPLE, H.L., 1949a, Crinoid Studies, Parts IV-VI: Bulletin of American Paleontology, v. 32, 43 p.

STRIMPLE, H.L., 1949b, Two new species of *Acrocrinus* from the Pennsylvanian of Oklahoma: American Journal of Science, v. 247, p. 900-904.

STRIMPLE, H.L., 1950, New species of *Utharocrinus* and *Lasanocrinus*: Journal of Paleontology, v. 24, p. 571-574.

STRIMPLE, H.L., 1951, Some new species of Carboniferous crinoids: Bulletin of American Paleontology, v. 33, 41 p.

STRIMPLE, H.L., 1952, The arms of *Perimestocrinus*: Journal of Paleontology, v. 26, p. 784-788.

STRIMPLE, H.L., 1977, Notes concerning *Delocrinus* and *Graffhamicrinus* (Crinoidea: Inadunata): Proceedings of the Iowa Academy of Science, v. 84, p. 157-162.

STRIMPLE, H.L., and MOORE, R.C., 1971, Crinoids of the LaSalle Limestone (Pennsylvanian) of Illinois: University of Kansas Paleontological Contributions, Echinodermata Article 11, 48 p.

TANNER, W.F., Jr., 1956, Geology of northeastern Osage County, Oklahoma: Oklahoma Geological Survey Circular 40, 76 p.

TAYLOR, K.G., and MACQUAKER, J.H.S., 2000, Spatial and temporal distribution of authigenic minerals in continental shelf sediments: Implications for sequence stratigraphic analysis: *in* Glenn, C. R., Prévôt, L., and Lucas, J., eds., Marine Authigenesis: From Global to Microbial: Society of Economic Paleontologists and Mineralogists Special Publication 66, p. 309-323.

TAYLOR, W.L., and BRETT, C E., 1996, Taphonomy and paleoecology of echinoderm Lagerstätten from the Silurian (Wenlockian) Rochester Shale: PALAIOS, v. 11, p. 118-140.

TAYLOR, W.L., and BRETT, C.E., 1999, Middle Silurian Rochester Shale of western New York, USA, and southern Ontario, Canada: *in* Hess, H., Ausich, W.I., Brett, C.E., and Simms, M.J., eds., Fossil Crinoids: Cambridge University Press, Cambridge, UK, p. 87-92.

TEDESCO, L.P., and WANLESS, H R., 1991, Generation of sedimentary fabrics and facies by repetitive excavation and storm infilling of burrow networks, Holocene of south Florida and Caicos Platform, B. W. I.: PALAIOS, v. 6, p. 326-343.

THOMKA, J.R., MOSHER, D., LEWIS, R.D., PABIAN, R.K., and HOLTERHOFF, P.F., 2009, Genus-level taphonomic variation within cladid crinoids, Upper Pennsylvanian Barnsdall Formation, northeastern Oklahoma: Geological Society of America Abstracts with Program, v. 41, p. 631.

THOMKA, J.R., MOSHER, D., LEWIS, R.D., HOLTERHOFF, P.F., and PABIAN, R.K., 2010, Taphonomy of disarticulated crinoids from the Upper Pennsylvanian Barnsdall Formation, northeastern Oklahoma: Geological Society of America Abstracts with Program, v. 42, p. 66-67.

VAN WAGONER, J.C., POSAMENTIER, H.W., MITCHUM, R.M., JR., VAIL, P.R., SARG, J.F., LOUITT, T.S., and HARDENBOL, J., 1988, An overview of the fundamentals of sequence stratigraphy and key definitions: *in* Wilgus, C.K., Hastings, B.S., St. C. Kendall, G.C., Posamentier, H.W., Ross, C.A., and Van Wagoner, J.C., eds., Sea-level Changes: An Integrated Approach: Society of Economic Paleontologists and Mineralogists Special Publication 42, p. 39-45.

VAN WAGONER, J C., MITCHUM, R.M., CAMPION, K.M., and RAHMANIAN, V.D., 1990, Siliciclastic sequence stratigraphy in well logs, core and outcrop: American Association of Petroleum Geologists Methods of Exploration 7, 55 p.

WATNEY, W.L., FRENCH, J.A., and FRANSEEN, E.K., 1989, Sequence Stratigraphic Interpretation and Modeling of Cyclothems: Kansas Geological Society 41st Annual Field Conference Guidebook, 211 p.

WEBBER, A.J., MEYER, D.L., and MILSON, C.V., 2008, New observations on taphonomy

and paleoecology of *Uintacrinus socialis* Grinnel (Crinoidea; Upper Cretaceous): *in* Ausich, W.I., and Webster, G.D., eds., Echinoderm Paleobiology: Indiana University Press, Bloomington, p. 93-113.

WEBSTER, G.D., 1997, Lower Carboniferous echinoderms from northern Utah and western Wyoming: Utah Geological Survey Bulletin 128, Paleontology Series, v. 1, p. 1-65.

WESTROP, S., 1986, Taphonomic versus ecologic controls on taxonomic relative abundance patterns in tempestites: Lethaia, v. 19, p. 123-132.

WETZEL, A., and MEYER, C.A., 2006, The dangers of high-rise living on a muddy seafloor: An example of crinoids from shallow-water mudstones (Aalenian, northern Switzerland): PALAIOS, v. 21, p. 155-167.

WETZEL, A., and UCHMANN, A., 1998, Biogenic sedimentary structures in mudstones—an overview: *in* Schieber, J., Zimmerle, W., and Sethi, P., eds., Shales and Mudstones I: Basin Studies, Sedimentology, and Paleontology: E. Schweizerbart'sche Verlagsbuchhandlung, Stuttgart, p. 350-369.

WHEATCROFT, R.A., 1990, Preservation potential of sedimentary event layers: Geology, v. 18, p. 843-845.

WHITICAR, M.J., FABER, E., and SCHOELL, M., 1986, Biogenic methane formation in marine and freshwater environments: CO_2 reduction versus acetate fermentation—Isotope evidence: Geochimica et Cosmochimica Acta, v. 50, p. 693-709.

XIONG, B., and HECKEL, P.H., 1996, Cementation patterns and diagenesis in the Stanton Limestone/cyclothem (Missourian, Upper Pennsylvanian) in the northern Midcontinent: *in* Witzke, B. J., Ludvigson, G. A., and Day, J., eds., Paleozoic Sequence Stratigraphy: Views from the North American Craton: Geological Society of America Special Paper 306, p. 373-387.

ZUSCHIN, M., HARZHAUSER, M., and MANDIC, O., 2005, Influence of size-sorting on diversity estimates from tempestitic shell beds in the Middle Miocene of Austria: PALAIOS, v. 20, p. 142-158.

APPENDIX 1

Data from mudstone disaggregation

Below Main Crinoid Bed:

B-1
Total Weight: 475.88 g
Fossil Weight: 22.84 g (48.00 g fossil / kg sample)
Fossil, >3 mm: 11.22 g (23.58 g fossil / kg sample)
Fossil, 2-3 mm: 1.73 g (3.64 g fossil / kg sample)
Fossil, 1-2 mm: 4.54 g (9.54 g fossil / kg sample)
Fossil, 0.5-1mm: 5.35 g (11.24 g fossil / kg sample)
Crinoid Weight: 8.73 g (18.34 g crinoid / kg sample)
Crinoid, >3 mm: 4.15 g (8.72 g crinoid kg sample)
Crinoid, 2-3 mm: 1.14 g (2.40 g crinoid / kg sample)
Crinoid, 1-2 mm: 2.16 g (4.54 g crinoid / kg sample)
Crinoid, 0.5-1mm: 1.28 g (2.69 g crinoid / kg sample)
Encrustation: 56
Breakage: 6
Articulation: 46
Offset: 11
Pluricolumnals: 46
Columnals: 21
Crown Plates: 36
Arm Segments: 0

B-2
Total Weight: 351.50 g
Fossil Weight: 10.02 g (28.51 g fossil / kg sample)
Fossil, >3 mm: 1.79 g (5.09 g fossil / kg sample)
Fossil, 2-3 mm: 0.79 g (2.25 g fossil / kg sample)
Fossil, 1-2 mm: 2.68 g (7.62 g fossil / kg sample)
Fossil, 0.5-1 mm: 4.76 g (13.54 g fossil / kg sample)
Crinoid Weight: 1.83 g (5.21 g crinoid / kg sample)
Crinoid, >3 mm: 0.05 g (0.14 g crinoid / kg sample)
Crinoid, 2-3 mm: 0.26 g (0.74 g crinoid / kg sample)
Crinoid, 1-2 mm: 0.80 g (2.28 g crinoid / kg sample)
Crinoid, 0.5-1 mm: 0.72 g (2.05 g crinoid / kg sample)
Encrustation: 4
Breakage: 3
Articulation: 7
Offset: 0
Pluricolumnals: 7
Columnals: 0
Crown Plates: 6
Arm Segments: 0

B-3
Total Weight: 141.28 g
Fossil Weight: 6.76 g (47.85 g fossil / kg sample)
Fossil, >3 mm: 1.37 g (9.70 g fossil / kg sample)
Fossil, 2-3 mm: 0.66 g (4.67 g fossil / kg sample)
Fossil, 1-2 mm: 2.38 g (16.85 g fossil / kg sample)
Fossil, 0.5-1 mm: 2.35 g (16.63 g fossil / kg sample)
Crinoid Weight: 2.20 g (15.57 g crinoid / kg sample)
Crinoid, >3 mm: 0.17 g (1.20 g crinoid / kg sample)
Crinoid, 2-3 mm: 0.27 g (1.91 g crinoid / kg sample)
Crinoid, 1-2 mm: 1.28 g (9.06 g crinoid / kg sample)
Crinoid, 0.5-1 mm: 0.48 g (3.40 g crinoid / kg sample)
Encrustation: 9
Breakage: 0
Articulation: 4
Offset: 1
Pluricolumnals: 4
Columnals: 2
Crown Plates: 16
Arm Segments: 0

Main Crinoid Bed:

M-3
Total Weight: 314.80 g
Fossil Weight: 17.46 g (55.46 g fossil / kg sample)
Fossil, >3 mm: 4.41 g (14.01 g fossil / kg sample)
Fossil, 2-3 mm: 1.97 g (6.26 g fossil / kg sample)
Fossil, 1-2 mm: 4.72 g (14.99 g fossil / kg sample)
Fossil, 0.5-1 mm: 6.36 g (20.20 g fossil / kg sample)
Crinoid Weight: 2.42 g (7.67 g crinoid / kg sample)
Crinoid, >3 mm: 0.81 g (2.57 g crinoid / kg sample)
Crinoid, 2-3 mm: 0.33 g (1.05 g crinoid / kg sample)
Crinoid, 1-2 mm: 0.80 g (2.54 g crinoid / kg sample)
Crinoid, 0.5-1 mm: 0.48 g (1.52 g crinoid / kg sample)
Encrustation: 15
Breakage: 3
Articulation: 9
Offset: 0
Pluricolumnals: 9
Columnals: 1
Crown Plates: 13
Arm Segments: 0

M-7
Total Weight: 531.09 g
Fossil Weight: 51.32 g (96.63 g fossil / kg sample)
Fossil, >3 mm: 13.27 g (24.99 g fossil / kg sample)
Fossil, 2-3 mm: 15.19 g (28.60 g fossil / kg sample)
Fossil, 1-2 mm: 10.95 g (20.62 g fossil / kg sample)
Fossil, 0.5-1 mm: 11.91 g (22.43 g fossil / kg sample)
Crinoid Weight: 3.91 g (7.36 g crinoid / kg sample)
Crinoid, >3 mm: 0.81 g (1.53 g crinoid / kg sample)
Crinoid, 2-3 mm: 0.62 g (1.17 g crinoid / kg sample)
Crinoid, 1-2 mm: 1.52 g (2.86 g crinoid / kg sample)
Crinoid, 0.5-1 mm: 0.96 g (1.81 g crinoid / kg sample)
Encrustation: 36
Breakage: 5
Articulation: 29
Offset: 3
Pluricolumnals: 28
Columnals: 6
Crown Plates: 12
Arm Segments: 1

M-8
Total Weight: 1598.00 g
Fossil Weight: 74.97 g (46.91 g fossil / kg sample)
Fossil, >3 mm: 19.42 g (12.15 g fossil / kg sample)
Fossil, 2-3 mm: 6.99 g (4.37 g fossil / kg sample)
Fossil, 1-2 mm: 26.40 g (16.52 g fossil / kg sample)
Fossil, 0.5-1 mm: 22.16 g (17.00 g fossil / kg sample)
Crinoid Weight: 13.63 g (8.53 g crinoid / kg sample)
Crinoid, >3 mm: 3.87 g (2.42 g crinoid / kg sample)
Crinoid, 2-3 mm: 2.56 g (1.60 g crinoid / kg sample)
Crinoid, 1-2 mm: 4.48 g (2.80 g crinoid / kg sample)
Crinoid, 0.5-1 mm: 2.72 g (1.70 g crinoid / kg sample)
Encrustation: 116
Breakage: 16
Articulation: 82
Offset: 10
Pluricolumnals: 72
Columnals: 48
Crown Plates: 53
Arm Segments: 10

M-9
Total Weight: 2131.30 g
Fossil Weight: 120.01 g (56.31 g fossil / kg sample)
Fossil, >3 mm: 37.65 g (17.66 g fossil / kg sample)
Fossil, 2-3 mm: 11.03 g (5.18 g fossil / kg sample)
Fossil, 1-2 mm: 32.17 g (15.09 g fossil / kg sample)
Fossil, 0.5-1 mm: 39.16 f (18.37 g fossil / kg sample)
Crinoid Weight: 26.54 g (12.45 g crinoid / kg sample)
Crinoid, >3 mm: 6.39 g (3.00 g crinoid / kg sample)
Crinoid, 2-3 mm: 4.63 g (2.17 g crinoid / kg sample)
Crinoid, 1-2 mm: 10.08 g (4.73 g crinoid / kg sample)
Crinoid, 0.5-1 mm: 5.44 g (2.55 g crinoid / kg sample)
Encrustation: 211
Breakage: 27
Articulation: 131
Offset: 7
Pluricolumnals: 123
Columnals: 98
Crown Plates: 146
Arm Segments: 8

M-10
Total Weight: 686.50 g
Fossil Weight: 46.59 g (67.87 g fossil / kg sample)
Fossil, >3 mm: 8.25 g (12.02 g fossil / kg sample)
Fossil, 2-3 mm: 4.12 g (6.00 g fossil / kg sample)
Fossil, 1-2 mm: 12.12 g (17.65 g fossil / kg sample)
Fossil, 0.5-1 mm: 15.17 g (22.10 g fossil / kg sample)
Crinoid Weight: 7.41 g (10.79 g crinoid / kg sample)
Crinoid, >3 mm: 1.38 g (2.12 g crinoid / kg sample)
Crinoid, 2-3 mm: 1.55 g (2.26 g crinoid / kg sample)
Crinoid, 1-2 mm: 2.72 g (3.96 g crinoid / kg sample)
Crinoid, 0.5-1 mm: 1.76 g (2.56 g crinoid / kg sample)
Encrustation: 65
Breakage: 12
Articulation: 41
Offset: 2
Pluricolumnals: 40
Columnals: 24
Crown Plates: 53
Arm Segments: 1

Top of Main Crinoid Bed / Base of Bed 0

M-1
Total Weight: 125.72 g
Fossil Weight: 5.96 g (47.41 g fossil / kg sample)
Fossil, >3 mm: 2.66 g (21.16 g fossil / kg sample)
Fossil, 2-3 mm: 0.33 g (2.62 g fossil / kg sample)
Fossil, 1-2 mm: 1.40 g (11.14 g fossil / kg sample)
Fossil, 0.5-1 mm: 1.57 g (12.49 g fossil / kg sample)
Crinoid Weight: 0.57 g (4.53 g crinoid / kg sample)
Crinoid, >3 mm: 0.04 g (0.32 g crinoid / kg sample)
Crinoid, 2-3 mm: 0.07 g (0.56 g crinoid / kg sample)
Crinoid, 1-2 mm: 0.38 g (3.02 g crinoid / kg sample)
Crinoid, 0.5-1 mm: 0.08 g (0.64 g crinoid / kg sample)
Encrustation: 6
Breakage: 1
Articulation: 2
Offset: 0
Pluricolumnals: 2
Columnals: 1
Crown Plates: 5
Arm Segments: 0

M-2
Total Weight: 749.10 g
Fossil Weight: 24.76 g (33.05 g fossil / kg sample)
Fossil, >3 mm: 4.52 g (6.03 g fossil / kg sample)
Fossil, 2-3 mm: 1.97 g (2.63 g fossil / kg sample)
Fossil, 1-2 mm: 7.60 g (10.15 g fossil / kg sample)
Fossil, 0.5-1 mm: 10.67 g (14.24 g fossil / kg sample)
Crinoid Weight: 5.20 g (6.94 g crinoid / kg sample)
Crinoid, >3 mm: 1.05 g (1.40 g crinoid / kg sample)
Crinoid, 2-3 mm: 0.87 g (1.16 g crinoid / kg sample)
Crinoid 1-2 mm: 2.00 g (2.67 g crinoid / kg sample)
Crinoid, 0.5-1 mm: 1.28 g (1.71 g crinoid / kg sample)
Encrustation: 35
Breakage: 6
Articulation: 16
Offset: 1
Pluricolumnals: 15
Columnals: 19
Crown Plates: 44
Arm Segments: 1

M-4
Total Weight: 141.28 g
Fossil Weight: 12.94 g (91.24 g fossil / kg sample)
Fossil, >3 mm: 5.29 g (37.30 g fossil / kg sample)
Fossil, 2-3 mm: 0.82 g (5.78 g fossil / kg sample)
Fossil, 1-2 mm: 3.32 g (23.41 g fossil / kg sample)
Fossil, 0.5-1 mm: 3.51 g (24.75 g fossil / kg sample)
Crinoid Weight: 1.69 g (11.92 g crinoid / kg sample)
Crinoid, >3 mm: 0.87 g (6.13 g crinoid / kg sample)
Crinoid, 2-3 mm: 0.10 g (0.71 g crinoid / kg sample)
Crinoid, 1-2 mm: 0.48 g (3.38 g crinoid / kg sample)
Crinoid, 0.5-1 mm: 0.24 g (1.69 g crinoid / kg sample)
Encrustation: 5
Breakage: 0
Articulation: 11
Offset: 1
Pluricolumnals: 5
Columnals: 1
Crown Plates: 6
Arm Segments: 6

M-5
Total Weight: 353.13 g
Fossil Weight: 18.85 g (53.38 g fossil / kg sample)
Fossil, >3 mm: 8.28 g (23.45 g fossil / kg sample)
Fossil, 2-3 mm: 1.10 g (3.12 g fossil / kg sample)
Fossil, 1-2 mm: 4.45 g (12.60 g fossil / kg sample)
Fossil, 0.5-1 mm: 5.02 g (14.22 fossil / kg sample)
Crinoid Weight: 1.87 g (5.30 g crinoid / kg sample)
Crinoid, >3 mm: 0.37 g (1.05 g crinoid / kg sample)
Crinoid, 2-3 mm: 0.18 g (0.51 g crinoid / kg sample)
Crinoid, 1-2 mm: 1.00 g (2.83 g crinoid / kg sample)
Crinoid, 0.5-1 mm: 0.32 g (0.91 g crinoid / kg sample)
Encrustation: 11
Breakage: 2
Articulation: 8
Offset: 2
Pluricolumnals: 5
Columnals: 2
Crown Plates: 18
Arm Segments: 3

M-6
Total Weight: 148.12 g
Fossil Weight: 4.45 g (30.04 g fossil / kg sample)
Fossil, >3 mm: 0.86 g (5.81 g fossil / kg sample)
Fossil, 2-3 mm: 0.36 g (2.43 g fossil / kg sample
Fossil, 1-2 mm: 1.49 g (10.06 g fossil / kg sample)
Fossil, 0.5-1 mm: 1.74 g (11.75 g fossil / kg sample)
Crinoid Weight: 1.68 g (11.34 g crinoid / kg sample)
Crinoid, >3 mm: 0.71 g (4.79 g crinoid / kg sample)
Crinoid, 2-3 mm: 0.33 g (2.23 g crinoid / kg sample)
Crinoid, 1-2 mm: 0.40 g (2.70 g crinoid / kg sample)
Crinoid, 0.5-1 mm: 0.24 g (1.62 g crinoid / kg sample)
Encrustation: 9
Breakage: 0
Articulation: 28
Offset: 0
Pluricolumnals: 3
Columnals: 5
Crown Plates: 3
Arm Segments: 25

Lower Bed 0

0-3
Total Weight: 185.73 g
Fossil Weight: 5.18 g (27.89 g fossil / kg sample)
Fossil, >3 mm: 2.43 g (13.08 g fossil / kg sample)
Fossil, 2-3 mm: 0.68 g (3.66 g fossil / kg sample)
Fossil, 1-2 mm: 0.85 g (4.56 g fossil / kg sample)
Fossil, 0.5-1 mm: 1.22 g (6.57 g fossil / kg sample)
Crinoid Weight: 0.19 g (1.02 g crinoid / kg sample)
Crinoid, >3 mm: 0.00 g (0.00 g crinoid / kg sample)
Crinoid, 2-3 mm: 0.03 g (0.16 g crinoid / kg sample)
Crinoid, 1-2 mm: 0.08 g (0.43 g crinoid / kg sample)
Crinoid, 0.5-1 mm: 0.08 g (0.43 g crinoid / kg sample)
Encrustation: 0
Breakage: 0
Articulation: 2
Offset: 0
Pluricolumnals: 2
Columnals: 0
Crown Plates: 0
Arm Segments: 0

0-4
Total Weight: 272.18 g
Fossil Weight: 11.20 g (41.15 g fossil / kg sample)
Fossil, >3 mm: 3.24 g (11.90 g fossil / kg sample)
Fossil, 2-3 mm: 0.92 g (3.38 g fossil / kg sample)
Fossil, 1-2 mm: 2.81 g (10.32 g fossil / kg sample)
Fossil, 0.5-1 mm: 4.23 g (15.54 g fossil / kg sample)
Crinoid Weight: 3.55 g (13.04 g fossil / kg sample)
Crinoid, >3 mm: 1.63 g (5.99 g fossil / kg sample)
Crinoid, 2-3 mm: 0.44 g (1.62 g fossil / kg sample)
Crinoid, 1-2 mm: 0.92 g (3.38 g fossil / kg sample)
Crinoid, 0.5-1 mm: 0.56 g (2.06 g fossil / kg sample)
Encrustation: 24
Breakage: 1
Articulation: 25
Offset: 6
Pluricolumnals: 23
Columnals: 5
Crown Plates: 6
Arm Segments: 2

0-5
Total Weight: 1677.10 g
Fossil Weight: 94.18 g (56.16 g fossil / kg sample)
Fossil, >3 mm: 22.41 g (13.36 g fossil / kg sample)
Fossil, 2-3 mm: 8.57 g (5.11 g fossil / kg sample)
Fossil, 1-2 mm: 27.45 g (16.37 g fossil / kg sample)
Fossil, 0.5-1 mm: 35.75 g (21.32 g fossil / kg sample)
Crinoid Weight: 15.74 g (9.39 g crinoid / kg sample)
Crinoid, >3 mm: 3.21 g (1.91 g crinoid / kg sample)
Crinoid, 2-3 mm: 2.18 g (1.30 g crinoid / kg sample)
Crinoid, 1-2 mm: 10.24 g (6.11 g crinoid / kg sample)
Crinoid, 0.5-1 mm: 3.84 g (2.29 g crinoid / kg sample)
Encrustation: 136
Breakage: 24
Articulation: 53
Offset: 2
Pluricolumnals: 53
Columnals: 46
Crown Plates: 56
Arm Segments: 0

0-6
Total Weight: 3660.11 g
Fossil Weight: 214.02 g (58.47 g fossil / kg sample)
Fossil, >3 mm: 44.80 g (12.24 g fossil / kg sample)
Fossil, 2-3 mm: 19.65 g (5.37 g fossil / kg sample)
Fossil, 1-2 mm: 87.92 g (24.02 g fossil / kg sample)
Fossil, 0.5-1 mm: 61.65 g (16.84 g fossil / kg sample)
Crinoid Weight: 27.12 g (7.41 g crinoid / kg sample)
Crinoid, >3 mm: 4.62 g (1.26 g crinoid / kg sample)
Crinoid, 2-3 mm: 3.30 g (0.90 g crinoid / kg sample)
Crinoid, 1-2 mm: 14.08 g (3.85 g crinoid / kg sample)
Crinoid, 0.5-1 mm: 5.12 g (1.40 g crinoid / kg sample)
Encrustation: 133
Breakage: 14
Articulation: 60
Offset: 7
Pluricolumnals: 50
Columnals: 86
Crown Plates: 103
Arm Segments: 10

0-7
Total Weight: 358.43 g
Fossil Weight: 16.25 g (45.34 g fossil / kg sample)
Fossil, >3 mm: 7.01 g (19.56 g fossil / kg sample)
Fossil, 2-3 mm: 0.98 g (2.73 g fossil / kg sample)
Fossil, 1-2 mm: 3.53 g (9.85 g fossil / kg sample)
Fossil, 0.5-1 mm: 4.73 g (13.20 g fossil / kg sample)
Crinoid Weight: 2.50 g (6.97 g crinoid / kg sample)
Crinoid, >3 mm: 1.25 g (3.49 g crinoid / kg sample)
Crinoid, 2-3 mm: 0.13 g (0.36 g crinoid / kg sample)
Crinoid, 1-2 mm: 0.64 g (1.79 g crinoid / kg sample)
Crinoid, 0.5-1 mm: 0.48 g (1.34 g crinoid / kg sample)
Encrustation: 5
Breakage: 0
Articulation: 4
Offset: 0
Pluricolumnals: 4
Columnals: 5
Crown Plates: 5
Arm Segments: 0

0-8
Total Weight: 538.73 g
Fossil Weight: 58.52 g (108.63 g fossil / kg sample)
Fossil, >3 mm: 29.62 g (54.98 g fossil / kg sample)
Fossil, 2-3 mm: 5.02 g (9.32 g fossil / kg sample)
Fossil, 1-2 mm: 10.99 g (20.40 g fossil / kg sample)
Fossil, 0.5-1 mm: 12.89 g (23.93 g fossil / kg sample)
Crinoid Weight: 8.85 g (16.43 g crinoid / kg sample)
Crinoid, >3 mm: 3.54 g (6.57 g crinoid / kg sample)
Crinoid, 2-3 mm: 1.71 g (3.17 g crinoid / kg sample)
Crinoid, 1-2 mm: 2.32 g (4.31 g crinoid / kg sample)
Crinoid, 0.5-1 mm: 1.28 g (2.38 g crinoid / kg sample)
Encrustation: 60
Breakage: 2
Articulation: 62
Offset: 10
Pluricolumnals: 62
Columnals: 30
Crown Plates: 54
Arm Segments: 0

Upper Bed 0:

0-1
Total Weight: 106.67 g
Fossil Weight: 4.97 g (46.59 g fossil / kg sample)
Fossil, >3 mm: 1.71 g (16.03 g fossil / kg sample)
Fossil, 2-3 mm: 0.27 g (2.53 g fossil / kg sample)
Fossil, 1-2 mm: 1.49 g (13.97 g fossil / kg sample)
Fossil, 0.5-1 mm: 1.50 g (14.06 g fossil / kg sample)
Crinoid Weight: 1.34 g (12.56 g crinoid / kg sample)
Crinoid, >3 mm: 0.67 g (6.28 g crinoid / kg sample)
Crinoid, 2-3 mm: 0.11 g (1.03 g crinoid / kg sample)
Crinoid, 1-2 mm: 0.32 g (3.00 g crinoid / kg sample)
Crinoid, 0.5-1 mm: 0.24 g (2.25 g crinoid / kg sample)
Encrustation: 9
Breakage: 2
Articulation: 8
Offset: 2
Pluricolumnals: 8
Columnals: 2
Crown Plates: 7
Arm Segments: 0

0-2
Total Weight: 359.53 g
Fossil Weight: 21.67 g (60.27 g fossil / kg sample)
Fossil, >3 mm: 8.96 g (24.92 g fossil / kg sample)
Fossil, 2-3 mm: 1.15 g (3.20 g fossil / kg sample)
Fossil, 1-2 mm: 4.75 g (13.21 g fossil / kg sample)
Fossil, 0.5-1 mm: 6.81 g (18.94 g fossil / kg sample)
Crinoid Weight: 3.13 g (8.71 g crinoid / kg sample)
Crinoid, >3 mm: 0.94 g (2.61 g crinoid / kg sample)
Crinoid, 2-3 mm: 0.43 g (1.20 g crinoid / kg sample)
Crinoid, 1-2 mm: 1.12 g (3.12 g crinoid / kg sample)
Crinoid, 0.5-1 mm: 0.64 g (1.78 g crinoid / kg sample)
Encrustation: 22
Breakage: 3
Articulation: 9
Offset: 1
Pluricolumnals: 9
Columnals: 10
Crown Plates: 24
Arm Segments: 0

Bed 1:

1-1
Total Weight: 280.22 g
Fossil Weight: 8.41 g (30.01 g fossil / kg sample)
Fossil, >3 mm: 1.42 g (5.07 g fossil / kg sample)
Fossil, 2-3 mm: 0.53 g (1.89 g fossil / kg sample)
Fossil, 1-2 mm: 2.26 g (8.07 g fossil / kg sample)
Fossil, 0.5-1 mm: 4.20 g (14.99 g fossil / kg sample)
Crinoid Weight: 1.11 g (3.96 g crinoid / kg sample)
Crinoid, >3 mm: 0.05 g (0.18 g crinoid / kg sample)
Crinoid, 2-3 mm: 0.14 g (0.50 g crinoid / kg sample)
Crinoid, 1-2 mm: 0.60 g (2.14 g crinoid / kg sample)
Crinoid, 0.5-1 mm: 0.32 g (1.14 g crinoid / kg sample)
Encrustation: 7
Breakage: 0
Articulation: 2
Offset: 0
Pluricolumnals: 2
Columnals: 0
Crown Plates: 7
Arm Segments: 0

1-2
Total Weight: 831.70 g
Fossil Weight: 54.07 g (65.01 g fossil / kg sample)
Fossil, >3 mm: 15.13 g (18.19 g fossil / kg sample)
Fossil, 2-3 mm: 5.84 g (7.02 g fossil / kg sample)
Fossil, 1-2 mm: 15.51 g (18.65 g fossil / kg sample)
Fossil, 0.5-1 mm: 17.59 g (21.15 g fossil / kg sample)
Crinoid Weight: 19.35 g (23.27 g crinoid / kg sample)
Crinoid, >3 mm: 7.30 g (8.78 g crinoid / kg sample)
Crinoid, 2-3 mm: 2.93 g (3.52 g crinoid / kg sample)
Crinoid, 1-2 mm: 5.92 g (7.12 g crinoid / kg sample)
Crinoid, 0.5-1 mm: 3.20 g (3.85 g crinoid / kg sample)
Encrustation: 170
Breakage: 16
Articulation: 95
Offset: 17
Pluricolumnals: 93
Columnals: 58
Crown Plates: 58
Arm Segments: 2

Lower Bed 2:

2-2
Total Weight: 1556.20 g
Fossil Weight: 103.50 g (66.51 g fossil / kg sample)
Fossil, >3 mm: 25.48 g (16.37 g fossil / kg sample)
Fossil, 2-3 mm: 7.35 g (4.72 g fossil / kg sample)
Fossil, 1-2 mm: 33.25 g (21.37 g fossil / kg sample)
Fossil, 0.5-1 mm: 37.42 g (24.05 g fossil / kg sample)
Crinoid Weight: 9.08 g (5.83 g crinoid / kg sample)
Crinoid, >3 mm: 1.83 g (1.18 g crinoid / kg sample)
Crinoid, 2-3 mm: 1.01 g (0.65 g crinoid / kg sample)
Crinoid, 1-2 mm: 3.68 g (2.36 g crinoid / kg sample)
Crinoid, 0.5-1 mm: 2.56 g (2.65 g crinoid / kg sample)
Encrustation: 57
Breakage: 9
Articulation: 18
Offset: 2
Pluricolumnals: 17
Columnals: 17
Crown Plates: 55
Arm Segments: 1

2-3
Total Weight: 665.70 g
Fossil Weight: 28.45 g (42.74 g fossil / kg sample)
Fossil, >3 mm: 9.19 g (13.81 g fossil / kg sample)
Fossil, 2-3 mm: 2.03 g (3.05 g fossil / kg sample)
Fossil, 1-2 mm: 7.98 g (11.99 g fossil / kg sample)
Fossil, 0.5-1 mm: 9.25 g (13.90 g fossil / kg sample)
Crinoid Weight: 5.38 g (8.08 g crinoid / kg sample)
Crinoid, >3 mm: 0.71 g (1.07 g crinoid / kg sample)
Crinoid, 2-3 mm: 0.67 g (1.01 g crinoid / kg sample)
Crinoid, 1-2 mm: 2.72 g (4.09 g crinoid / kg sample)
Crinoid, 0.5-1 mm: 1.28 g (1.92 g crinoid / kg sample)
Encrustation: 38
Breakage: 5
Articulation: 11
Offset: 1
Pluricolumnals: 11
Columnals: 19
Crown Plates: 28
Arm Segments: 0

Bed 3:

3-1
Total Weight: 121.88 g
Fossil Weight: 7.68 g (63.01 g fossil / kg sample)
Fossil, >3 mm: 1.88 g (15.43 g fossil / kg sample)
Fossil, 2-3 mm: 0.46 g (3.77 g fossil / kg sample)
Fossil, 1-2 mm: 2.20 g (18.05 g fossil / kg sample)
Fossil, 0.5-1 mm: 3.14 g (25.76 g fossil / kg sample)
Crinoid Weight: 1.36 g (11.16 g crinoid / kg sample)
Crinoid, >3 mm: 0.61 g (5.00 g crinoid / kg sample)
Crinoid, 2-3 mm: 0.03 g (0.25 g crinoid / kg sample)
Crinoid, 1-2 mm: 0.40 g (3.28 g crinoid / kg sample)
Crinoid, 0.5-1 mm: 0.32 g (2.63 g crinoid / kg sample)
Encrustation: 6
Breakage: 1
Articulation: 3
Offset: 0
Pluricolumnals: 3
Columnals: 3
Crown Plates: 2
Arm Segments: 0

3-2
Total Weight: 94.28 g
Fossil Weight: 8.32 g (88.25 g fossil / kg sample)
Fossil, >3 mm: 2.70 g (28.64 g fossil / kg sample)
Fossil, 2-3 mm: 1.09 g (11.56 g fossil / kg sample)
Fossil, 1-2 mm: 2.41 g (25.56 g fossil / kg sample)
Fossil, 0.5-1 mm: 2.12 g (22.49 g fossil / kg sample)
Crinoid Weight: 0.99 g (10.50 g crinoid / kg sample)
Crinoid, >3 mm: 0.35 g (3.69 g crinoid / kg sample)
Crinoid, 2-3 mm: 0.12 g (1.27 g crinoid / kg sample)
Crinoid, 1-2 mm: 0.40 g (4.24 g crinoid / kg sample)
Crinoid, 0.5-1 mm: 0.12 g (1.27 g crinoid / kg sample)
Encrustation: 4
Breakage: 1
Articulation: 4
Offset: 0
Pluricolumnals: 3
Columnals: 2
Crown Plates: 3
Arm Segments: 0

3-3
Total Weight: 1138.32 g
Fossil Weight: 97.10 g (85.30 g fossil / kg sample)
Fossil, >3 mm: 32.09 g (28.19 g fossil / kg sample)
Fossil, 2-3 mm: 10.18 g (8.94 g fossil / kg sample)
Fossil, 1-2 mm: 25.09 g (22.04 g fossil / kg sample)
Fossil, 0.5-1 mm: 29.74 g (26.13 g fossil / kg sample)
Crinoid Weight: 30.82 g (27.07 g crinoid / kg sample)
Crinoid, >3 mm: 11.35 g (9.97 g crinoid / kg sample)
Crinoid, 2-3 mm: 5.23 g (4.59 g crinoid / kg sample)
Crinoid, 1-2 mm: 9.76 g (8.57 g crinoid / kg sample)
Crinoid, 0.5-1 mm: 4.48 g (3.94 g crinoid / kg sample)
Encrustation: 260
Breakage: 31
Articulation: 139
Offset: 13
Pluricolumnals: 138
Columnals: 165
Crown Plates: 85
Arm Segments: 1

Lower Bed 4:

4-4
Total Weight: 989.80 g
Fossil Weight: 61.85 g (62.49 g fossil / kg sample)
Fossil, >3 mm: 11.47 g (11.59 g fossil / kg sample)
Fossil, 2-3 mm: 5.31 g (5.36 g fossil / kg sample)
Fossil, 1-2 mm: 19.93 g (20.14 g fossil / kg sample)
Fossil, 0.5-1 mm: 25.14 g (25.40 g fossil / kg sample)
Crinoid Weight: 17.32 g (17.50 g crinoid / kg sample)
Crinoid, >3 mm: 4.81 g (4.86 g crinoid / kg sample)
Crinoid, 2-3 mm: 2.11 g (2.13 g crinoid / kg sample)
Crinoid, 1-2 mm: 6.56 g (6.63 g crinoid / kg sample)
Crinoid, 0.5-1 mm: 3.84 g (3.88 g crinoid / kg sample)
Encrustation: 119
Breakage: 8
Articulation: 69
Offset: 1
Pluricolumnals: 58
Columnals: 35
Crown Plates: 73
Arm Segments: 11

4-5
Total Weight: 1486.13 g
Fossil Weight: 97.24 g (65.43 g fossil / kg sample)
Fossil, >3 mm: 29.54 g (19.88 g fossil / kg sample)
Fossil, 2-3 mm: 11.21 g (7.54 g fossil / kg sample)
Fossil, 1-2 mm: 25.94 g (17.45 g fossil / kg sample)
Fossil, 0.5-1 mm: 30.55 g (20.56 g fossil / kg sample)
Crinoid Weight: 23.30 g (15.68 g crinoid / kg sample)
Crinoid, >3 mm: 7.65 g (5.15 g crinoid / kg sample)
Crinoid, 2-3 mm: 3.17 g (2.13 g crinoid / kg sample)
Crinoid, 1-2 mm: 8.00 g (5.38 g crinoid / kg sample)
Crinoid, 0.5-1 mm: 4.48 g (3.01 g crinoid / kg sample)
Encrustation: 152
Breakage: 14
Articulation: 66
Offset: 13
Pluricolumnals: 66
Columnals: 7
Crown Plates: 90
Arm Segments: 0

4-6
Total Weight: 526.48 g
Fossil Weight: 38.27 g (72.69 g fossil / kg sample)
Fossil, >3 mm: 10.02 g (19.03 g fossil / kg sample)
Fossil, 2-3 mm: 3.73 g (7.08 g fossil / kg sample)
Fossil, 1-2 mm: 11.27 g (21.41 g fossil / kg sample)
Fossil, 0.5-1 mm: 13.25 g (25.17 g fossil / kg sample)
Crinoid Weight: 9.13 g (17.34 g crinoid / kg sample)
Crinoid, >3 mm: 3.08 g (5.85 g crinoid / kg sample)
Crinoid, 2-3 mm: 1.49 g (2.83 g crinoid / kg sample)
Crinoid, 1-2 mm: 2.64 g (5.01 g crinoid / kg sample)
Crinoid, 0.5-1 mm: 1.92 g (3.65 g crinoid / kg sample)
Encrustation: 76
Breakage: 9
Articulation: 54
Offset: 10
Pluricolumnals: 50
Columnals: 33
Crown Plates: 56
Arm Segments: 4

4-7
Total Weight: 1276.10 g
Fossil Weight: 64.40 g (50.47 g fossil / kg sample)
Fossil, >3 mm: 8.43 g (6.61 g fossil / kg sample)
Fossil, 2-3 mm: 7.03 g (5.51 g fossil / kg sample)
Fossil, 1-2 mm: 20.06 g (15.72 g fossil / kg sample)
Fossil, 0.5-1 mm: 28.88 g (22.63 g fossil / kg sample)
Crinoid Weight: 14.05 g (11.01 g crinoid / kg sample)
Crinoid, >3 mm: 3.37 g (2.64 g crinoid / kg sample)
Crinoid, 2-3 mm: 2.60 g (2.04 g crinoid / kg sample)
Crinoid, 1-2 mm: 5.20 g (4.14 g crinoid / kg sample)
Crinoid, 0.5-1 mm: 2.88 g (2.26 g crinoid / kg sample)
Encrustation: 108
Breakage: 9
Articulation: 68
Offset: 4
Pluricolumnals: 67
Columnals: 42
Crown Plates: 100
Arm Segments: 2

Middle Bed 4:

4-1
Total Weight: 136.39 g
Fossil Weight: 7.04 g (51.62 g fossil / kg sample)
Fossil, >3 mm: 0.92 g (6.75 g fossil / kg sample)
Fossil, 2-3 mm: 1.08 g (7.92 g fossil / kg sample)
Fossil, 1-2 mm: 2.51 g (18.40 g fossil / kg sample)
Fossil, 0.5-1 mm: 2.53 g (18.55 g fossil / kg sample)
Crinoid Weight: 1.31 g (9.60 g crinoid / kg sample)
Crinoid, >3 mm: 0.21 g (1.54 g crinoid / kg sample)
Crinoid, 2-3 mm: 0.30 g (2.20 g crinoid / kg sample)
Crinoid, 1-2 mm: 0.40 g (2.93 g crinoid / kg sample)
Crinoid, 0.5-1 mm: 0.40 g (2.93 g crinoid / kg sample)
Encrustation: 11
Breakage: 0
Articulation: 7
Offset: 1
Pluricolumnals: 7
Columnals: 4
Crown Plates: 9
Arm Segments: 0

4-2
Total Weight: 273.83 g
Fossil Weight: 21.09 g (77.01 g fossil / kg sample)
Fossil, >3 mm: 6.61 g (24.14 g fossil / kg sample)
Fossil, 2-3 mm: 1.83 g (6.68 g fossil / kg sample)
Fossil, 1-2 mm: 6.18 g (22.57 g fossil / kg sample)
Fossil, 0.5-1 mm: 6.57 g (23.63 g fossil / kg sample)
Crinoid Weight: 3.73 g (13.62 g crinoid / kg sample)
Crinoid, >3 mm: 0.52 g (1.90 g crinoid / kg sample)
Crinoid, 2-3 mm: 0.73 g (2.67 g crinoid / kg sample)
Crinoid, 1-2 mm: 1.68 g (6.14 g crinoid / kg sample)
Crinoid, 0.5-1 mm: 0.80 g (2.92 g crinoid / kg sample)
Encrustation: 47
Breakage: 2
Articulation: 21
Offset: 5
Pluricolumnals: 21
Columnals: 26
Crown Plates: 12
Arm Segments: 0

4-9
Total Weight: 1085.35 g
Fossil Weight: 63.54 g (58.54 g fossil / kg sample)
Fossil, >3 mm: 16.28 g (15.00 g fossil / kg sample)
Fossil, 2-3 mm: 5.86 g (5.40 g fossil / kg sample)
Fossil, 1-2 mm: 19.30 g (17.78 g fossil / kg sample)
Fossil, 0.5-1 mm: 22.10 g (20.36 g fossil / kg sample)
Crinoid Weight: 11.96 g (11.02 g crinoid / kg sample)
Crinoid, >3 mm: 1.52 g (1.40 g crinoid / kg sample)
Crinoid, 2-3 mm: 2.60 g (2.40 g crinoid / kg sample)
Crinoid, 1-2 mm: 5.60 g (5.16 g crinoid / kg sample)
Crinoid, 0.5-1 mm: 2.24 g (2.06 g crinoid / kg sample)
Encrustation: 100
Breakage: 6
Articulation: 64
Offset: 11
Pluricolumnals: 63
Columnals: 46
Crown Plates: 39
Arm Segments: 1

4-10
Total Weight: 2479.80 g
Fossil Weight: 179.33 g (72.32 g fossil / kg sample)
Fossil, >3 mm: 43.05 g (17.36 g fossil / kg sample)
Fossil, 2-3 mm: 17.16 g (6.92 g fossil / kg sample)
Fossil, 1-2 mm: 66.48 g (26.81 g fossil / kg sample)
Fossil, 0.5-1 mm: 52.64 g (21.23 g fossil / kg sample)
Crinoid Weight: 30.84 g (12.44 g crinoid / kg sample)
Crinoid, >3 mm: 7.43 g (3.00 g crinoid / kg sample)
Crinoid, 2-3 mm: 5.81 g (2.34 g crinoid / kg sample)
Crinoid, 1-2 mm: 12.16 g (4.90 g crinoid / kg sample)
Crinoid, 0.5-1 mm: 5.44 g (2.19 g crinoid / kg sample)
Encrustation: 207
Breakage: 19
Articulation: 174
Offset: 29
Pluricolumnals: 173
Columnals: 89
Crown Plates: 77
Arm Segments: 1

Upper Bed 4:

4-3
Total Weight: 303.55 g
Fossil Weight: 9.81 g (32.32 g fossil / kg sample)
Fossil, >3 mm: 2.72 g (8.96 g fossil / kg sample)
Fossil, 2-3 mm: 0.74 g (2.44 g fossil / kg sample)
Fossil, 1-2 mm: 2.49 g (8.20 g fossil / kg sample)
Fossil, 0.5-1 mm: 3.86 g (12.72 g fossil / kg sample)
Crinoid Weight: 0.96 g (3.16 g crinoid / kg sample)
Crinoid, >3 mm: 0.11 g (0.36 g crinoid / kg sample)
Crinoid, 2-3 mm: 0.17 g (0.56 g crinoid / kg sample)
Crinoid, 1-2 mm: 0.28 g (0.92 g crinoid / kg sample)
Crinoid, 0.5-1 mm: 0.40 g (1.32 g crinoid / kg sample)
Encrustation: 8
Breakage: 0
Articulation: 6
Offset: 0
Pluricolumnals: 5
Columnals: 1
Crown Plates: 7
Arm Segments: 1

4-8
Total Weight: 3901.10 g
Fossil Weight: 290.63 g (74.50 g fossil / kg sample)
Fossil, >3 mm: 87.97 g (22.55 g fossil / kg sample)
Fossil, 2-3 mm: 25.86 g (6.63 g fossil / kg sample)
Fossil, 1-2 mm: 97.38 g (24.96 g fossil / kg sample)
Fossil, 0.5-1 mm: 79.42 g (20.36 g fossil / kg sample)
Crinoid Weight: 62.31 g (15.97 g crinoid / kg sample)
Crinoid, >3 mm: 29.96 g (7.68 g crinoid / kg sample)
Crinoid, 2-3 mm: 7.71 g (1.98 g crinoid / kg sample)
Crinoid, 1-2 mm: 16.96 g (4.35 g crinoid / kg sample)
Crinoid, 0.5-1 mm: 7.68 g (1.97 g crinoid / kg sample)
Encrustation: 429
Breakage: 23
Articulation: 329
Offset: 42
Pluricolumnals: 404
Columnals: 188
Crown Plates: 180
Arm Segments: 1